Role of acid sphingomyelinase in T lymphocyte activation

Inaugural-Dissertation

Zur

Erlangung des Doktorgrades

Dr. rer. nat.

der Fakultät für

Biologie

an der

Universität Duisburg-Essen

vorgelegt von

Salina Begum

aus Dhaka, Bangladesh

August 2018

Die der vorliegenden Arbeit zugrundeliegenden Experimente wurden am Institut für Molekularbiologie, Universität Duisburg-Essen durchgeführt.

1. Gutachter: Prof. Dr. Erich Gulbins

2. Gutachter: Prof.´in Dr. Wiebke Hansen

3. Gutachter: Prof. Dr. Jürgen Becker

Vorsitzender des Prüfungsausschusses: Prof. Dr. Jürgen Becker

Tag der mündlichen Prüfung: 22 November 2018

Table of Contents

Abbreviations

AC	Acid ceramidase (AC for human, Ac for murine)
APC	Antigen-presenting cells
AICD	Activation-induced cell death
ASM	Acid sphingomyelinase (ASM for human, Asm for murine)
a.u.	Arbitrary unit
ATP	Adenosine triphosphate
BCG	Bacillus Calmette-Guerin
CFSE	Carboxyfluorescein succinimidyl ester
CRMP	Ceramide-rich membrane platform
CTLA	Cytotoxic T lymphocyte antigen
DAG	Diacylglycerol
DC	Dendritic cell
ELISA	Enzyme-linked immunosorbent assay
EDTA	Ethylenediaminetetraacetic acid
ECL	Enhanced chemiluminescence
ER	Endoplasmic reticulum
FCS	Fetal calf serum
FIASMA	Functional inhibitors of acid sphingomyelinase
GFP	Green fluorescent protein
Gly	Glycine
h	Hour
His	Histidine
i.v.	Intravenous
IL	Interleukin
ICAM	Intercellular adhesion molecule
IP_3	Inositol 1,4,5-triphosphate
ITAM	Immunoreceptor tyrosine-based activation motif
LAT	Linker for activation of T cells
LFA	Lymphocyte function-associated antigen
L-ASM	Lysosomal acid sphingomyelinase

LN	Lymph node
MAPK	Mitogen-activated protein kinase
mTOR	Mammalian target of rapamycin
MFI	Mean fluorescence intensity
MHC	Major histocompatibility complex
Mtb	*Mycobacterium tuberculosis*
min	Minute
NK	Natural killer cell
NFAT	Nuclear factor of activated T-cell
NSM	Neutral sphingomyelinase
NO	Nitric oxide
PBMC	Peripheral blood mononuclear cell
PAGE	polyacrylamide gel electrophoresis
PBS	Phosphate-buffered saline
PHA	Phytohaemagglutinin
p-	Phospho-
PMSF	Phenylmethanesulfonyl fluoride
PM	Plasma membrane
PD1	Programmed cell death protein 1
PI3K	Phosphoinositide 3-kinase
PIP2	Phosphatidylinositol 4,5-bisphosphate
PKC	Protein kinase C
PLC	Phospholipase C
ROS	Reactive oxygen species
S-ASM	Secretory acid sphingomyelinase
SM	Sphingomyelin
SMPD1	Sphingomyelin phosphodiesterase 1
S1P	Sphingosine-1-phosphate
Ser	Serine
SDP	Sodium dodecyl sulfate
Tg	Transgenic

TLC	Thin layer chromatography
Thr	Threonine
TNFα	Tumor necrosis factor α
TB	Tuberculosis
Tyr	Tyrosine
TCR	T cell receptor
TGF β	Transforming growth factor β
WT	Wild-type
ZAP	ζ-chain associated protein kinase

Abstract

Acid sphingomyelinase and ceramide modulate several aspects of T lymphocyte activation. T lymphocytes are the vital players in adaptive immune response against invading pathogens. Tuberculosis is one of the most common infectious diseases, still imposing a huge death toll every year.

This project investigates the role of acid sphingomyelinase in tuberculosis-specific peptide25 T cell receptor (TCR) transgenic CD4+ T cells, murine primary lymphocytes and human Jurkat cells.

Data reveals that pharmacological inhibition of acid sphingomyelinase by Imipramine significantly impairs the activation of several TCR signaling kinases, however genetic deficiency of acid sphingomyelinase only shows limited effects. Moreover, examination of peptide25-induced activation of TCR transgenic CD4+ T cells demonstrates that Imipramine significantly inhibits the late activation events, i.e., proliferation, differentiation, cytokine production and induces cell death following stimulation due to ineffective initial activation. In contrast, acid sphingomyelinase-deficient transgenic (P25/Asm$^{-/-}$) CD4+ T cells present very similar responses regarding the late activation events, compared to wild-type control cells (P25/Asm$^{+/+}$). In parallel, systemic infection of wild-type and acid sphingomyelinase-deficient mice with Bacillus Calmette-Guerin, which is a live attenuated form of *Mycobacterium bovis* with a similar antigenic profile to *Mycobacterium tuberculosis*, reveals the insignificant function of acid sphingomyelinase in both CD4+ and CD8+ T cell activation *in vivo*. In addition, mass spectrometry analysis of lipid composition of Jurkat cells following Imipramine treatment reveals a diminished level of sphingosine and sphingosine-1-phosphate. This indicates that the inhibitory effects of Imipramine in T cell signaling and late activation events might not be entirely due to the inhibition of acid sphingomyelinase but also acid ceramidase. Thus, this project gives some new insights into the role of acid sphingomyelinase in T lymphocyte activation.

Zusammenfassung

Die Saure Sphingomyelinase und Ceramid modulieren diverse Aspekte der T-Zellaktivierung. T-Lymphozyten kommt bei der adaptiven Immunabwehr von Pathogenen eine zentrale Rolle zu. Tuberkulose ist eine der häufigsten Infektionskrankheiten (weltweit), die jährlich noch immer zu einer Vielzahl an Todesfällen führt.

In diesem Projekt wird die Rolle der Sauren Sphingomyelinase in der Signaltransduktion von T-Zellen näher beleuchtet. Dies wird anhand dreier T-Zellmodelle vollzogen: 1) transgene CD4-positive T-Zellen, die einen T-Zellrezeptor exprimieren, welcher das tuberkulosespezifische Peptid25 erkennt, sowie 2) primäre Mauslymphozyten und 3) Jurkat-Zellen, eine humane Leukämiezelllinie, die von T-Zellen abstammt.

Die pharmakologische Inhibition der sauren Sphingomyelinase durch Imipramin beeinträchtigt die Aktivierung verschiedener Kinasen signifikant, während die genetische Defizienz der Sauren Sphingomyelinase nur zu geringfügigen Effekten führt. Darüber hinaus wurde die Bedeutung der Sauren Sphingomyelinase für die Aktivierung von T-Zellrezeptor-transgenen CD4-positiven T-Zellen durch das tuberkulosespezifische Peptid25 untersucht. Hierbei wurde gezeigt, dass unter Imipramineinfluss die initiale Aktivierung der Signalwege durch die Stimulation mit Peptid25 weniger effektiv erfolgt, welches wiederum zu einer deutlichen Reduktion der Proliferation, Differenzierung und Zytokinproduktion führt und zudem zur Induktion des Zelltodes beiträgt. Im Gegensatz dazu zeigen T-Zellrezeptor-transgene CD4-positive T-Zellen, die defizient für die Saure Sphingomyelinase sind, sehr ähnliche Reaktionen in Bezug auf späte Aktivierungsereignisse wie solche, die die Saure Sphingomyelinase exprimieren. Das Bacillus Calmette-Guerin ist eine attenuierte Form des *Mycobacterium bovis* mit einem Antigen-Profil, welches dem des *Mycobacterium tuberculosis* sehr ähnlich ist. In Analogie zu den Befunden *in vitro* zeigt die systemische Infektion mit dem Bacillus Calmette-Guerin von Saure Sphingomyelinase-defizienten im Vergleich mit genetisch unveränderten Mäusen ebenfalls, dass die Saure Sphingomyelinase im Kontext der Aktivierung von CD4- und CD8-positiven T-Zellen *in vivo* nur eine untergeordnete Rolle spielt. Weiterhin hat die massenspektrometrische Analyse der

Lipidzusammensetzung von Jurkatzellen gezeigt, dass die Behandlung mit Imipramin zu verringerten Sphingosin- und Sphingosin-1-phosphat-Spiegeln führt. Dies deutet darauf hin, dass die Effekte der Gabe von Imipramin nicht allein auf die Inhibition der Sauren Sphingomyelinase, sondern auch auf die Beeinträchtigung der Funktion der Sauren Ceramidase zurückzuführen sein könnten. Diese Arbeit gibt somit neue Einblicke in die Bedeutung der Sauren Sphingomyelinase in Bezug auf die T-Zellaktivierung.

1 Introduction

1.1 Cell biology of acid sphingomyelinase and ceramide

1.1.1 Sphingolipids structure and synthesis

Sphingolipids consist of a broad range of lipid molecules that are involved in a wide range of cellular functions (Airola and Hannun et al. 2013). To understand the diversity of their functions in health and disease, it is essential to understand their chemical structure, cellular metabolism and the role of metabolizing enzymes. There are almost 300 different sphingolipids found to be produced by different mammalian cells. At the basic structural level, sphingolipids are composed of a long-chain sphingoid base, an amide-linked fatty acid and a polar head group at the 1-position (**Figure 1.1**). Almost all the sphingolipids contain carbohydrate head groups. Exceptions are ceramide and sphingomyelin (SM), which have a hydroxyl and phosphorylcholine head group at 1-position, respectively (Hannun and Bell et al. 1989).

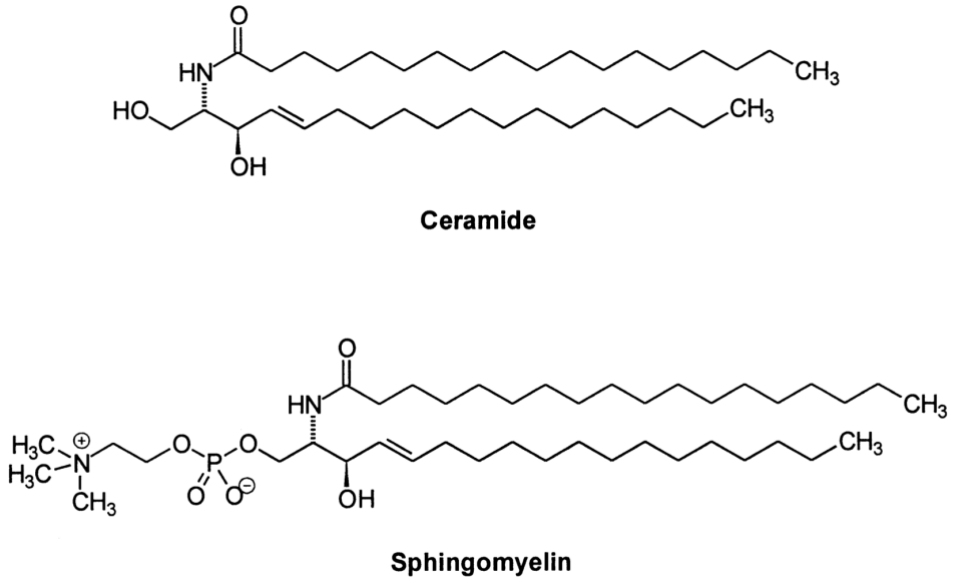

Figure 1.1: Chemical structure of ceramide and SM (Huwiler et al. 2000).

Sphingolipid biosynthesis occurs in the endoplasmic reticulum (ER) and the Golgi apparatus (Gault et al. 2010),(Bartke and Hannun et al. 2009). The initial step of *de novo* synthesis of simplest sphingolipid, ceramide is catalyzed by the enzyme serine palmitoyltransferase (SPT), which condenses L-serine and palmitoyl-CoA to form 3-keto-dihydrosphingosine (Airola and Hannun et al. 2013),(Huwiler et al. 2000). The carbonyl group of 3-keto-dihydrosphingosine is then reduced to form dihydrosphingosine by the enzyme 3-keto-dihydrosphingosine reductase (KDHR). Afterwards, the enzyme (dihydro) ceramide synthase (CerS) adds a fatty acid chain (the acyl chain) by N-acylation to form (dihydro) ceramide. Finally, desaturation of the C4-C5 carbon-carbon bond on the sphingoid backbone by dihydroceramide desaturase (DES) generates ceramide (Gault et al. 2010).

After being produced in ER, ceramide is transported to the Golgi apparatus either through vesicular transport or via transport proteins. Considering ceramide as the central point, sphingolipid metabolism can go in several directions. These include the phosphorylation of ceramide by ceramide kinase (CerK) to produce ceramide-1-phosphate (C1P), the addition of phosphocholine by sphingomyelin synthase (SMS) to produce SM and the addition of a sugar molecule by glucosyl- or galactosyl-ceramide synthases to create glucosylceramide (GluCer) or galactosylceramide (GalCer), respectively (Airola and Hannun et al. 2013).

Findings in the recent years identified a novel mechanism of ceramide accumulation from the catabolism of complex sphingolipids that are eventually broken down into sphingosine, which is then reused through re-acylation to produce ceramide. This pathway is known as sphingolipid recycling or the salvage pathway. Key enzymes involved in this process are sphingomyelinases, glucocerebrosidase (acid-β-glucosidase), ceramidases and (dihydro) ceramide synthases (Kitatani et al. 2008). On the other hand, ceramide can be broken down by ceramidases to produce sphingosine. Sphingosine can be reconverted to ceramide by CerS or can be phosphorylated by sphingosine kinase (SK) to produce sphingosine-1-phosphate (S1P) (Airola and Hannun et al. 2013) (**Figure 1.2**). Ceramide can also be generated from SM hydrolysis by various sphingomyelinases. Peak activity of these enzymes depends on pH.

Depending on the pH for the optimum activity they are classified as acid, neutral and alkaline sphingomyelinases (Henry et al. 2013).

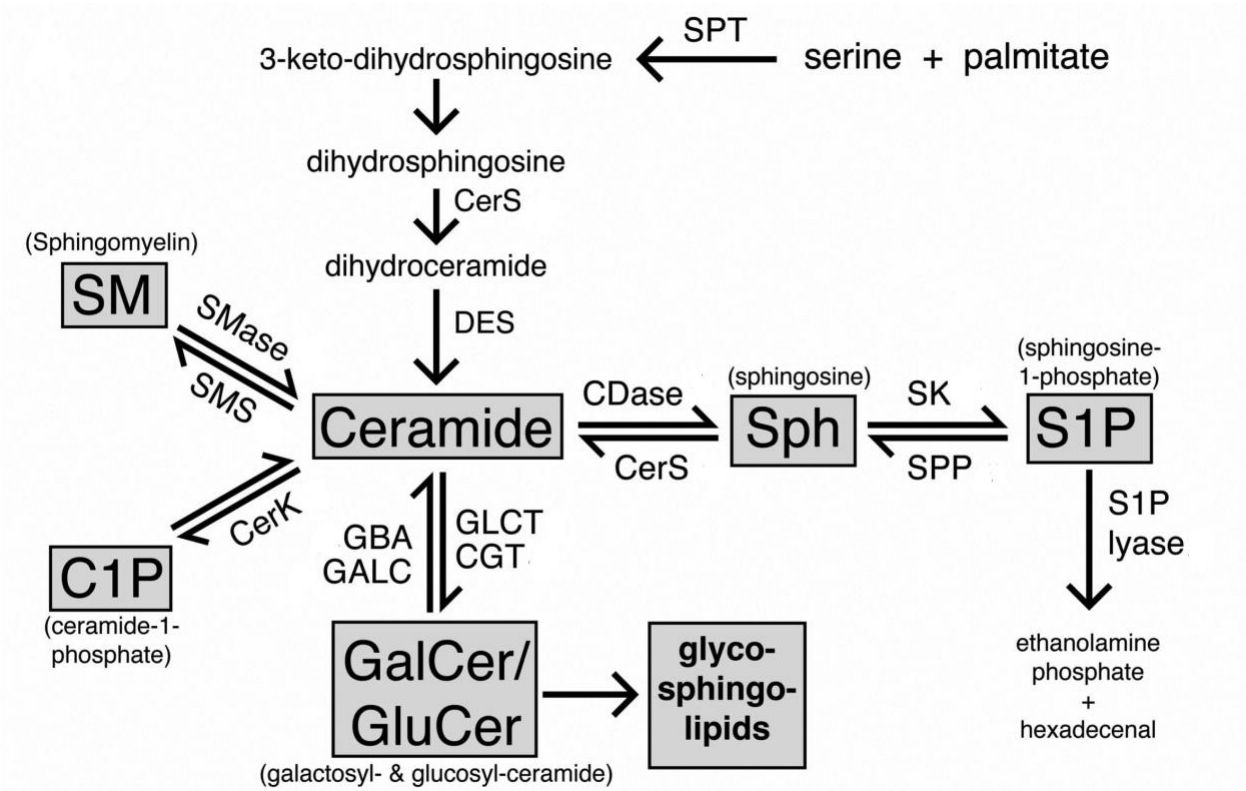

Figure 1.2: Sphingolipid metabolism.
Diagram of sphingolipid metabolism showing the major lipid species in grey boxes and sphingolipid metabolizing enzymes on top of them. Abbreviations: SPT = serine palmitoyltransferase, CerS = (dihydro) ceramide synthase, DES = dihydroceramide desaturase, SMase = sphingomyelinase, SMS = sphingomyelin synthase, CerK = ceramide kinase, GBA = glucosylceramidase, GALC = galactosylceramidase, GCLT= ceramide glucosyltransferase, CGT = ceramide galactosyltransferase, CDase = ceramidase, SK= sphingosine kinase, SPP =S1P-phosphatase (Airola and Hannun et al. 2013).

1.1.2 Acid sphingomyelinase and ceramide system

Acid sphingomyelinase (ASM for human and Asm for murine) is a lipid hydrolase which catalyzes the breakdown of SM by cleavage of the phosphorylcholine linkage, thereby producing ceramide. It is encoded by one conserved gene in human and mice and symbolled as *SMPD1* and *Smpd1*, respectively. *SMPD1* gene is 5-6 kb long and localizes to chromosome 11p15.1–11p15.4 containing six exons and five introns (Da et al. 1991). Encoded ASM cDNA is 629 amino acids (aa) long. At present, there are 7 different isoforms of ASM have been identified, among them only ASM1 is catalytically active (Schuchman et al. 1991),(Rhein et al. 2012).

Recent publications proposed the crystal structures of human ASM. Xiong and his group proposed that ASM is composed of three primary domains: The N-terminal saposin domain, the proline-rich connector domain and the catalytic domain. Overall, the enzyme has the shape of a large shallow depression, at the base of which resides two-zinc ions. Saposin domain constitutes the arc-shaped lip along the edge. The active site of the enzyme is at the center of the bowl and the six glycosylation sites are located on the back side of the bowl (**Figure 1.3**) (Gorelik et al. 2016),(Xiong et al. 2016).

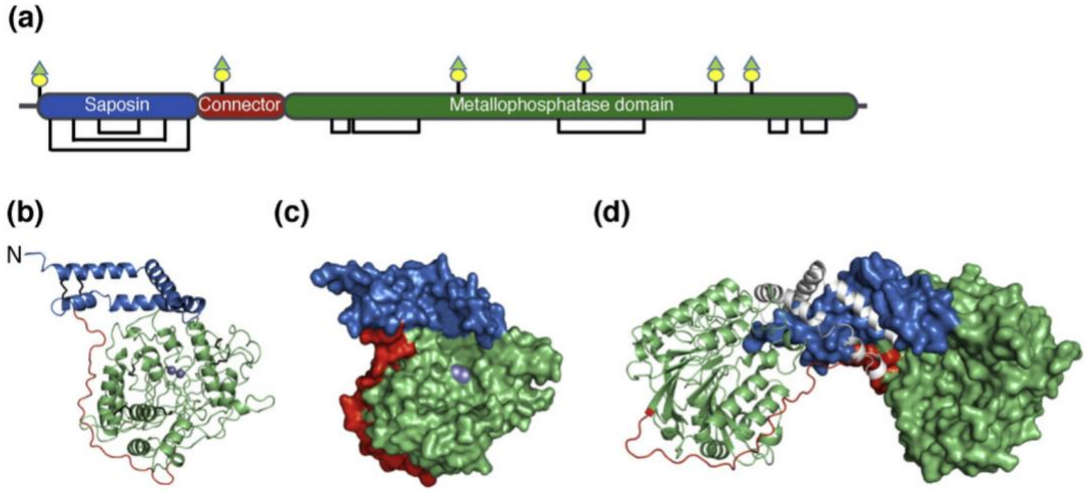

Figure 1.3. Structure of ASM.
Domain organization of ASM, indicating the glycosylation sites and disulfide bonds (a). Crystal structure of ASM in ribbon and surface representation (b, c), with coloring as in panel (a). Disulfide bonds are shown as black lines and the zinc ions at the active site are shown as grey spheres. ASM homodimer in the crystal formed by the association of the two saposin domains (d). One chain is represented as a surface and the other as a ribbon with a gray saposin domain (Xiong et al. 2016).

In vitro experiments revealed the optimum pH for ASM activity is 4.5-5.0. This finding indicated that the enzyme might be solely located in the lysosome (Fowler et al. 1969). However, recent studies have demonstrated that acidic microenvironment can exist on the outer leaflet of the plasma membrane (PM) as well. Moreover, membrane lipid composition alters the Michaelis constant (Km) of the enzyme, makes it active at a higher pH (Schissel et al. 1998a). These data indicate that the activity of ASM is not lysosome restricted (Henry et al. 2013).

After SDS–PAGE analysis of ASM purified from various sources, revealed its estimated molecular weight of 72 kDa. Metabolic labeling experiments indicate the existence of 75 kDa ASM as a preproenzyme. The preproenzyme enters the Golgi apparatus and then subjected to partial cleavage to generate the proenzyme with a molecular weight of 72 kDa (Hurwitz et al. 1994). ASM can be located in the lysosome or can be secreted as well (Schissel et al. 1998b). The post-translational cleavage processing depends on the subcellular location of the protein (Ferlinz et al. 1994). Lysosomal (L-ASM) and secretory (S-ASM) forms of ASM are cleaved at Gly66 and His60 sites, respectively. Mature protein undergoes glycosylation which is required for its activity and determines the trafficking of the enzyme. L-ASM is glycosylated by N-linked oligomannose groups in the Golgi apparatus. In contrary, S-ASM shows complex glycosylation. Mannose-6-phosphate glycosylation permits the binding of mannose-6-phosphate receptors (M6P-R) to L-ASM, which directs the enzyme to the lysosome. On the other hand, complex glycosylated S-ASM is directed to be secreted (Schissel et al. 1998b),(Newrzella and Stoffel et al. 1996),(Ferlinz et al. 1994). Besides, M6P-R system another sorting system which segregates ASM to the lysosome has been proposed by Ni and co-workers (Ni and Morales et al. 2006). In this study, they demonstrated that sortillin, which is a member of the Vps10p sorting receptor family, is also involved in L-ASM trafficking from trans-Golgi network to endosome/lysosome in a M6P-R-independent way.

Further, ASM is a metalloenzyme. As shown earlier (**Figure:1.3**), it has several Zn^{2+} binding sites. However, the requirements of Zn^{2+} for its activation differs between S-ASM and L-ASM. The lysosomal form of ASM encounters Zn^{2+} in the lysosome. Though, the secretory form remains excluded from Zn^{2+} through the Golgi secretory

pathway. For this reason, it requires additional Zn^{2+} to be activated (Schissel et al. 1998b). However, the molecular mechanism of ASM activation is not fully understood. Zhang and colleagues showed that the enzyme can be directly activated by oxidation *in vitro* (Li et al. 2010). Oxidation at cysteine residue-629 results in dimerization and activation of the enzyme. In contrary, ASM activation by DR5 or Cu^{2+} is inhibited by reactive oxygen species (ROS) scavengers (Dumitru and Gulbins et al. 2006),(Lang et al. 2007), although these studies did not clarify whether ASM activity is directly modulated by ROS or by unknown intermediates. In addition, caspase enzymes are also found to be involved in ASM activation. For example, it has been shown that treating Jurkat T cells with caspase inhibitor Ac-YVAD-chloromethylketone, prevents ASM activation induced by CD95 (Brenner et al. 1998). Tumor necrosis factor α (TNFα) is known to induce ceramide production by ASM activation. A potential mechanism could be the interaction of TNF-receptor with caspase-7 leads to receptor internalization into endosome. Following fusion of an endosome with the lysosome, caspase-7 cleaves lysosomal ASM and activates the enzyme (Edelmann et al. 2011). Phosphorylation at serine-508 by protein kinase C (PKC) might also be an essential step for ASM activation, as described in phorbol 12-myristate (PMA) treatment of MCF-7 cancer cells (Zeidan and Hannun et al. 2007). Besides activation, ASM is found to be inhibited by inositol-phosphates (Kolzer et al. 2003). Although, the physiological significance of this finding is not determined yet.

Genetic deficiency of ASM results in the accumulation of SM and causes lysosomal storage diseases named Niemann-Pick disease (NPD) type A and type B. Onset of type A NPD happens at infantile age, causes neurodegeneration, follows a rapidly progressive course which leads to death by the age of 2-3 years. On the other hand, type B is the milder form of the disease with residual ASM activity. It occurs at a later age, usually without any neurological symptoms. However, different organ abnormalities can appear with disease progression (Schuchman et al. 2010),(Schuchman et al. 1992).

1.1.3 Lipid rafts and ceramide enriched domains

According to the fluid mosaic model of Singer and Nicolson, PM is a “sea’’ of lipid bilayer where proteins are floating as icebergs (Singer and Nicolson et al. 1972).

However, works over the last decades have provided evidence that the PM is not a random ocean of lipids. Rather, there are structures within this “sea’’ of lipids that in turn impose organization on the distribution of proteins in the bilayer. The lipid structures within the membrane ocean are called lipid rafts (Pike et al. 2003). In recent years, many new findings introduced the different kinds of lipid molecules present in the PM.

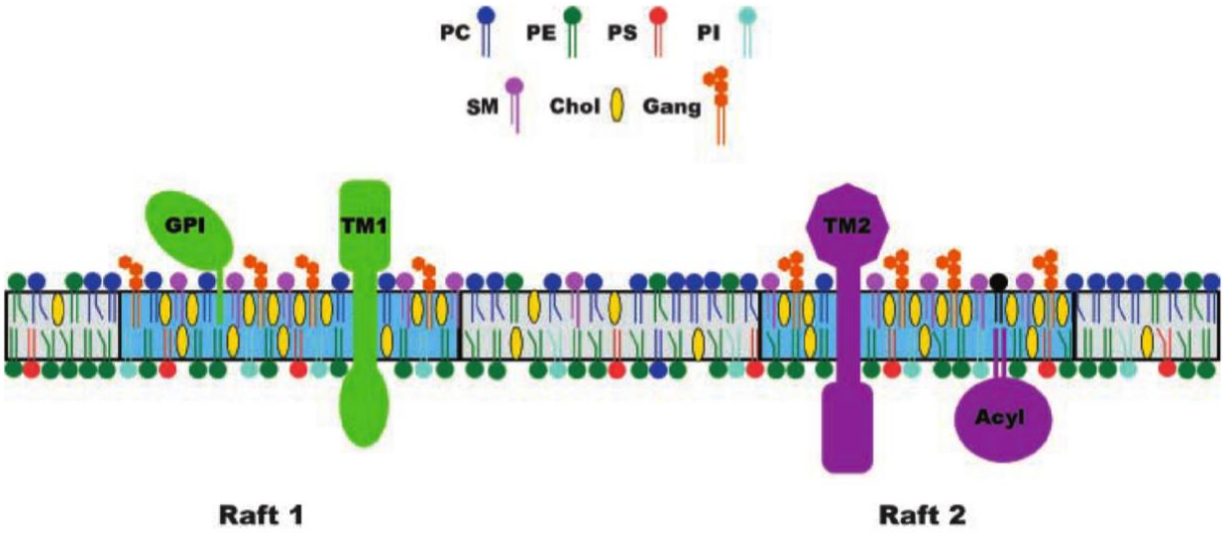

Figure 1.4: Structure of lipid rafts.
Lipid rafts (blue bilayer) are specialized membrane domains containing high concentrations of cholesterol, SM and gangliosides. They are also enriched in phospholipids that contain saturated fatty acyl chains (straight lines in lipid tails). This composition results in lateral phase separation and the generation of a liquid-ordered domain. Bulk PM (gray) contains less cholesterol (Chol), sphingomyelin (SM) and gangliosides (Gang) and more phospholipids with unsaturated acyl chains. As a result, it is more fluidic in nature than lipid rafts. A variety of proteins partition into lipid rafts: glycosylphosphatidylinositol (GPI)-anchored proteins; transmembrane proteins (TM); dually acylated proteins (Acyl). As shown in the diagram, not all lipid rafts have the identical protein or lipid composition (Raft 1 vs. Raft 2). Other abbreviations: Phosphatidylcholine (PC); phosphatidylethanolamine (PE); phosphatidylserine (PS); phosphatidylinositol (PI) (Pike et al. 2003).

SM is the major sphingolipid component of the PM and it is abundant at the outer leaflet (**Figure 1.4**). Sphingolipids interact with each other via hydrophilic interactions between their head groups and hydrophobic interactions between their side chains. They are tightly packed in the membrane because of their saturated hydrocarbon chains. Cholesterol provides additional support by interacting with SM via hydrogen bonds and

hydrophobic van der Waals interactions of sterol ring and ceramide moiety of SM. This tight and stable packaging of sphingolipids results in the lateral phase separation from phospholipid bulk, forming cholesterol-rich sphingolipid raft, described as ‘‘lipid raft’’ earlier (Brown and London et al. 1998).

Many stimuli trigger the translocation of ASM containing secretory lysosomes to the PM. Subsequent fusion of lysosomes with the PM exposes ASM to the extracellular leaflet, where it hydrolyzes SM to ceramide (Henry et al. 2013). Increase in the ceramide content results in increased lipid-order in phospholipid bilayers. Ceramide has unique biophysical properties such as preferential self-association and ability to induce membrane fusion, which ultimately leads to lateral phase separation and formation of ceramide-enriched domains. Domains can get together and make large platforms known as ceramide-rich membrane platforms (CRMP) (Veiga et al. 1999). The diameter of these CRMPs could be from 200 nm up to several microns, which can be visualized by light/fluorescence microscopy (Brown and London et al. 1998),(Stancevic and Kolesnick et al. 2010). As discussed earlier, hydrolysis of SM is the principal source of ceramide and SM is abundant in lipid rafts. That is why it is speculated that CRMPs are originated from lipid rafts. Various stimuli can induce the generation of CRMPs in various cells in a cell-type and stimulus-specific way. To mention a few: ligation of CD95 (Dumitru and Gulbins et al. 2006), DR5, FcγRII (Shakor et al. 2004); infection with *Pseudomonas aeruginosa* (Zhang et al. 2008), *Neisseria gonorrhoeae* (Hauck et al. 2000), *Staphylococcus aureus* (Esen et al. 2001), Measles virus (Avota et al. 2011), Rhinovirus (Grassmé et al. 2005a); different stress stimuli like UV (Zeidan et al. 2008), chemotherapeutic drugs (Lovat et al. 2004),(Perrotta et al. 2007) and gamma radiation (Haimovitz-Friedman et al. 1994).

1.1.4 ASM/ceramide in signal transduction

It was only 50 years ago; lipids were considered as the inert component of the cell membrane, providing only structural support. Continuous research unfolded their important role in different biological processes such as signal transduction. The first indication of the involvement of lipids in cell singling was the discovery of the phosphoinositide cycle (Berridge and Taylor et al. 1988),(Rhee et al. 1989). In this cycle, phospholipase C (PLC) hydrolyzes phosphatidylinositol 4,5-bisphosphate (PIP2) into inositol 1,4,5-triphosphate (IP_3) and 1,2- diacylglycerol (DAG). IP_3 interacts with its receptor at the ER membrane and leads to calcium release from the intracellular stores, which in turn induces the influx of extracellular calcium. A rise in intracellular calcium level ($[Ca^{2+}]_i$) can activate diverse signaling pathways in many types of cells. On the other hand, DAG directly binds to the PKC and activates it, which leads to separate signaling pathways (Nishizuka et al. 1995).

Ceramide platforms modulate the signal transduction in a unique way. CRMPs provide a platform for trapping, clustering, sorting and re-organization (and re-compartmentalization) of receptors and other signaling molecules at the cell membrane (Grassmé et al. 2003). Clustering increases receptor density in a small area which facilitates signal amplification (Stancevic and Kolesnick et al. 2010). Furthermore, CRMPs can also exclude molecules which negatively regulate the signaling and ensure the transmission of signal to the downstream targets (Bock and Gulbins et al. 2003). Moreover, it has been shown that CRMPs can immobilize receptors and ligands at the PM, increase interaction affinity by limiting lateral diffusion (Grassmé et al. 2001),(Grassmé et al. 2002). However, the mechanism for this preferential partitioning is still not understood.

Formation of ceramide in the outer leaflet of PM promotes lipid exchange with the inner leaflet which leads to its free trans-bilayer flip-flop movement. This allows ceramide to directly interact with different intracellular target proteins (Contreras et al. 2003). For example, phospholipase A_2, atypical PKC isoforms, c-Raf-1, Cathepsin D and ceramide-activating protein phosphatases (CAPP) (Huwiler et al. 2001),(Zhang et al. 1997),(Dobrowsky and Hannun et al. 1993),(Heinrich et al. 1999). All these findings

make ceramide a valuable mediator for the signal transduction. One important issue to keep in mind that ASM activation does not always indicate the formation of CRMPs. So, all the biological effects produced by ASM might not be modulated by ceramide platforms as well.

1.2 Outlook of T cell activation

1.2.1 T cells in immunity

After encountering an infectious agent, T lymphocytes become activated, undergo clonal expansion by proliferation and differentiate into effector cells to restrict the invading pathogen. After the infection is controlled, the majority of the T cells undergo apoptosis; a phase described as “contraction phase’’ (Malek and Castro et al. 2010). A balance between the expansion and contraction phase is vital to define immunity and tolerance.

Activation of cytotoxic CD8+ and helper CD4+ T cells is the central event in immune responses. Naïve CD8+ T cells have no cytotoxic activity but once activated; they can kill virus-infected cells. This elimination is mediated by two contact-dependent pathways: perforin/granzymes granule exocytosis pathway and engagement of cell surface death receptors, e.g., CD95 pathway (Lieberman et al. 2003). Direct cell-cell contact is established when CD2 and lymphocyte function-associated antigen-1 (LFA-1) of CD8+ T cells bind to LFA-3 and intercellular adhesion molecules (ICAMs) of target cells, respectively (Makgoba et al. 1989). After binding, CD8+ T cells release the cytotoxic granules to the region of contact between the killer and the target cells. These granules are specialized lysosomes, containing: membrane-perturbing proteins such as perforin and granulysin; granzymes A, B; perforin inhibitor calreticulin; lysosomal enzymes cathepsin C, cathepsin B and CD95 ligands (L) (Lieberman et al. 2003). After getting the activation signals via T cell receptor (TCR), CD8+ T cells start the production of these granules and granule components. Following recognition of target cells, granules migrate to the contact site and secrete its content into the tight junction formed between the participating cells. In a calcium-dependent way, perforin polymerizes and form a channel, through which other granules-contents enter the target cells (Russell

and Ley et al. 2002). Perforin by itself cannot induce apoptosis, granzyme B is required for its action (Duke et al. 1989). Also, CD8+ T cells express CD95-L which can bind to CD95 on target cells and induce apoptotic cells death (Bossi et al. 1999). Granulysin damages the membrane directly and can cause the release of cytochrome-C from damaged mitochondria (Naval et al. 2018). Calreticulin inhibits perforin by sequestering calcium or by inhibiting granzyme (Hudig et al. 2018). One CD8+ T cell can kill multiple target cells by reorienting their granule release to another region of contact. Considering the large size of granzymes (30 to 65 kDa), it has been suggested that they cannot enter via perforin pore. They are believed to be taken up by endocytosis. Once inside the cell, granzyme is delivered from the endo-lysosomal compartment into the nucleus, where it induces DNA fragmentation and rapid apoptosis (Heusel et al. 1994).

Additionally, CD4+ T cells play a vital role in the immune system. In general, they promote macrophage function, help B cells to make antibody, maintain CD8+ T cells, provide protection against a wide variety of microorganisms (Zhu et al. 2010). As mentioned above, after CD4+ T cells encounter specific antigens from killed and processed pathogen, they differentiate into various effector cells, proliferate to increase in number and migrate to the site of infection to eradicate the pathogen, this is known as the primary immune response. However, the effector cells are short-lived. They are removed from the circulation by programmed cell death, known as activation-induced cell death (AICD). This is necessary for the regulation of homeostasis of antigen-reactive T cells (Baaten et al. 2010). During this process, another subset of cells is formed with long-termed survival, named as memory cells. They can remain in the secondary lymphoid organs (central memory cells) or in the recently infected tissue (effector memory cells). In case of re-exposer to the same pathogen, memory T cells undergo fast expansion resulting in faster and more effective immune response, known as the secondary immune response (Golubovskaya and Wu et al. 2016).

Major effector cells that derive from naïve CD4+T cells are: Th1, Th2, Th17 and regulatory T cells (Tregs). Cytokines are the central regulator of this lineages and determine the direction of differentiation. Over the past years it has been identified that IL-12 (Takatori et al. 2005) and IFNγ for Th1; IL-4 (Swain et al. 1990) and IL-2/IL-7 for

Th2; TGFβ and IL-6/IL-21/IL-23 for Th17 (Veldhoen et al. 2006) and TGFβ and IL-2 for Tregs (Chen et al. 2003) are the primary mediators. Moreover, their effector function is also determined by the cytokines they produce. Th1 cells produce IFNγ as their signature cytokine. They also produce TNFα and IL-2 (Zhu et al. 2010). IFNγ promotes the expression of major histocompatibility complexes-II (MHC-II) and the phagocytic ability of macrophages and supports the activation of immature CD8+ T cells to be fully cytotoxic. On the other hand, Th2 cells secret IL-4, IL-5 and IL-13 (Zhu et al. 2010) and support the activation of B cells to induce antibody production. They also contribute to helminthic infection and allergic reaction (Zhu and Paul et al. 2008). Th17 cells are the third dominant group of effector cells. They are characterized by the production of their signature cytokines IL-17 and IL-22 (Park et al. 2005). They provide host defense against various extracellular pathogens by mediating the recruitment of neutrophils and macrophages to infected tissues. Fourth effector cell types are Tregs. They produce cytokines IL-10 and TGFβ and are critical in maintaining self-tolerance and modulating immune response produced by Th1 cells (Belkaid and Tarbell et al. 2009).

Activation and differentiation of naïve T cells are characterized by expression of various surface molecules such as CD44, CD25 and PD1. CD44 is an adhesion protein that binds to the hyaluronic acid (HA) which is its major *in vivo* ligand (Ponta et al. 2003). In case of an infection, activated T cells elevate the expression of CD44. The expression is sustained on memory T cells, even after the clearance of infection. CD44 is involved in various T cells responses. Such as migration of activated T cells from the blood vessel to the site of infection/inflammation by extravasation and within the tissue stroma as well (DeGrendele et al. 1997). CD44 on T cells bind to the HA on the surface of dendritic cells (DC) leading to the cell clustering which is necessary to stabilize the T cell-DC interaction, augmenting T cell proliferation and cytokine production (Do et al. 2004). Additionally, CD44 can modulate AICD in T cells by sequestering CD95 and thereby preventing the assembly of death-inducing signaling complex (DISC). As a result, the downstream activation of caspase pathways of apoptosis is also inhibited. However, CD44 is also reported to activate the phosphoinositide-3-kinase (PI3K)/AKT pathway, providing survival signals for the respective cells (Larkin et al. 2006).

Another important activation marker for antigen-induced T cells is CD25, which is the α-chain of IL-2 receptor (IL-2R) and regulates T cell differentiation by modulating IL-2 signaling. IL-2R is composed of 3 subunits: IL-2Rα (CD25; 50-55 kDa), IL-2Rβ (CD122; 70-75 kDa) and IL-2Rγc (CD132; 65 kDa) (Hémar et al. 1995). It is constitutively expressed in Tregs, which contrasts with conventional T cells (Tcons) where both IL-2Rα and IL-2Rβ are absent in naïve stage and expressed only after antigenic activation. However, IL-2Rβ is constitutively expressed on NK, NKT and memory CD8+ T cells. Rγc is much less rigorously regulated and is constitutively expressed by all lymphoid cells (Malek and Castro et al. 2010).

Secreted IL-2 works in an autocrine or paracrine manner on IL-2R expressing cells. It first binds to IL-2Rα, which results in conformational changes in IL-2R that promote the association of IL-2Rβ. Upon binding of IL-2, all the subunits of IL-2R undergo internalization by endocytosis. However, it has been shown that IL-2Rα subunit is endocytosed separately from IL-2Rβ and IL-2Rγc subunits. Moreover, their intracellular destinations also differ. The α-chain is found to be restricted to early, sorting and recycling endosomes, while β-chain enters the late/pre-lysosomal compartments (Hémar et al. 1995). This indicates that the α-chain is recycled back to the cell surface. This recycling process of α-chain is supported by the findings in IARC 301.5 cells that IL-2Rα has a longer half-life (48 h) than IL-2Rβ and IL-2Rγc (55 and 70 min, respectively) (Hémar and Dautry-Varsat et al. 1990). Intracellularly, IL-2R signals through Janus kinase-1 (JAK1) and JAK3 tyrosine kinases leading to the activation of mitogen-activated protein kinase (MAPK) and PI3K pathways (Nelson and Willerford et al. 1998). Moreover, IL-2R chains have been proposed to be associated with p56 (Lck), p59 (Fyn) and p53/56 (Lyn) kinases as well (Kim et al. 1993),(Kobayashi et al. 1993). More recent findings reported that IL2-R subunits are selectively associated in lipid rafts which facilitates their oligomerization and signaling (Cho et al. 2010).

1.2.2 T cell receptor

T cells are the critical mediators of the adaptive immune system. They act through the activation of T cell receptor (TCR) upon ligand binding. TCRs are cell surface heterodimer proteins consisting of either disulfide-linked α- and β-chains or γ- and δ-chains (Rudolph et al. 2006). Most of the T cells (>95%) are $\alpha\beta$-T cells containing $\alpha\beta$-TCR, which binds to the antigens displayed by MHCs and MHC-like molecules (Eckle et al. 2013). MHCs are also cell surface molecules. During the cell-mediated immune response, antigens (mainly peptides) are displayed to $\alpha\beta$-T cells in complex with class I (for CD8) or class II (for CD4) MHC molecules. Both classes of MHC are heterodimers with similar architectures and are composed of three domains, one α-helix/β-sheet ($\alpha\beta$) super-domain that forms the peptide-binding site and two Ig-like domains. Class-I MHC molecules usually bind to peptides of 8-10 residues length. In class II MHC, bound peptides are usually longer than in MHC class-I (Rudolph et al. 2006).

TCR does not possess any intracellular signaling domains; instead it is non-covalently associated with a multi-subunit signaling apparatus, consisting of the CD3$\gamma\varepsilon$ and CD3$\delta\varepsilon$ heterodimers and the CD3$\zeta\zeta$ homodimer, which collectively form the TCR-CD3 complex (Wucherpfennig et al. 2010). The intracellular domains of these CD3 chains contain immunoreceptor tyrosine-based activation motifs (ITAMs). When a ligand binds to the antigen binding sites, ITAMs get phosphorylated and start a complex network of signaling pathways (**Figure 1.5-1.7)**.

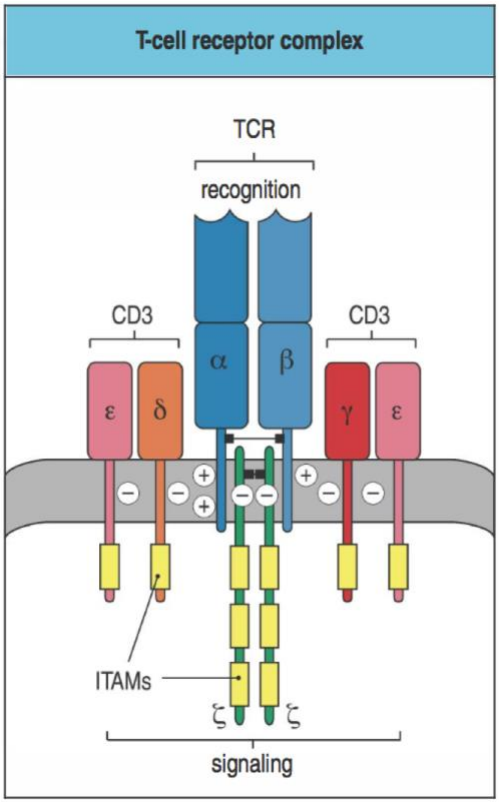

Figure 1.5: TCR-CD3 complex.
The functional TCR is composed of αβ heterodimer chains, which represents the antigen-binding site. Besides this, TCR heterodimer is associated with three different signaling chains remain as 2 heterodimers: δε, γε and 1 homodimer: ζζ. They are collectively called the CD3 complex. CD3 chains have ITAMs, shown as the yellow segments (Janeway's Immunobiology, 9th edition).

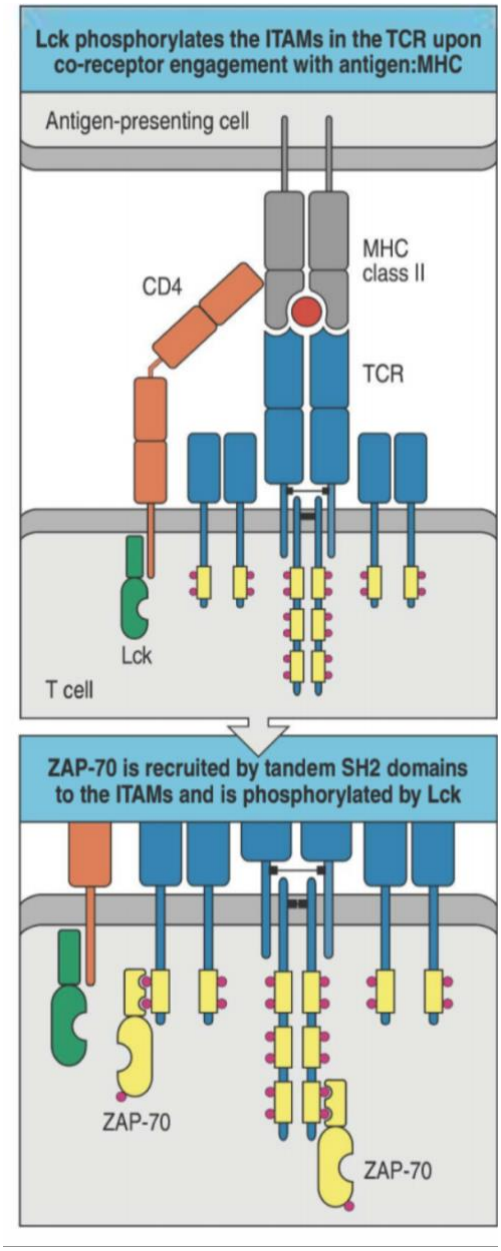

Figure 1.6: Initiation of TCR signal transduction. Upper panel: In CD4+ T cells, the CD4 co-receptor is located close to TCR-CD3 complex. Upon binding of peptide: MHC-II complexes on the surface of an antigen-presenting cell to the antigen binding site, TCR and co-receptor CD4 are brought together by the recruitment of the co-receptor-associated kinase Lck, which leads to phosphorylation of ITAMs in CD3γ, δ, ε and ζ-chains.

Lower panel: the tyrosine kinase ZAP70 binds to phosphorylated ITAMs through its SRC homology 2 (SH2) domain, enabling ZAP70 to be phosphorylated and activated by Lck. Afterwards, ZAP70 phosphorylates other downstream intracellular signaling molecules (Janeway's Immunobiology, 9th edition).

When T cells and antigen-presenting cells (APC) interact with each other, immunological synapse is formed at the interface. At first, micro-clusters are formed at the contact site, consisting of 11–17 TCRs per micro-cluster. Other signaling molecules such as CD2, CD4, CD8 and CD28 also contribute to its formation (Varma et al. 2006). This micro-cluster is known as the central supramolecular activation cluster (cSMAC). The cSMAC is surrounded by a ring of LFA-1 constituting the peripheral SMAC (pSMAC). The outermost ring is called the distal SMAC (dSMAC) which is rich in large proteins, such as CD45 and actin. Central, peripheral and distal SMAC, all together

generate the full immunological synapse (Brownlie and Zamoyska et al. 2013a). Besides commencing the TCR signal transduction, the immunological synapse may serve as a site for TCR internalization and degradation to limit signal strength or duration (Dustin et al. 2010). Following the formation of the immunological synapse, TCR bound ITAMs are phosphorylated by lymphocyte-specific protein tyrosine kinase (Lck) which belong to the group: Src family kinases. Lck is associated with CD4 and CD8 co-receptors. Once the ITAMs are phosphorylated by Lck, they start downstream signaling cascades.

1.2.3 TCR signaling pathways (activation and outcomes)

T cell activation promotes several signaling cascades that ultimately determine cell fate through regulating cytokine production, cell survival, proliferation and differentiation. As mentioned above, the earliest event in this process is phosphorylation of ITAMs on the cytosolic site of the TCR/CD3-complex by Lck (**Figure 1.6**). Phosphorylated ITAM works as a docking site for SH2-domain-containing proteins such as ζ-chain associated protein kinase (ZAP70), where it is phosphorylated and activated by Lck. Activated ZAP70 phosphorylates four key tyrosine residues on linker for activation of T cells (LAT), which recruits numerous signaling molecules to form "LAT-signalosome''. Phosphorylation of SH2-domain containing lymphocyte protein of 76 kDa (SLP-76) by ZAP70, promotes recruitment of Vav (a guanine nucleotide exchange factor), the adaptor proteins: non-catalytic region of tyrosine kinase (NCK), SLP-76/growth factor receptor-bound protein 2 (GRB2)-related adapter protein (GADS) and interleukin-2-inducible T cell kinase (ITK). Other Important molecules constituting the "LAT-signalosome'' are PLCγ1, GRB2 and adhesion- and degranulation-promoting adaptor protein (ADAP). It has been proposed that Vav1 activates Rac-GTPase and/or cell division control protein 42 homolog (Cdc42), which leads to actin polymerization. This step is essential for the translocation and activation of PKC-θ in the SMAC (Villalba et al. 2000). This Vav/Rac pathway of PKC-θ activation represents an alternative for the PLCγ1/DAG dependent pathway (Altman and Villalba et al. 2003). The latter pathway starts with ITK. ITK phosphorylates and activates PLCγ1. This activated PLCγ1 hydrolyses PIP2 to produce the second messenger DAG and IP_3.

DAG activates PKC-θ. Potential physiological targets for PKC-θ are activator protein-1 (AP-1) and nuclear factor-κB (NFκB). Both transcription factors are essential for the production of IL-2 and other cytokines of activated T cells. Signaling pathways leading from PKC to AP-1 and NFκB are not entirely understood. After a considerable amount of research, it has been shown that PKC activates cJun N-terminal kinases (JNK)/AP-1 pathway and IκB kinase (IKK)/NFκB pathway. MAPK/Erk kinase kinase 1 (MEKK1) mediates the cross-talk between these signaling cascades (Baier-Bitterlich et al. 1996),(Lin et al. 2000).

On the other hand, IP_3 binds to its receptors in the ER membrane which open the Ca^{2+} channels and releases Ca^{2+} into the cytosol. This generates a rapid transient rise in $[Ca^{2+}]_i$ that reaches a peak concentration of ~500 nM and returns to baseline within ~100 seconds. Ca^{2+} release from the ER promotes entry of extracellular Ca^{2+} into the cells through calcium release-activated Ca^{2+} (CRAC) channels which can be prolonged till 1 h (Donnadieu et al. 1992),(Lewis et al. 2001). The amplitude and duration of Ca^{2+} signals control various calcium-sensitive transcription factors. A transient rise in $[Ca^{2+}]_i$ is sufficient for activation of NFκB or JNK and its substrate: activating transcription factor-2 (ATF-2). In contrast to this, prolonged elevation is required for the activation of another vital transcription factor for IL-2 production: nuclear factor of activated T cells (NFAT) (Dolmetsch et al. 1997). The phosphorylation-dependent activation of TCR signaling cascade is negatively regulated by several tyrosine phosphatases such as CD45, protein tyrosine phosphatase non-receptor type 6 (PTPN6) and type 22 (PTPN22). Calcium-dependent phosphatase calcineurin is activated by calcium-bound calmodulin protein (Ca^{2+}/CaM). Calcineurin de-phosphorylates NFAT and translocates it to the nucleus which inhibits IL-2 production. Additionally, SLP-76 has been shown to impair the clustering of ZAP70 molecules. Such negative feedback regulation of TCR signal transduction at several points, allows different outcomes, depending on the cell and stimulation-type and surrounding tissue environment (Chen and Flies et al. 2013),(Brownlie and Zamoyska et al. 2013b) (**Figure 1.7**). In addition to these, downregulation of TCR surface expression is another feedback control mechanism. Two pathways have been identified for this. One pathway depends on PKC and CD3γ

Leucine-based motif, while the other pathway is dependent on tyrosine phosphorylation. Additional pathway has been proposed which is regulated by ceramide production. Experiments done in genetically modified Jurkat cells revealed that ceramide activates several caspases which cleaves the ζ- chain leading to TCR downregulation (Menne et al. 2001).

To be fully activated, T cells need total 3 signals. Signal 1 is delivered via TCR-MHC-peptide interaction. Signal 2 is provided via various co-stimulatory and co-inhibitory molecules. CD28 is the cognate co-stimulatory molecule which is constitutively expressed on the surface of naïve CD4+ and CD8+ T cells. Its ligands: B7-1 (also known as CD80) and B7-2 (also known as CD86) are expressed on APCs (Rudd et al. 2009). Although, their expression depends on the activation status of APCs. B7-2 is constitutively expressed at low levels. On the other hand, infection or stress can induce expression of both B7-1 and B7-2. CD28 associates with the P85 subunit of PI3K, which leads to the activation of AKT (also known as protein kinase B). PI3K-AKT pathway activates NF-κB, NFAT, B-cell lymphoma extra-large protein (Bcl-xL), mammalian target of rapamycin (mTOR) and other targets resulting in cell survival and proliferation. Moreover, CD28 recruits PKC-θ to immunological synapse, which is an essential step for its activation (Chen and Flies et al. 2013). Recently it has been shown that CD28 induces activation of Ras-GTPase and its targets AKT, JNK and Erk as well (Janardhan et al. 2011). Moreover, CD28 can also associate with Lck and promotes nuclear translocation of NFAT resulting in enhanced IL-2 production (Boomer and Green et al. 2010). Studies have revealed that these co-regulatory molecules follow distinct expression kinetics depending on the activation status of T cells. Abundant co-stimulatory molecules are expressed on naïve and activated T cells. At the peak of activation, both co-stimulatory and co-inhibitory molecules are expressed and determine the outcomes of initial activation. Later on, co-stimulatory molecules are replaced by the expression of co-inhibitory molecules (Chen and Flies et al. 2013). Well studied inhibitory molecules are cytotoxic T lymphocyte antigen-4 (CTLA-4) and programmed cell death protein-1 (PD1). Similarly to CD28, CTLA-4 binds to the same ligand, B7-2. Expression of CTLA-4 is upregulated following T cell activation, while CD28 is

downregulated by endocytosis which leads to the suppression of T cell responses (Qureshi et al. 2011),(Rudd et al. 2009).

PD1 is a transmembrane molecule which is expressed upon activation of CD4+ and CD8+ T cells, B cells, NKT cells and monocytes (Keir et al. 2008). It binds to two ligands (PD-L1 and PD-L2). PD1 signaling strongly antagonizes TCR signal transduction, which leads to abrogated cytokine production and cell cycle arrest. For these reasons, PD1 is considered as a co-inhibitory molecule which is necessary to inhibit uncontrolled immune activation (Freeman et al. 2000). Expression of the PD1 ligands is different depending on the activation status of the cells. In mice, PD-L2 expression is only induced upon the activation of DCs, macrophages and bone-marrow derived mast cells (Latchman et al. 2001). In contrary, PD-L1 is constitutively expressed by most hematopoietic cell types and can be further up-regulated following cell activation (Agata et al. 1996). At the molecular level, the cytoplasmic tail of PD1 contains an immunoreceptor tyrosine-based inhibitory motif (ITIM) and an immunoreceptor tyrosine-based switch motif (ITSM) (Sharpe et al. 2007). These two motifs recruit SH2-containing tyrosine phosphatases: SHPI and SHP2 (Chemnitz et al. 2004), which inhibits ZAP70 and PI3K phosphorylation as well as the downstream activation pathways (Sheppard et al. 2004). Moreover, it has been shown that PD1 is a potent inhibitor of CD28-mediated co-stimulation in primary human T cells (Chemnitz et al. 2004). In murine CD4+ T cells, PD1 expression can restrain the peptide-induced immunity (Konkel et al. 2010).

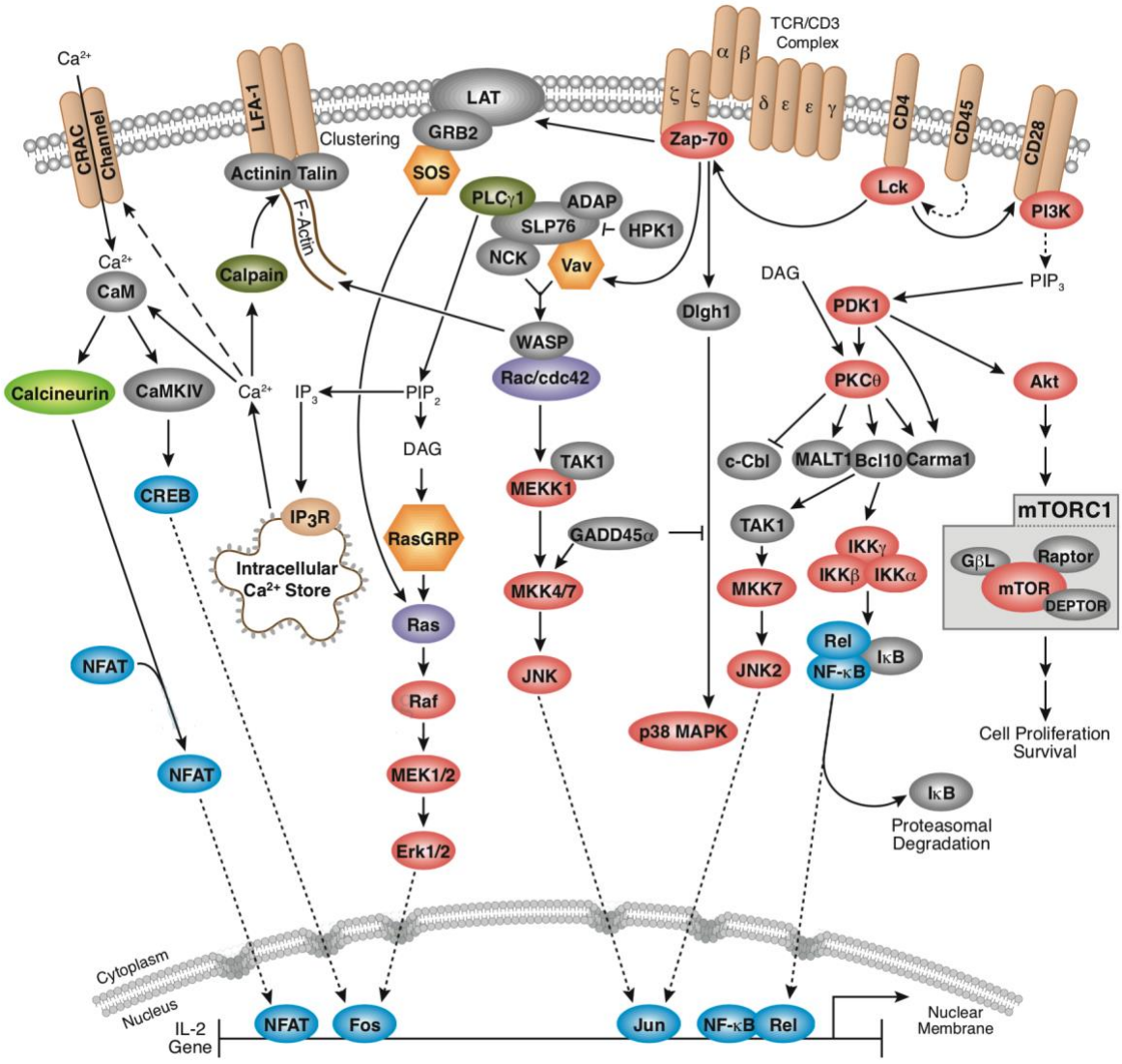

Figure 1.7: Summary of interactive TCR signaling pathways. (Courtesy to Cell Signaling Technology)

1.3 ASM/ceramide in T cell signaling

The role of ASM in CD4+ T cells is largely unknown and to some level controversial as well. It has been shown that the addition of exogenous C2-ceramide to IL-2 deprived CTLL-2 cells initially protects them from IL-2 deprivation-induced apoptosis. Later, when proliferating cells produce endogenous ceramide for a longer duration, it enhances apoptotic cell death (Mérida et al. 2018). Comparable to this study, both mitogenic and anti-mitogenic effect of ceramide and some other related lipids such as phosphatidylcholine, SM has also been demonstrated in human Kit-225 cells (Flores et al. 2000). These results suggest that the death-promoting effect of ceramide in T cells depends on the activation and differentiation status of the cells and the duration of the presence of ceramide in the cell environment. Ceramide also plays a role in negative feedback regulation of T cell-response by downregulating TCR surface expression (Menne et al. 2001).

Whether T cell stimulation leads to sphingomyelinases activation or not, is still conflicting among several studies. For many years, it was believed that CD28 is the primary mediator of ASM activation in T cells. In favor to this idea, It has been shown that ligation of CD28 but not CD3 in human resting and activated primary T cells and in Jurkat cells, induced ceramide production due to increased ASM activity (Boucher et al. 1995),(Chan and Ochi et al. 1995). Moreover, these studies reported that such stimulation only activates ASM but not neutral sphingomyelinase (NSM). However, opposite results have also been shown, where simulation of T cell hybridomas led to ceramide production specifically from increased NSM activity (Tonnetti et al. 1999). Another group indicated that in human primary CD4+ T cells, stimulation with anti-CD3 or anti-CD28 alone and co-stimulation with anti-CD3/CD28 activates various downstream activation signals in an ASM-dependent manner (Bai and Guo et al. 2017),(Bai et al. 2015). Contrarily, it is reported that increased ASM activity upon anti-CD28 ligation is entirely abrogated by anti-CD3/CD28 co-ligation in human primary T cells (Mueller et al. 2014). Previously in murine splenocytes, it was reported that either exogenous sphingomyelinases or C6-ceramide mimicked the CD28 signal leading to proliferation and IL-2 production (Chan and Ochi et al. 1995). On the other hand, the

addition of exogenous sphingomyelinase and/or C2-ceramide to human resting T cells cannot substitute for CD28 mediated co-stimulation, but drastically reduce proliferation and yet increase CD25, CD69 activation marker expression (O'Byrne and Sansom et al. 2000). Several functional inhibitors of ASM were shown to diminish IL-2 and INFγ release from human T cells (Xia et al. 1996). Nevertheless, it was also documented that ceramide is needed for the secretion but not for the production of IL-2 in anti-CD3/CD28 co-stimulated murine splenocytes (Stoffel et al. 1998).

All these findings are indicative for a putative role of ceramide generated by sphingomyelinases in activation and function of T lymphocytes. However, more research needs to be done to understand the cell-specific role of this metabolic process in the immune system. Indeed, the available knowledge makes this system a promising platform to work on for various pathological conditions ranging from infection to genetic diseases (Adam et al. 2002),(Hueber et al. 2000).

1.4 Imipramine as one of the FIASMAs

FIASMAs are the functional Inhibitors of ASM. Considering the importance of ASM and its product ceramide, many efforts were made to identify pharmacologic inhibitors of this pathway. Several functional inhibitors of the ASM have been identified. They are diverse in chemical structure yet show specific physicochemical properties such as most of them are weak bases. ASM is attached to the inner lysosomal membranes by electrostatic forces, where it is protected against the proteolytic inactivation by lysosomal enzymes (**Figure 1.8**). Weak organic bases like FIASMAs can detach ASM from the inner lysosomal membrane and make it available for subsequent proteolytic degradation (Kornhuber et al. 2010),(Kölzer et al. 2004). This mechanism of action of FIASMAs might explain why they do not work against S-ASM, NSM or alkaline sphingomyelinase (Mintzer et al. 2005). Since this particular group of molecules do not interact directly with ASM but inhibit its functional activity, they are considered as functional Inhibitors.

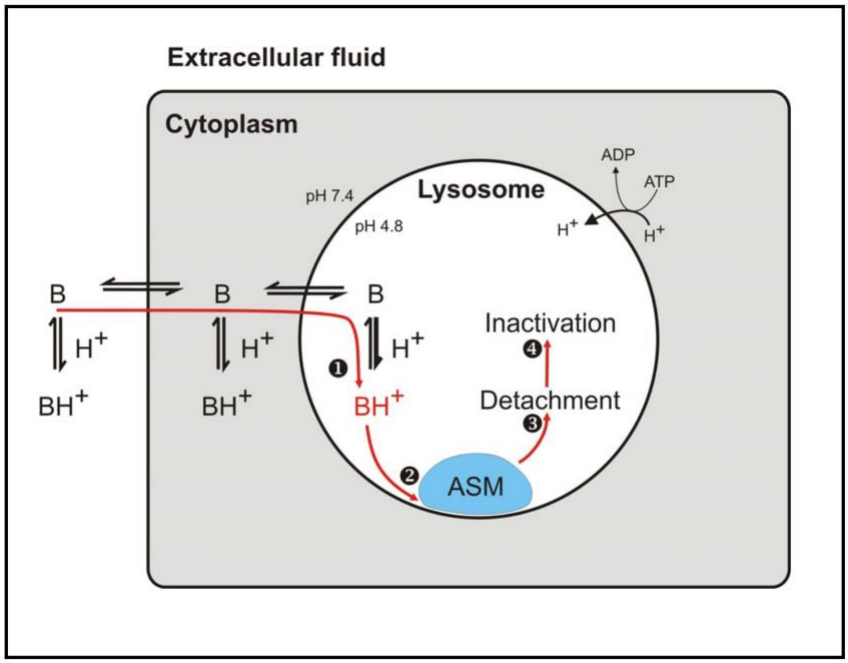

Figure 1.8: Schematic representation of the mechanism of action of FIASMAs.
Inside the lysosome, a low lysosomal pH is maintained by an ATP-driven proton pump. Lipophilic weak bases (BH), as well as FIASMAs, can accumulate preferably inside the lysosome due to their high lipophilicity. Inside the lysosome, the high concentration of the protonated bases disturbs the binding of ASM to the inner lysosomal membrane and results in the detachment of ASM and its subsequent inactivation, possibly involving proteolysis (Kornhuber et al. 2010).

Most of the identified FIASMAs are approved by the US Food and Drug Administration (FDA) and is used as prescription drugs for many diseases. They have favorable ADME (Absorption, Distribution, Metabolism and Excretion) properties, do not show habituation or rebound effects and can work as reversible inhibitors (Kornhuber et al. 2005). Combination use of more than one drug show additive inhibitory effect (Kornhuber et al. 2011). Moreover, their low toxicity, being able to cross blood-brain barrier and availability of data from long-term clinical experience make them a good target for treating diseases where anti-apoptotic effect is needed like in many neurodegenerative diseases such as Alzheimer's, Parkinson's disease, multiple sclerosis or where accumulation of ceramide happens like in the airways in cystic fibrosis disease (Kornhuber et al. 2011),(Malaplate-Armand et al. 2006),(Riethmüller et al. 2009). FIASMAs are distributed into limited groups of drugs. Tricyclic antidepressants are one of the large group. Amitriptyline, Desipramine, Imipramine are few of the mention-worthy

drugs of this group. These drugs have been used in the research of ASM/ceramide system in various bacterial infection such as *Neisseria gonorrhoeae* (Grassmé et al. 1997), *Escherichia coli* (Molnár et al. 1983), *Pseudomonas aeruginosa*, *Staphylococcus aureus* (Hendricks et al. 2003); Rhinovirus infection (Grassmé et al. 2005b), Ebolavirus infection (Miller et al. 2012); study of T cell biology (Bai et al. 2015),(Chentouf et al. 2010); cancer biology; chronic conditions like inflammatory bowel disease (Bauer et al. 2009).

To achieve the inhibition of ASM, FIASMAs require high lysosomal concentrations (Kölzer et al. 2004). Regarding the specificity towards ASM, experimental data showed that FIASMAs do not work as a general inhibitor of lysosomal hydrolases. However, a limited number of hydrolases are inhibited by FIASMAs, such as acid ceramidase (AC for human, Ac for murine), acid lipase and phospholipase A and C (Kornhuber et al. 2010),(Kornhuber et al. 2011). Desipramine is one of the first identified drugs to show AC inhibition in parallel to ASM. However, the extent and specificity of inhibition largely vary depending on the drugs being used. It has been documented that Desipramine treatment of DU145, SSC-14A, Hela cell lines resulted in higher ceramide level, which indicates inhibition of AC (Elojeimy et al. 2006). In contrary, another study showed that treatment with Amitriptyline or Fluoxetine reduced the concentration of ceramide in the hippocampus of experimental animals, indicative of ASM inhibition (Gulbins et al. 2013). These discrepancies indicate that the effects of FIASMAs differ between *in vitro* and *in vivo* models and might be that different drugs exhibit their inhibitory effects in a different extent or they might have the preference for ASM over AC or vice versa (Kornhuber et al. 2010). Moreover, most of the FIASMAs target enzymes, receptors or transporters. Therefore, the produced pharmacological effects by them might not be only from the inhibition of ASM but also from the action on the molecular targets.

1.5 Tuberculosis

1.5.1 General pathophysiology

Tuberculosis (TB) is an infectious disease caused by the bacteria *Mycobacterium tuberculosis* (Mtb). The pathogen enters the host as respiratory droplets and deposits in

the distal alveoli, where it is engulfed by alveolar macrophages (Philips and Ernst et al. 2012). After infection with Mtb, in the majority of the cases, the pathogen can stay inside the host's body for lifelong without causing any active disease. This stage is known as latent infection. During this stage, bacteria are not actively replicating. The only indication of infection is immune responses to mycobacterial antigens. It is believed that approximately one-third of the world's population is in this latent infection stage. In exceptional cases, which represents 5–10% of infected individuals, when the immune system is compromised the active disease can develop.

The active stage of TB is highly contagious. Bacteria can spread from person to person via respiratory droplets (Philips and Ernst et al. 2012). As mentioned above, once another person inhales the infected droplet, the pathogen reaches the distal alveoli, where it is engulfed by alveolar macrophages and most probably by DCs as well (Wolf et al. 2007). Uptake of Mtb into the host cells is mediated through various receptors such as C-type lectin receptors (CLRs), scavenger receptors (SRs) and complement receptors (CRs), macrophage mannose receptor (MMR), DC-specific intracellular adhesion molecule 3-grabbing non-integrin (DC-SIGN) (Philips and Ernst et al. 2012). Once taken up, the intracellular fate of the bacteria depends on the receptor type. For instance, it has been shown that uptake via MMR inhibits phagosome maturation. On the other hand, DC-SIGN or Fc receptors uptake ensure delivery of the bacteria to the lysosome (Kang et al. 2005),(Armstrong B and Hart et al. 1975).

The maneuver behind the lifelong infection by Mtb is believed to be their ability to prevent phagosome maturation and phagosome-lysosome fusion (Russell et al. 2001), inhibition of acidification of lysosomal environment, capacity to escape phagosomes and replicate in the cytosol (Philips and Ernst et al. 2012). Although Mtb can survive inside the resting macrophages, activated macrophages play the central role in bacterial clearance. Activation occurs after the onset of adaptive immunity through various cytokine signals like IFNγ (mainly from CD4+ T lymphocytes) and TNFα. The cytokine, IFNγ is the key macrophage activating agent. *In vitro* studies have shown that TNFα synergizes with IFNγ to induce anti-mycobacterial capacity of macrophages (Flesch and Kaufmann et al. 1990). Both of these cytokines can induce the production of nitric oxide

(NO) and related reactive nitrogen intermediates (RNIs) by macrophages via the action of the inducible form of nitric oxide synthase (NOS) (Kursar et al. 2007).

Granulomas are the histopathological hallmark of TB lesions. A granuloma is an organized aggregate of different kinds of macrophages such as mature macrophages, differentiated or epithelioid macrophages, foamy macrophages and (or Langhans) giant cells (Tsai et al. 2006). Although macrophages are sufficient for granuloma formation, during the development, it is also infiltrated by other immune cells such as DCs, CD4+, CD8+ T cells, B cells and neutrophils (Puissegur et al. 2004),(Tsai et al. 2006). By using *Mycobacterium marinum* as a model, it has been shown that at the initial stage, bacteria freely replicate inside the infected macrophage. After that, many non-infected macrophages are recruited to the initial site and form cellular aggregates representing initial granuloma (Davis et al. 2002). After the death of infected cells, replicated new bacteria are released into the extracellular space and ingested by recruited macrophages which expand the granuloma (Davis and Ramakrishnan et al. 2009). Infected macrophages can leave the preliminary granuloma and spread the infection to distal sites (Davis and Ramakrishnan et al. 2009).

Considering the host defense, granulomas are like the double-edged sword. It provides sanctuaries for bacteria to survive and causes persistent infection. On the other hand, it facilitates the close accumulation of pathogen-infected APCs, such as macrophages and DCs at the site of infection, to T lymphocytes for the initiation of adaptive immune responses (Davis and Ramakrishnan et al. 2009). This step is crucial for protective immunity against TB as macrophages are not able to clear the infection by themselves.

1.5.2 Role of T cells in TB

An essential role of CD4+ T cells for TB pathogenesis became evident from the studies of HIV-infected individuals, where only modest reductions in CD4+ T cell count is shown to be sufficient to increase the TB infection rate by 5 to 10 fold (Kwan and Ernst et al. 2011). Among several subsets of CD4+ T cells involved in TB immunity, Th1 cells are the best studied. They secret their signature cytokine IFNγ, which is a primary stimulant

of the antimicrobial capacity of macrophages and also improves expression of MHC class II for better antigen presentation (Philips and Ernst et al. 2012). Moreover, IFNγ regulates inflammation at the site of infection by working on non-hematopoietic cells (Desvignes and Ernst et al. 2009). Many studies well established the necessity of IFNγ in TB immunity. However, it has been reported that its secretion does not correlate to the protection in human. Similarly, it has been shown that after Bacillus Calmette-Guerin (BCG) vaccination of newborns, T cell frequency and cytokines profile do not correspond with the protection provided by the vaccine (Kagina et al. 2010).

Another subset of T cells, Th17 cells have recently been recognized to contribute to TB immunity, although their roles are still being defined. Their cognate cytokine IL-17 has been shown to be essential for granuloma maturation in BCG-infected mice. In contrary, IL-17 is found to be involved in pathological inflammation in cattle infected with BCG (Blanco et al. 2011).

Tregs are also newly emerged contributors to TB immunity. Experiments done by infecting Mtb or BCG specific peptide25 TCR transgenic (Tg) mice with Mtb showed that Tregs could recognize bacterial peptide as well and the frequency of both Tregs and effector T cells were increased upon infection. Moreover, depletion of Tregs in mice resulted in the reduction of the bacterial burden in the lungs, which also suggests that Tregs impose a delay on the arrival of effector T cells in the lung during the early stage of TB (Shafiani et al. 2010). In another experiment, during active TB disease, Tregs frequencies are found to be higher in patients than healthy controls (Chen et al. 2007). Thus, these studies indicate the involvement of Tregs in TB immune response.

Until the present time, evidence for the direct association between TB and CD8+ T cells in human is not available (Philips and Ernst et al. 2012). However, in mice, it has been shown that CD8+ T cell-deficient mice deceased earlier than wild-type (WT) mice after infection with Mtb (Mogues et al. 2001). Mtb inhibits apoptosis of infected macrophages and instead of apoptosis, they promote necrotic cell death which facilitates bacterial phagosome escape and spread inside the host (Divangahi et al. 2010). Apoptosis of infected macrophage can deliver apoptotic vesicles containing bacterial antigens to

DCs. Then DCs can process and present the antigen to CD8+ T cells to kill the infected cells. This phenomenon is known as cross-presentation. This pathway represents a promising way of utilizing CD8+ T cells for protection against TB (Divangahi et al. 2010).

1.5.3 Involvement of ASM/ceramide in TB

Gatfield and co-workers showed that cholesterol accumulates at the site of mycobacterial entry into J774A.1 macrophages and depletion of cholesterol inhibits bacterial entry (Gatfield and Pieters et al. 1997). Anes and colleagues revealed the involvement of several lipids in phagosomal processes such as actin assembly, fusion and acidification; and its effect in the pathogenic mycobacterial killing (Anes et al. 2003). Actin nucleation is important for phagosome maturation. They showed that phagosomes containing pathogenic mycobacteria (*Mycobacterium avium*) failed to initiate actin nucleation in comparison to non-pathogenic mycobacteria (*Mycobacterium smegmatis*), indicating this process as a defense mechanism exploited by pathogenic mycobacteria. Incubation of cells with selected lipids like ceramide, sphingosine, arachidonic acid increased the percentage of the nucleated phagosome. Moreover, they reported that similar treatment with lipids can activate phagosome-lysosome fusion and acidification of phagosome and specifically ceramide can increase the NO release in macrophages infected with pathogenic mycobacteria (Anes et al. 2003). Similar findings were demonstrated by Utermöhlen and his group in Asm-deficient mice infected with *Listeria monocytogenes*. They revealed that ceramide produced by Asm promotes the fusogenicity of cellular membranes at the intra-(phago-lysosomal fusion) and intercellular (between PM of individual macrophages) levels (Utermöhlen et al. 2008). Moreover, longer retention of late phagosomal markers M6PR and Rab7 and lack of acquisition of late endosomal/lysosomal marker Lamp1 was observed in Asm-deficient macrophages after infection with *Listeria monocytogenes* (Schramm et al. 2008).

1.6 Aim of the study

Activation of T cells is an extremely complicated process. The multiple possibilities for naïve T cells to differentiate into different effector cells, bring more complexity to the mechanism. TCR is a signaling complex consisting of TCR by itself coupled with CD3-molecules and other co-stimulatory molecules, e.g., CD28. Recent studies indicated controversial results on the role of ASM in T cells. In the search for the involvement of ASM in T cell signaling/activation, the first question was asked, which one of these molecules mediates the activation of ASM or which one of them is activated by this enzyme. In 1995, studies done in Jurkat cells and human peripheral resting T cells, showed that only cross-linking of CD28 but not CD3, activates ASM (Boucher et al. 1995). In the same year, similar results were published in murine splenic T cells. The study showed that only anti-CD28 but not anti-CD3 stimulation degrades SM and produces ceramide with similar kinetics, indicating the activation of Asm followed by ceramide production from SM hydrolysis. Moreover, the referred study revealed that the addition of extracellular ceramide induces proliferation and IL-2 production by murine spleen cells (Chan and Ochi et al. 1995). These data suggest that activation of ASM and production of ceramide positively modulate the activation of both human and murine T cells. Stoffel and co-workers showed that anti-CD3/CD28 co-stimulation of splenocytes from Asm-deficient mice shows reduced proliferation and IL-2 secretion than WT control mice. However, interestingly, Asm-deficient cells had more intracellular IL-2 than WT cells. They proposed that the impaired proliferation of Asm-deficient cells is not because Asm-produced ceramide is needed for CD28 mediated co-stimulation but due to the reduced secretion of IL-2 (Stoffel et al. 1998). More recently, it has been shown that in human primary CD4+ T cells CD28 ligation significantly increases ASM activity. However, this response was abrogated upon anti-CD3/CD28 co-stimulation (Mueller et al. 2014). In contrary to these findings, another group revealed that anti-CD3/CD28 co-stimulation activates ASM in human peripheral blood-derived CD4+ T cells. Moreover, by immunoprecipitation and confocal microscopy, they demonstrated that both CD3 and CD28 molecules are physically associated with ASM at the outer leaflet of PM in human CD4+ T cells (Bai et al. 2015).

Thus, this current situation demands more research to understand the extent of the involvement of ASM in T cell activation in a cell-specific manner. Therefore, this project aimed to explore the effects of ASM in 3 completely different models/systems, i.e., peptide25-induced stimulation of TCR Tg CD4+ T cells, physiological or classic anti-CD3/CD28 activation of murine primary naïve T lymphocytes and OKT3 stimulation of Jurkat cells.

2 Materials

2.1 Chemicals

Acetic acid	Merck KGaA, Darmstadt, Germany
Acetone	Merck KGaA, Darmstadt, Germany
Acrylamide (C_3H_5NO)	Carl-Roth GmbH & Co, Karlsruhe
Agarose	Gibco, Invitrogen, Karlsruhe Sigma-Aldrich
Ammonium persulfate (APS)	Carl-Roth GmbH & Co, Karlsruhe
Annexin V	BioLegend San Diego, USA
Bovine serum albumin (BSA)	Sigma-Aldrich Chemie GmbH, Steinheim
β-mercaptoethanol	Sigma-Aldrich Chemie GmbH, Steinheim
Bromphenol blue	Sigma-Aldrich Chemie GmbH, Steinheim
Calcium chloride ($CaCl_2$)	Sigma-Aldrich Chemie GmbH, Steinheim
Chloroform ($CHCl_3$)	Applichem, GmbH, Darmstadt, Germany
CDP-STAR with Nitro-Block II enhancer	PerkinElamer, Boston, USA
CFSE	BioLegend San Diego, USA
CD90.2 Microbeads	Miltenyi Biotec
Dimethylsulfoxide (DMSO)	Sigma-Aldrich Chemie GmbH, Steinheim
Ethanol (C_2H_5OH)	Sigma-Aldrich Chemie GmbH, Steinheim
Ethylenediaminetetraacetic acid (EDTA)	Serva Electrophoresis GmbH, Heidelberg
Fetal calf serum (FCS)	Gibco, Invitrogen, Karlsruhe
Fluo-4 AM cell permeant	Thermo Fisher scientific
Formamide	Sigma-Aldrich Chemie GmbH, Steinheim
Gentamycin	Sigma-Aldrich Chemie GmbH, Steinheim
Glucose ($C_6H_{12}O_6$)	Sigma-Aldrich Chemie GmbH, Steinheim
Glycerol ($C_3H_8O_3$)	Fluka Chemie GmbH, Buchs
Glycine ($C_2H_5NO_2$)	Applichem, GmbH, Darmstadt, Germany
HEPES	Carl-Roth GmbH & Co, Karlsruhe
Hydrochloric acid (HCl)	Sigma-Aldrich Chemie GmbH, Steinheim
Isopropanol	Sigma-Aldrich Chemie GmbH, Steinheim
Magnesium Chloride ($MgCl_2$)	Sigma-Aldrich Chemie GmnH, Steinheim
Methanol	Fluka Chemie GmbH, Buchs

Monopotassium phosphate (KH_2PO_4)	Merck KGaA, Darmstadt, Germany
Mowiol	Kuraray Specialties GmbH, Frankfurt
NP-40 (IGEPAL)	Sigma-Aldrich Chemie GmbH, Steinheim
Paraformaldehyde (PFA)	Sigma-Aldrich Chemie GmbH, Steinheim
Pierce ECL Western blotting substrate	Thermo Fisher Scientific
Potassium chloride (KCl)	Sigma-Aldrich Chemie GmbH Steinheim
Protease Inhibitor	Carl-Roth GmbH & Co, Karlsruhe
Propidium iodide	BioLegend San Diego, USA
Pan T cell isolation kit II	Miltenyi Biotec
Saposin	Serva Electrophoresis GmbH, Heidelberg
Sodium acetate	Sigma-Aldrich Chemie GmbH, Steinheim
Sodium chloride	Carl-Roth GmbH & Co, Karlsruhe
Sodium dodecyl Sulphate (SDS)	Serva Electrophoresis GmbH, Heidelberg
Sodium fluoride	Sigma-Aldrich Chemie GmbH, Steinheim
Sodium hydroxide	Sigma-Aldrich Chemie GmbH, Steinheim
Sodium phosphate	Merck, Darmstadt
Sodium pyrophosphate	Sigma-Aldrich Chemie GmbH, Steinheim
Triton X-100	Sigma-Aldrich Chemie GmbH, Steinheim
Tween-20	Sigma-Aldrich Chemie GmbH, Steinheim
Tris-HCL and Tris-Base	Carl-Roth GmbH & Co, Karlsruhe
Xylene	Applichem GmbH, Darmstadt

2.2 Antibodies

Donkey anti-rabbit AF647	Jackson ImmunoResearch UK
Mouse anti-CD4 PE	BioLegend London, UK
Mouse anti-CD8 PE	BioLegend London, UK
Mouse anti-CD44 PECy7	BD Biosciences, New Jersey, USA
Mouse anti-CD25 AF488	BD Biosciences, New Jersey, USA
Mouse anti-PD1 BV605	BD Biosciences, New Jersey, USA
Mouse anti-CD4 BUV737	BD Biosciences, New Jersey, USA
Mouse anti-IL2 PE	BioLegend London, UK
Mouse anti-Ras	Merck Millipore, Darmstadt, Germany
Mouse anti-β Actin HRP	Santa Cruz, USA
Rabbit anti-phospho-Erk 1/2	Cell Signaling Technology, Frankfurt
Rabbit anti-phospho-AKT	Cell Signaling Technology, Frankfurt
Rabbit anti-phospho-ZAP70	Cell Signaling Technology, Frankfurt
Rabbit anti-phospho-PLCγ1	Cell Signaling Technology, Frankfurt
Rabbit anti-phospho-PI3K	Cell Signaling Technology, Frankfurt
Rabbit anti-phospho-mTOR	Cell Signaling Technology, Frankfurt
Rabbit anti-phospho-AMPKα	Cell Signaling Technology, Frankfurt
Rabbit anti-phospho-Lck (Tyr 416)	Cell Signaling Technology, Frankfurt
Rabbit anti-phospho-Lck (Tyr 505)	Cell Signaling Technology, Frankfurt
Rabbit anti-phospho-JNK	Cell Signaling Technology, Frankfurt
Rabbit anti-phospho-cJun	Cell Signaling Technology, Frankfurt
Rabbit anti-mouse IgG	Abcam Cambridge, UK

2.3 Tissue culture materials

RPMI 1640	Gibco/Invitrogen, Karlsruhe
Fetal calf serum (FCS)	Gibco/Invitrogen, Karlsruhe
L-Glutamine	Gibco/Invitrogen, Karlsruhe
Penicillin/Streptomycin	Gibco/Invitrogen, Karlsruhe
Sodium pyruvate	Gibco/Invitrogen, Karlsruhe

2.4 Equipment

Cell culture 6, 24, 96 well plates	Corning Inc., NY, USA
Cell culture flask	Corning Inc., NY, USA
Cell culture incubator	Thermo Fisher Scientific, MA, USA
Cell strainer	Becton Dickinson Labware, France
Conical centrifuge tubes	BD Falcon, USA
Cuvettes	Sarstedt, Nümbrecht, Germany
Leica DMI-4000 fluorescence microscope	Leica Microsystem, Mannheim, Germany
Leica TCS SP5 confocal microscope	Leica Microsystem, Mannheim, Germany
Microscopic slides	Becton Dickinson Labware, France
Nitrocellulose membrane	GE Healthcare, USA
Parafilm	Pechiney, Chicago, IL, USA
Rotary agitator	Neolab Migge Laborbedarf-Vertriebs GmbH., Germany
Silica G60 TLC plates	Merck, Darmstadt, Germany
SpeedVac	Thermo Fisher Scientific, MA, USA
Thermomixer	Eppendorf, Germany
Typhoon FLA 9500 laser scanner	GE Healthcare Life Sciences, USA
X-ray films	FUJIFILM Medical Systems, USA

2.5 Buffers

Agarose gel (0.8%)	0.8 g agarose
	100 ml TAE buffer
Alkaline phosphatase wash buffer	100 mM Tris/ HCl pH 9.5
	100 mM NaCl
HEPES	132 mM NaCl
	20 mM Hepes pH 7.4
	5 mM KCl
	1 mM $CaCl_2$
	0.7 mM $MgCl_2$
	0.8 mM $MgSO_4$
Mowiol	6 g Glycerol
	2.4 g Mowiol
	6 ml ddH_2O
	12 ml 0.2 M Tris-Base, pH 8.5
	0.1% DABCO
Phosphate buffered saline (PBS)	137 mM NaCl
	2.7 mM KCl
	10 mM Na_2HPO_4
	1.8 mM KH_2PO_4
PBST	137 mM NaCl
	2.7 mM KCl
	10 mM Na_2HPO_4
	1.8 mM KH_2PO_4
	0.05 % Tween 20
Running buffer	25 mM Tris
	192 mM glycine
	0.1 % SDS
SDS laemmli buffer (5X)	250 mM Tris pH 6.8
	20 % Glycine
	4 % SDS

	8 % β-mercaptoethanol
	0.2 % bromophenol blue
TBST	20 mM Tris
	150 mM NaCl
	0.05 % Tween 20
Transfer buffer	25 mM Tris
	192 mM glycine
	20% Methanol

3 Methods

3.1 Mice and cells

Asm-deficient (Horinouchi et al. 1995) mice and their WT littermates; Asm-deficient peptide25 TCR transgenic (Tg) mice (P25/Asm$^{-/-}$) and their WT peptide25 TCR Tg littermates (P25/Asm$^{+/+}$) (Tamura et al. 2004),(Wolf et al. 2008) were maintained on a C57BL/6J background. P25/Asm$^{-/-}$ and P25/Asm$^{+/+}$ mice were generated by crossing peptide25 TCR Tg mice with mice lacking Asm (heterozygous for Asm, Asm$^{+/-}$). These peptide25 TCR Tg mice contain CD4+ T cells expressing a Tg TCR that recognizes peptide25 (aa 240-254) of Mtb and BCG derived antigen-85B (Ag85B) bound to I-Ab. These Tg mice are widely used to study the process of adaptive immune responses to Mtb and BCG infection (Wolf et al. 2008),(Tamura et al. 2004). The genotype of mice was verified by polymerase chain reaction. WT and Asm-deficient mice were used at the age of 6 to 8 weeks to avoid SM accumulation (Lozano et al. 2001). Mice were bred in the animal facility of the University of Duisburg-Essen under specific pathogen-free (SPF) conditions according to the criteria of the Federation of Laboratory Animal Science. All procedures performed on mice were approved by the State Agency for Nature, Environment and Consumer Protection (LANUV) NRW in Düsseldorf, Germany.

Jurkat E6.1 cells were maintained in complete RPMI 1640 (Gibco) medium supplemented with 10% FCS (Gibco), 10 mM HEPES (Roth GmbH; pH 7.4), 2 mM L-glutamine, 1 mM sodium pyruvate, 100 µM non-essential amino acids, 100 U/mL penicillin and 100 µg/mL streptomycin (Gibco) in a confluency of ~5x10^5 cells/ml.

3.2 *Ex vivo* stimulation experiments

Three different stimulation models were tested to evaluate the involvement of ASM in T cell signaling, i.e., peptide25 and anti-CD28-induced activation of murine primary TCR Tg CD4+ T cells, anti-CD3 and anti-CD28 co-stimulation of murine primary T cells and OKT3 antibody induced activation of human Jurkat cells.

To study peptide25-induced activation of TCR Tg CD4+ T cells, single cell suspensions from lymph nodes (LN) and spleens were prepared from P25/Asm$^{+/+}$ and P25/Asm$^{-/-}$ mice.

CD4+ T cells from LNs were purified with mouse Pan T Cell Isolation Kit II (Miltenyi Biotec, cat#130-095-130) and APCs were prepared from spleens using CD90.1 MicroBeads (Miltenyi Biotec, cat#130-094-523) by magnetic-activated cell sorting (MACS) according to the manufacturer's protocol. APCs were pre-loaded with peptide25 (15 μg/ml) for 30 min at 37°C. To induce activation, CD4+ T cells were mixed with pre-loaded APCs from the autologous animal at a ratio of 1:10 in HEPES/Saline (H/S). Soluble anti-CD28 (1 μg/ml) was added to provide the co-stimulatory signal. Cell mixtures were pelleted by centrifugation at 400xg for 30 seconds at 4°C, followed by stimulation at 37°C for 2, 5, 10 and 15 min or left unstimulated. Stimulation was stopped by adding ice-cold modified RIPA lysis buffer (0.1% SDS, 25 mM HEPES, 0.5% deoxycholate, 0.1% Triton X-100, 10 mM EDTA, 10 mM sodium pyrophosphate, 10 mM sodium fluoride, 125 mM sodium chloride) containing freshly added phosphatase inhibitors: 10 mM sodium orthovanadate and 1 mM of PMSF and 10 μg/ml of the protease inhibitors: Aprotinin/Leupeptin (A/L). Lysates were incubated for 5 min on ice. Cell debris was removed by centrifugation at 14,000 rpm at 4°C for 5 min. Collected supernatant was reduced by boiling for 5 min at 95°C with 5x SDS laemmli buffer. The phosphorylated form of different kinases was detected by Western blotting and considered to be indicative of activation of respective signaling pathways.

Next, the signaling pathway activation was studied in murine primary T cells after anti-CD3 and anti-CD28 co-stimulation. Lymphocytes were isolated from LNs of WT and Asm-deficient mice. 24-well tissue culture plates were coated with 1 μg/ml of anti-CD3ε (clone: 145-2C11) for 2 h at 37°C. Plates were washed 2 times with PBS to remove unbound antibodies. $3x10^6$ cells in 250 μl of PBS containing anti-CD28 (1 μg/ml) and 25 μg/ml of rabbit anti-mouse IgG (Abcam, cat# ab6709) were added to each well and incubated at 37°C for 2, 5, 10 and 15 min or left inactivated. Activation of signaling cascades was studied as mentioned above.

Lastly, Jurkat cells were stimulated with OKT3 antibody (Orthoclone OKT3, Janssen-Cilag, Germany) and the activation of signaling pathways was tested. OKT3 is a mouse monoclonal antibody which recognizes the CD3-complex on mature human T cells

(Goldstein et al. 1987). Cells were harvested and washed two times with cold PBS and adjusted to ~0.5x10^6 cells/100 μl of PBS. Imipramine was used as ASM inhibitor. To evaluate the dose-dependent inhibitory effect of Imipramine, cells were incubated with different doses (5, 10 and 25 μM) of Imipramine for 30-40 min at 37°C or left untreated. OKT3 antibody was added to cells at a concentration of 1 μg/ml and incubated at 37°C according to desired durations of stimulation which were 1, 2, 5, 10, 20 and 30 min or left unstimulated. Preparation of cell lysate and detection of various phospho-kinases were done as described above.

3.3 Western blotting and pull-down assay

Western blotting was performed to detect the protein level of phosphorylated kinases after stimulation. Lysates were prepared as mentioned above. Proteins were separated by 7.5%, 10%, 12% and 15% (depending on the size of desired proteins) by SDS-PAGE and transferred to nitrocellulose membranes, followed by blocking with Starting Block (PBS) blocking buffer (Thermo Fisher Scientific) for 1 h at room temperature. Blots were incubated overnight at 4°C with anti-phospho-AKT (Ser473), anti-phospho-Erk1/2 (Thr202/Tyr204), anti-phospho-Lck(Tyr416), anti-phospho-Lck(Tyr505), anti-phospho-mTOR (Ser2448), anti-phospho-PLCγ1 (Tyr783) (clone: D6M9S), anti-phospho-ZAP70 (Tyr493), anti-phospho-AMPKα (Thr172) (clone: 40H9), anti-phospho-SAPK/JNK (Thr183/Tyr185) and anti-phospho-cJun (Ser63) antibodies. All antibodies were from Cell Signaling Technology and used at 1:1000 dilution in blocking buffer. Blots were washed and incubated with alkaline phosphatase (AP)-coupled secondary antibodies (Santa Cruz Biotechnology Inc.) at 1:20,000 dilution in TBST containing 10% blocking buffer for 1 h at room temperature. Membranes were developed using the CDP-STAR with Nitro-Block II enhancer (PerkinElmer, Boston, USA). For detection of β-actin, membranes were washed and blocked as before and incubated with HRP-conjugated mouse anti-β-actin antibody for 1 h at room temperature. Membranes were developed with Pierce ECL Western blotting substrate.

Expression of Ras-GTP was detected using the Ras Activation Assay Kit (Merck Millipore, cat# 17-218) according to the manufacturer's instructions. Briefly, stimulated

and unstimulated Jurkat cells were lysed with lysis buffer containing 125 mM HEPES, 750 mM NaCl, 5% IGEPAL CA-630, 50 mM $MgCl_2$, 5 mM EDTA, 10% glycerol, 10 μg/mL A/L and 1 mM sodium orthovanadate for 5 min on ice. Insoluble cell debris from the lysate was removed by centrifugation for 5 min at 14,000 rpm at 4°C. The supernatant was collected and aliquots were snap frozen in liquid nitrogen and kept at -80°C for later use. Two μl of the Ras Assay Reagent (Raf-1 RBD, agarose) containing agarose beads was added to 100 μl of cell extract. The Mixture was Incubated for 45 min at 4°C with gentle agitation. Agarose beads were pelleted by brief centrifugation (10 seconds, 14,000 rpm, 4°C) and washed 3 times with lysis buffer. Beads were re-suspended in 40 μl of 2x laemmli sample buffer and boiled for 5 min at 95°C. Proteins were detected by Western blotting using 0.5 μg/mL anti-Ras antibody (clone: Ras10) as primary antibody and AP-coupled anti-mouse secondary antibody (1:20,000; Santa Cruz Biotechnology Inc.). Membranes were developed as described above.

3.4 Intracellular Calcium measurement using flow cytometry

To detect $[Ca^{2+}]_i$ in Jurkat cells, cells were washed twice in PBS, adjusted to $1x10^6$ cells/ml and incubated with 5, 10 and 25 μM of Imipramine for 30-40 min at 37°C. Cells were pelleted by centrifugation at 300xg, for 5 min and re-suspended in pre-warmed complete RPMI 1640 medium containing 2.5 μM of Fluo-4 AM as a calcium indicator and 2.5 μM of Sulfinpyrazone as an organic anion-transport inhibitor. Cells were incubated for 45 min at 37°C with 300 rpm agitation. Cells were washed once, re-suspended in complete RPMI 1640 medium containing 2.5 μM of Sulfinpyrazone and incubated for another 45 min at 37°C. Afterwards, cells were analyzed on an Attune NxT (Thermo Fisher scientific) flow cytometer and acquired immediately after adding OKT3 antibody.

In case of murine primary lymphocytes, cells were isolated from LNs of WT and Asm-deficient mice and loaded with Fluo-4 AM calcium indicator as described above except cells were co-stained with Allophycocyanin (APC)-conjugated anti-CD4 antibody as well. Cells were stimulated with anti-CD3 (1 μg/ml) and anti-CD28 (1 μg/ml) and acquired by flow cytometer as mentioned above.

3.5 Cell activation and CFSE proliferation assay

To study the late events of T cell activation upon peptide25 stimulation, spleens from P25/Asm$^{+/+}$ and P25/Asm$^{-/-}$ mice were removed under sterile conditions and gently teased on 70 μM cell strainer (Sigma), to obtain a single cell suspension. Red blood cells (RBC) in the cell pellet were eliminated by incubating the cells with RBC lysis buffer (BioLegend) on ice for 5 min. Followed by washing twice with ice-cold PBS, cell-suspensions were adjusted to 1.5x10^6 cells/ml and incubated with 25 μM Imipramine in plain RPMI 1640 medium for 30 min at 37°C or left untreated. Afterwards, cells were washed once and re-suspended in 5 μM CFSE in PBS in the presence or absence of Imipramine. After incubation for 20 min at 37°C, cells were washed 2 times with serum-containing medium. CFSE loaded cells were activated with peptide25 (1 μg/ml) and anti-CD28 (1 μg/ml) and cultured in complete RPMI 1640 medium for 24, 48, 72 and 96 h depending on the experiments performed. β-mercaptoethanol was freshly added to the medium at a concentration of 0.05 mM. Cell division was analyzed by measuring CFSE intensity by flow cytometry.

3.6 Trypan blue cell viability assay

Spleen cells from P25/Asm$^{+/+}$ and P25/Asm$^{-/-}$ mice were stimulated with peptide25 plus anti-CD28 in the presence or absence of 25 μM Imipramine. In another experiment, cells from LNs and spleens of WT mice were activated with anti-CD3 and anti-CD28 antibodies in the presence or absence of Imipramine (1, 5, 10 and 25 μM). Following stimulation, cells were cultured in 96-well plates at a density of 1.5x10^6 cells/ml in a volume of 200 μl. Cell viability in the culture was measured by Trypan blue staining after 6, 12, 24, 48, 72 and 96 h for TCR Tg spleen cells or after 2, 4, 6, 12, 24 and 48 h for WT cells. For counting, 50 μl of cell suspension was collected by gentle pipetting to break down any clump to get single cell suspension and mixed with equal volume of 0.4% Trypan blue buffer. Cell mixture (10 μl) was counted using a hemocytometer under a light microscope. Dead cells are stained as dark blue and viable cells are colorless. For proliferation assay, only viable cells were counted. For Imipramine toxicity assay both dead and viable cells were counted.

3.7 Alamar blue proliferation assay

Alamar blue dye (Thermo Fisher Scientific) was developed to indirectly determine the mitogen-induced proliferation of lymphocytes by Ansar Ahmed and colleagues (Ahmed et al. 1994). Alamar blue dye contains an indicator that is oxidation-reduction sensitive. In *in vitro* culture, different metabolites are released from proliferating cells, which reduce the dye to induce a change in color from deep blue to shades of red. The intensity of change to the red color reflects the extent of proliferation (Zhi-Jun et al. 1997).

Spleen cells from P25/Asm$^{+/+}$ and P25/Asm$^{-/-}$ mice were stimulated with peptide25 plus anti-CD28 in the presence or absence of 25 μM Imipramine and cultured as described earlier. After 48 and 72 h of activation, 100 μl of cell suspensions were re-plated in 96-well sterile culture plates (Corning, NY). 10% (v/v) Alamar blue dye was added to cells and incubated for another 2 h at 37°C. As an indication of proliferation, changes in fluorescence intensity of Alamar blue were measured by Tecan Infinite M1000pro microplate reader with excitation at 530 nm and emission at 590 nm.

3.8 Flow cytometry

Flow cytometry was used to determine the expression of different cell-surface markers and the apoptotic cell death. Cells were harvested from the culture and adjusted to the concentration of 1x10^6 cells/100 μl in PBS. Cells were incubated for 30 min at 4°C with anti-mouse CD16/32 antibody to block Fcγ receptors followed by incubation with primary antibodies for 45 min at 4°C. After washing 2 times with PBS; cells were re-suspended in PBS and acquired with BD LSRFortessa™ flow cytometer (BD Biosciences). Following antibodies were used: anti-CD4-brilliant ultraviolet-737 (BUV737) (BD Biosciences), anti-CD25-Alexa Fluor 488 (AF488) (clone: PC61), anti-PD1-brilliant violet-605 (BV605) (clone: 29F.1A12), anti-CD44-phycoerythrin cyanine-7 (PECy7) (clone: IM7) (BD Biosciences), APC-conjugated Annexin V, Propidium iodide (PI); all antibodies were from BioLegend, except where stated otherwise. Data were analyzed using FlowJo software v10 (LLC, Ashland, Oregon).

3.9 Detection of cytokine production and secretion

To determine the frequency of IL-2 producing cells among CD4+ T cells, splenocytes from P25/Asm$^{+/+}$ and P25/Asm$^{-/-}$ mice were treated with Imipramine or left untreated. Afterwards, cells were activated with peptide25 and anti-CD28 for 6 h in the presence of Brefeldin-A (BioLegend) as an inhibitor of intracellular protein transport. Intracellular staining for IL-2 was performed using BD cytofix/cytoperm kit according to the manufacturer's protocol. Briefly, after harvesting, cells were washed and stained for the surface marker CD4 for 30 min at 4°C, followed by fixation with fixation/permeabilization solution for 20 min at 4°C. After washing 2 times with perm/wash buffer, cells were stained with anti-IL-2-PE antibody (BioLegend) (clone: JES6-5H4) for 45 min at 4°C in the same solution. Data were acquired with a BD LSRFortessa™ flow cytometer (BD Biosciences) and analyzed using FlowJo software v10.

Secretion of IL-2 and INFγ was determined by measuring their level in culture supernatant using enzyme-linked immunosorbent assay (ELISA) kits from BioLegend, according to the manufacturer's protocol.

3.10 Assay for ASM and AC activity

ASM activity was measured with BODIPY FL C12-SM (Thermo Fisher Scientific) as a substrate. Unstimulated cells were treated with Imipramine or left untreated and in a separate experiment, untreated cells were stimulated or left unstimulated; followed by lysis in 250 mM sodium acetate (pH 5.0), 1% Nonidet P-40 and 100 μM $ZnCl_2$ for 5 min on ice. Cells were further disrupted by sonication for 10 min in ice bath sonicator (Bandelin Electronic). The protein concentration was measured by Bradford protein assay (BioRad) and 4.5 μg of protein for murine primary lymphocytes and 20 μg of protein for Jurkat cells were diluted in 20 μl of lysis buffer. BODIPY FL C12-SM was diluted (1:2000) in the assay buffer containing 250 mM sodium acetate (pH 5.0) and 100 μM $ZnCl_2$ and sonicated for 10 min in a bath sonicator to obtain micelles. This dilution gives the concentration of 100 pmol SM/sample. The samples were incubated at 37°C for 1 h while shaking at 300 rpm. The reaction was stopped by adding 250 μl of freshly prepared chloroform: methanol (2:1, v/v) followed by centrifugation for 5 min at 14,000

rpm at 4°C. The lower phase (120 μl) was collected and dried in a SpeedVac Concentrator (Thermo Fisher Scientific) for 30-40 min. Pellets were re-suspended in 20 μl of chloroform: methanol (2:1, v/v). The samples were spotted on a thin-layer chromatography (TLC) plate (Merck, Germany) drop by drop at a volume of 3.5 μl each time. Transferred lipids were separated by running the plates in chloroform: methanol (80:20, v/v). After air-drying, plates were scanned with a Typhoon FLA 9500 laser scanner (GE Healthcare Life Sciences, USA) and analyzed with ImageQuant software (GE Healthcare Life Sciences, USA).

For AC activity assay, C12 NBD ceramide (Cayman Chemical) was used as a substrate. Cell lysates were prepared by incubating cells with 250 mM sodium acetate (pH 4.5), 1% Nonidet P-40 for 5 min on ice. After sonication and protein concentration measurement, 20 μg of protein was incubated with 100 pmol substrate for 4.5 h at 37°C. Lipid extraction and collection were done as described above. Dried lipids were re-dissolved in chloroform: methanol (2:1, v/v) and spotted onto TLC plate. The plate run was conducted with ethyl acetate: acetic acid (100:1, v/v) as the running buffer. The plates were imaged and quantified similarly as outlined above.

3.11 BCG infection experiments

In vivo infections were performed with green fluorescent protein-expressing BCG (GFP-BCG). To construct the GFP-BCG strain, BCG was transformed with the dual reporter plasmid pSMT3LxEGFP (Humphreys et al. 2006). Bacteria were cultured with continuous shaking at 120 rpm at 37°C in Erlenmeyer flasks with 10 ml Middlebrook 7H9 Broth with Glycerol (BD Biosciences, Heidelberg, Germany) supplemented with 50 μg/ml Hygromycin to maintain the GFP plasmid. Bacteria were used after 5 to 7 days of culture. After collection by centrifugation at 2000 rpm for 10 min, bacteria were re-suspended in H/S and vortexed continuously for 5 min. Bacteria were bath-sonicated for 5 min in the presence of ice and passed for 10-15 times through a 21G needle attached to a 10-ml syringe. Clumps of bacteria were removed by centrifugation for 2 min at 1000 rpm. The supernatant containing single cells of GFP-BCG was carefully collected. Single bacteria were further concentrated by centrifugation at 3200 rpm for 10 min and

re-suspended in PBS at the desired density. $1x10^7$ GFP-BCG in 200 μl PBS/mouse were injected Intravenously. After 3 days, the animals were sacrificed by cervical dislocation and spleens were removed for further processing.

3.12 Lipid measurements via mass spectrometry

Jurkat cells were stimulated with OKT3 antibody in the presence or absence of Imipramine. After the desired duration, stimulation was stopped by adding ice-cold PBS. Cells were pelleted by brief centrifugation and snap frozen in liquid nitrogen. After that, cells were re-suspended in cold methanol and sent to the University of Potsdam on dry ice. All the mass spectrometry analyses were performed by Dr. Fabian Schumacher, University of Potsdam. Cell pellets were further loosened by ultrasonication on ice for 15 min. Aliquots of the cell samples (20 μl) were subjected to lipid extraction using 1.5 mL of methanol: chloroform (2:1, v/v). The extraction solvent contained C17-ceramide, C16-d_{31}-SM, d_7-sphingosine, d_7-S1P as internal standards (all from Avanti Polar Lipids, Alabaster, USA). After lipid extraction, samples were saponified using 150 μl of 1 M methanolic potassium hydroxide for 2 h at 37°C with gentle shaking (120 rpm). Then, samples were neutralized with 12 μl glacial acetic acid and centrifuged at 200xg for 10 min at 4°C. Organic supernatants were evaporated to dryness through vacuum centrifugation using a Savant SpeedVac concentrator from Thermo Fisher Scientific (Dreieich, Germany). Dried residues were reconstituted in 200 μl of a 95:5 (v/v) mixture of acetonitrile: methanol (1:1, v/v) and water, both acidified with 0.1% formic acid, thoroughly vortexed for 10 min at 1500 rpm, centrifuged at 200xg for 10 min at 4°C and subjected to mass spectrometric sphingolipid quantification. Ceramide and SM were analyzed using a 1200 series HPLC coupled to a quadrupole time-of-flight 6530 mass spectrometer (Agilent Technologies, Waldbronn, Germany). Sphingosine and S1P measurements were conducted with a 1260 Infinity HPLC system coupled to a 6490 triple quadrupole mass spectrometer (Agilent Technologies). Both instruments were interfaced with an electrospray ion source operating in the positive ion mode (ESI+). Sphingosine, S1P, ceramide and SM were analyzed in MS/MS mode utilizing the fragmentation of the respective precursor ions into the product ion *m/z* 282.3 (for

sphingosine), *m/z* 264.3 (for S1P and all ceramide) or *m/z* 184.07 (for all SM). Quantification was performed using the MassHunter software (Agilent Technologies).

3.13 Immunohistochemistry

Following collection, spleens were embedded in Tissue-Tec (Sakura Finetek USA) and snap-frozen in the environment of liquid nitrogen. Sections of 6 μm thickness were cut with a cryotome (Leica CM1850 UV). Sections were kept in -80°C for later use. For staining, sections were thawed, air-dried and fixed in ice-cold Acetone for 10 min at room temperature. After washing once with PBS, tissues were blocked with 5% FCS/PBS for 15 min at room temperature. Staining was done with PE-conjugated anti-CD4, anti-CD8 and unconjugated anti-phospho-AKT (Ser473), anti-phospho-Erk1/2 (Thr202/Tyr204), anti-phospho-ZAP70 (Tyr493) and anti-phospho-JNK (Thr183/Tyr185) antibodies for 45 min at room temperature. All antibodies were diluted in 0.05% Tween-20 in H/S. After washing in PBS containing 0.05% Tween-20, tissues were incubated with Alexa Fluor 647-conjugated F(ab')2 fragments of donkey anti-rabbit IgG (Jackson ImmunoResearch) for 45 min at room temperature. After that, the samples were washed and mounted with Mowiol (Kuraray Specialties Europe GmbH, Germany). After air-drying for overnight in the dark, samples were visualized with a Leica TCS SP5 confocal microscope using 40x, 63x and 100x oil immersion lens and images were analyzed with Leica LCS software (Leica Microsystems).

3.14 Statistics

Data are expressed as arithmetic means ± standard deviation (SD) unless otherwise indicated. Two-way analysis of variance (ANOVA) followed Bonferroni posttest was used to test data with two variables (e.g., time and treatment), one-way ANOVA was used to measure a single variable (e.g., treatment) between multiple groups and pairwise comparisons were performed with unpaired t-test. Statistical significance was set at the level of $p < 0.05$. All data were obtained from independent measurements. The GraphPad Prism statistical software program (GraphPad Software, USA) was used for the analyses.

4 Results

4.1 Effects of Asm deficiency on peptide25-induced signal transduction

As discussed in the introduction, over the past years many studies have been conducted to identify the role of ASM/ceramide in T cell signal transduction. However, most of the findings are not conclusive enough. It is fair to say that the involvement of ASM is cell-type and stimulant specific. To add new insights to this topic, in this project peptide25-induced activation of signaling pathways in TCR Tg CD4+ T cells was studied.

Purified CD4+ T cells were stimulated with peptide25 pre-loaded APCs in the presence of anti-CD28 for 2, 5, 10 and 15 min or left unstimulated. Detection of different phospho-kinases by Western blotting showed that this antigenic stimulation leads to the activation of PLCγ1 (b), Erk1/2 (c) and AKT (e) in both P25/Asm$^{+/+}$ and P25/Asm$^{-/-}$ cells. In P25/Asm$^{+/+}$ cells, PLCγ1 and AKT activation happened quickly after 2 min, while Erk1/2 was activated only after 5 min of stimulation. On the other hand, P25/Asm$^{-/-}$ cells showed a trend of reduced phosphorylation of PLCγ1, AKT and Erk1/2, which was statistically significant at 2 min for PLCγ1. Unexpectedly, there was no significant increase of phosphorylation of ZAP70 (a) in P25/Asm$^{+/+}$ cells upon stimulation. In P25/Asm$^{-/-}$ cells, its phosphorylation was also unchanged before and after stimulation. In addition, there was no activation of PI3K (d) neither in P25/Asm$^{+/+}$ nor P25/Asm$^{-/-}$ cells.

To summarize, peptide25 and anti-CD28 co-stimulation causes activation of PLCγ1, AKT and Erk1/2 in both P25/Asm$^{+/+}$ and P25/Asm$^{-/-}$ CD4+ T cells. However, Asm deficiency diminishes the early (2 min) activation of PLCγ1 and AKT. Otherwise, Asm deficiency has little effect on other signaling pathways.

a) p-ZAP70

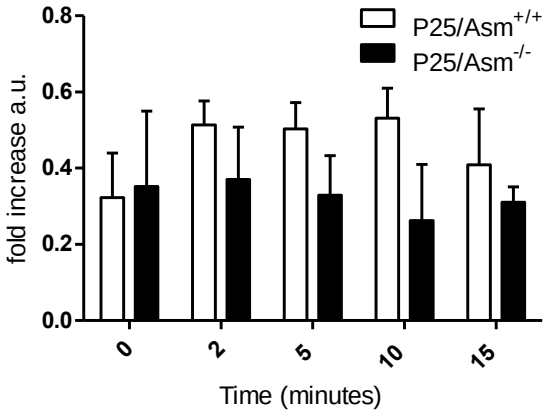

b) p-PLCg1

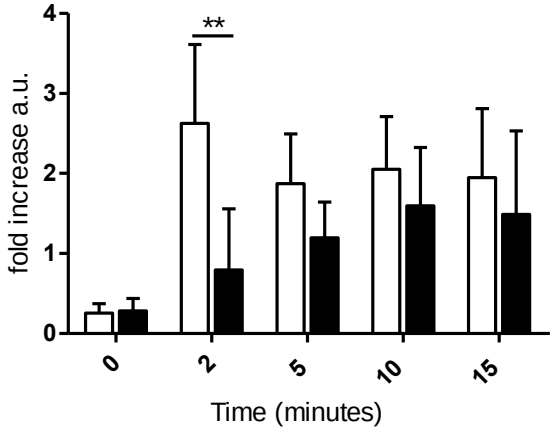

c) p-Erk1/2

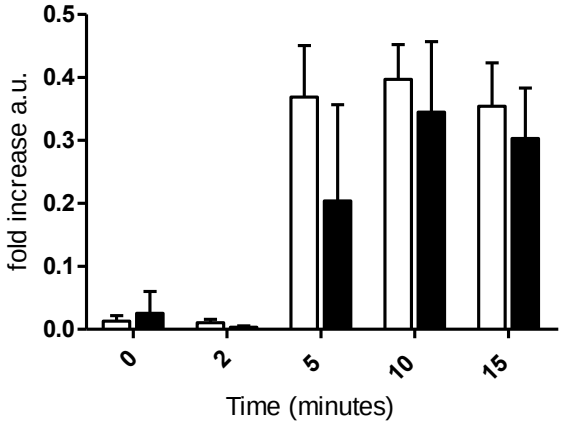

d) p-PI3K

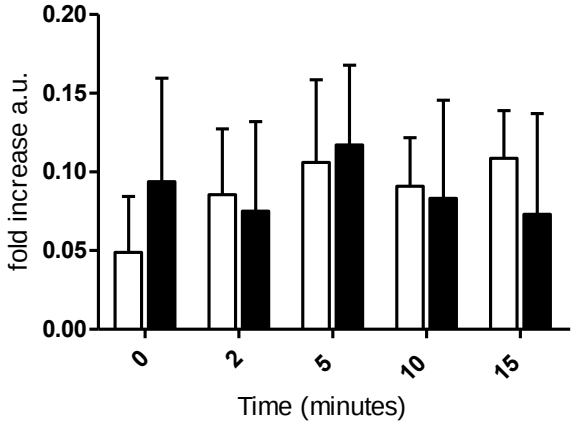

e) p-AKT

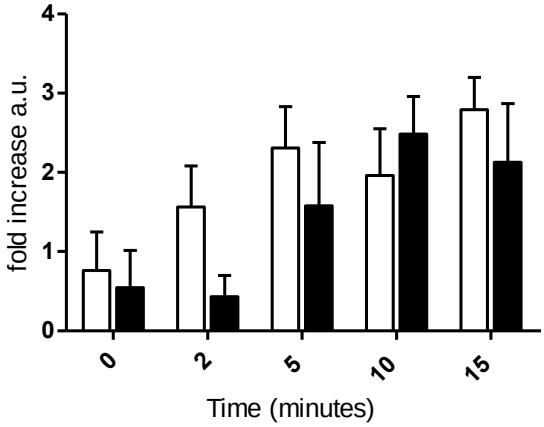

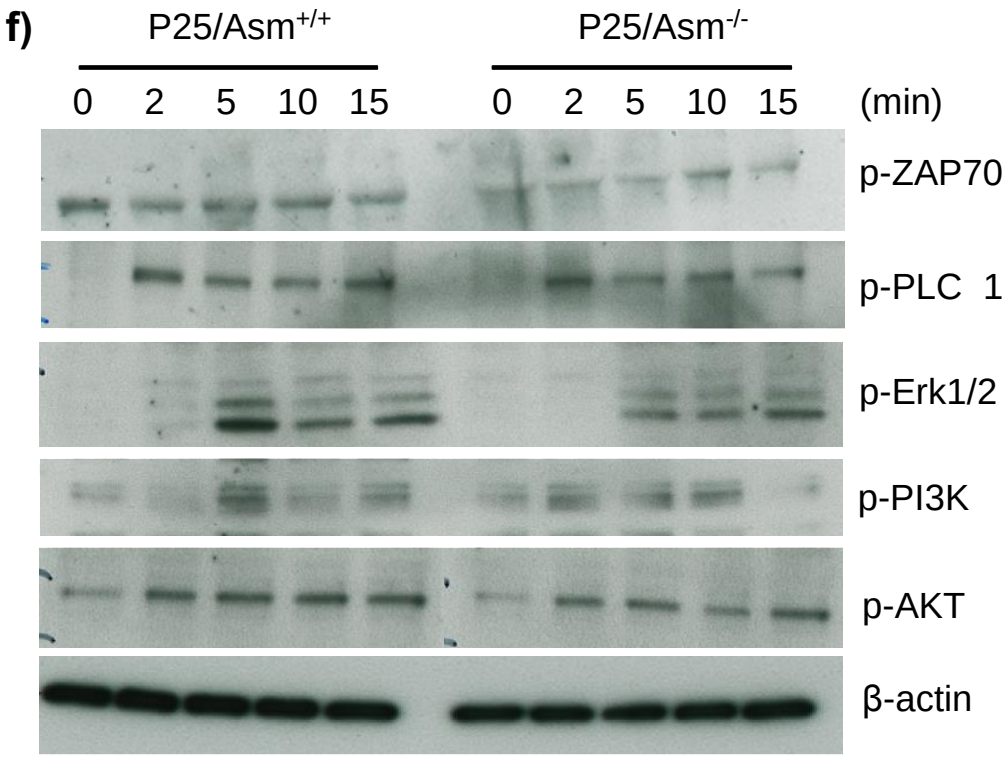

Figure 4.1: Role of Asm on peptide25-induced activation of naïve TCR Tg CD4+ T cell signaling cascades.

Tg CD4+ T cells were activated with peptide25-loaded APCs in the presence of soluble anti-CD28 for indicated time points and signaling pathway activation was determined using Western blotting with specific phospho-kinase antibodies (names mentioned as the title of the graphs). Densitometry signals were quantified by ImageStudioLite software. β-actin was used as loading control. Expression of proteins is represented as 'fold increase a.u.' (a-e). Scanned pictures of representative Western blot films are also shown (f). Data are representative of 3 independent experiments. Error bars represent mean ± SD. ** ($p<0.01$) as assessed by two-way ANOVA followed Bonferroni posttest.

4.2 Asm has a negligible role in physiological-stimulation of naïve T cells

Next, the effect of Asm deficiency in physiological anti-CD3/CD28-activated pathways was tested in murine primary lymphocytes isolated from LNs.

Freshly isolated lymphocytes from WT and Asm-deficient mice were activated with plate-bound anti-CD3 and soluble anti-CD28, cross-linked with mouse IgG for 2, 5, 10 and 15 min or left inactivated. Phosphorylation of several kinases of T cell signaling cascade was determined by Western blotting. Results showed that anti-CD3/CD28 co-stimulation leads to activation of ZAP70 (c), PLCγ1 (d), Erk1/2 (e) and AKT (h) in both WT and Asm-deficient cells soon after stimulation (2 min). However, there was no difference between these two groups regarding the phosphorylation level of tested kinases except for PLCγ1, where Asm-deficient cells showed reduced phosphorylation than WT control.

As discussed earlier, Src-family kinases such as Lck initiates signal transduction in T cells by phosphorylating ZAP70. Both the activation and inactivation of Lck depend on tyrosine phosphorylation but at separate sites. Phosphorylation at Tyr416 in the activation loop of the kinase domain upregulates enzyme activity (Hunter et al. 1987). On the other hand, phosphorylation of the carboxyl-terminal Tyr505 downregulates Lck activity (Chow et al. 1993). In the present study, the phosphorylation of both active (Tyr416) and inactive (Tyr505) form of Lck was determined. Level of basal p-Lck(Tyr416) in the unstimulated sample (0 min) was significantly lower in Asm-deficient cells compared to WT control (a). Upon stimulation, the phosphorylation of Lck(Tyr416) went further down in WT cells, which directly contradicts the increased phosphorylation of its substrate ZAP70 (c). However, no change of p-Lck(Tyr416) upon stimulation could be detected in Asm-deficient cells. Unexpectedly, the inactive p-Lck(Tyr505) level was slightly increased in WT cells following stimulation (b). Similar to the p-Lck(Tyr416), the p-Lck(Tyr505) level was unchanged in Asm-deficient cells before and after stimulation. This is hard to explain why stimulation led to Lck inactivation in WT cells. Despite this, no changes of both p-Lck(Tyr416) and p-Lck(Tyr505) in Asm-deficient cells indicate that Asm might be involved in the regulation of the balance between these two forms of Lck in murine lymphocytes. PI3K was activated only in WT cells but not in Asm-deficient

cells (g). After 15 min of stimulation, the level of p-PI3K was significantly lower in Asm-deficient cells than WT control. There was no elevated phosphorylation of AMPKα (f) and mTOR (i) upon stimulation. Moreover, the p-AMPKα level went further down after stimulation for both cell types.

These results led to the conclusion that anti-CD3/CD28 co-stimulation causes activation of ZAP70, PLCγ1, AKT and Erk1/2 in both WT and Asm-deficient cells. Reduced phosphorylation of PLCγ1 in Asm-deficient cells and activation of PI3K only in WT cells indicate that Asm is needed for the regulation of these kinases.

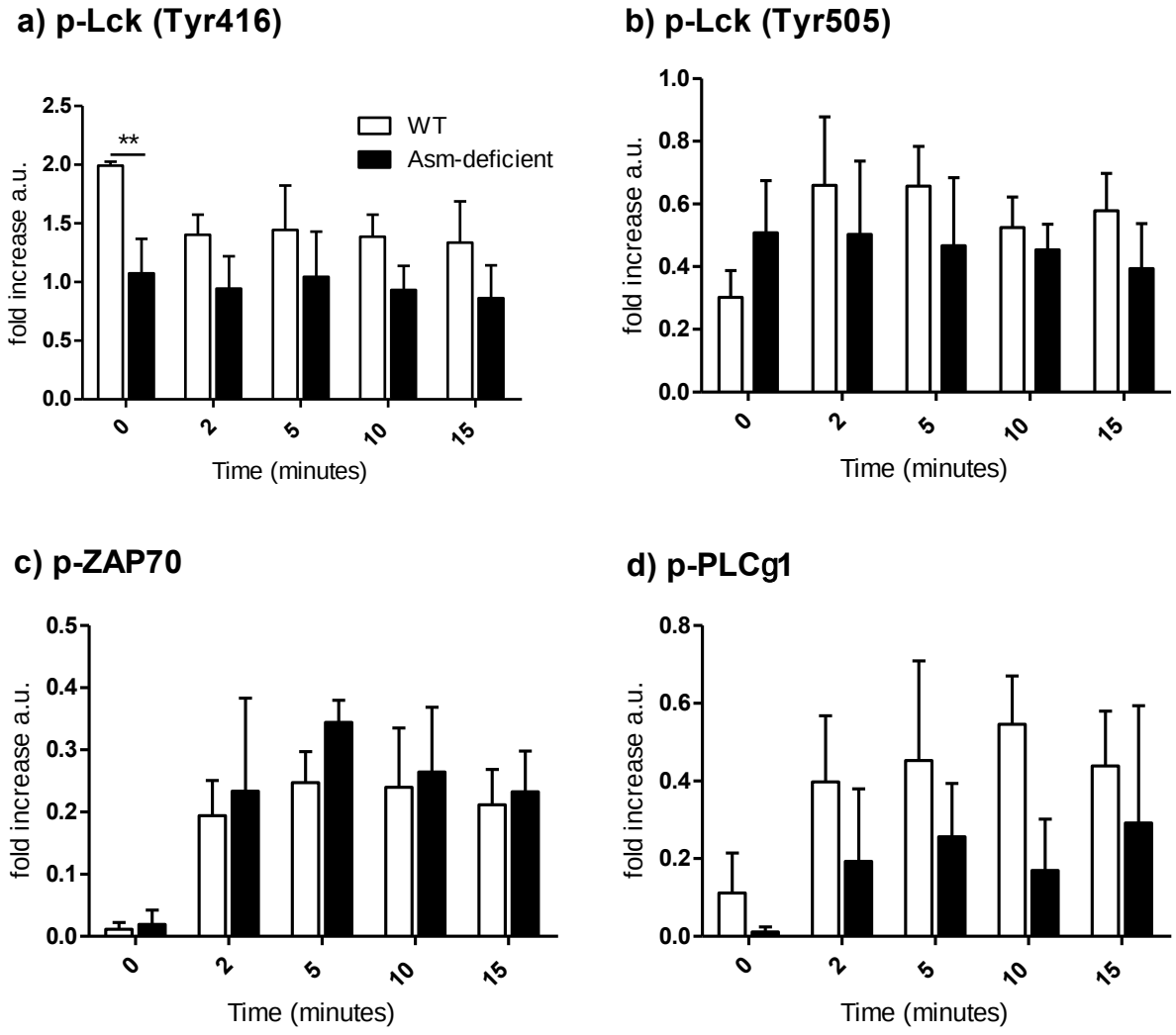

e) p-Erk1/2

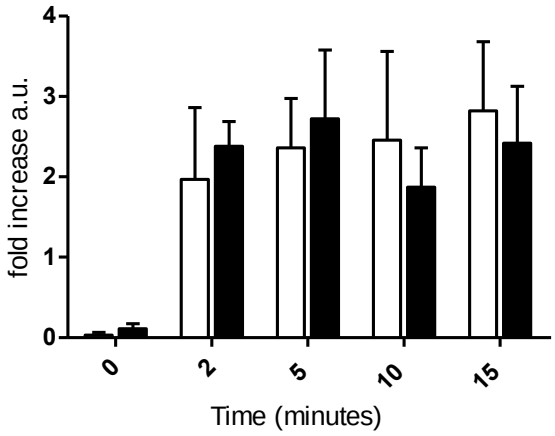

f) p-AMPKa

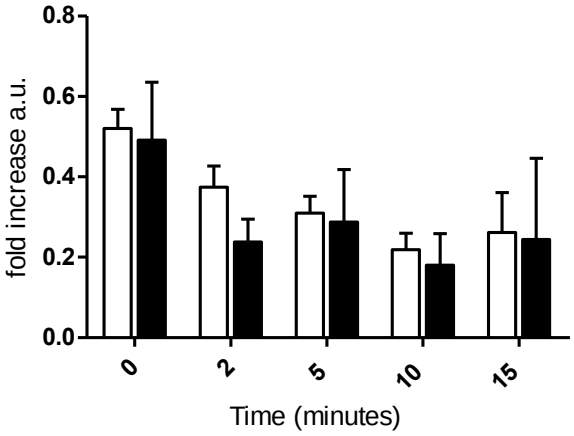

g) p-PI3K

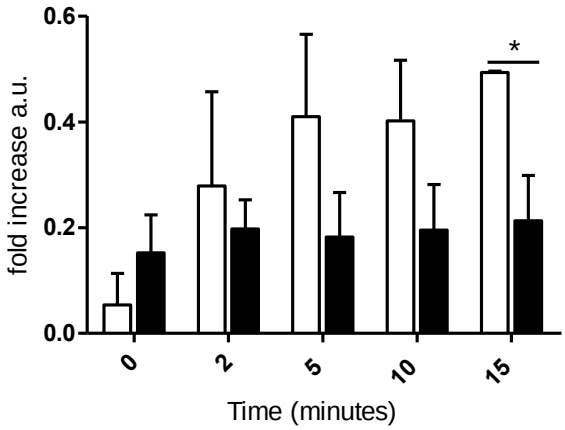

h) p-AKT

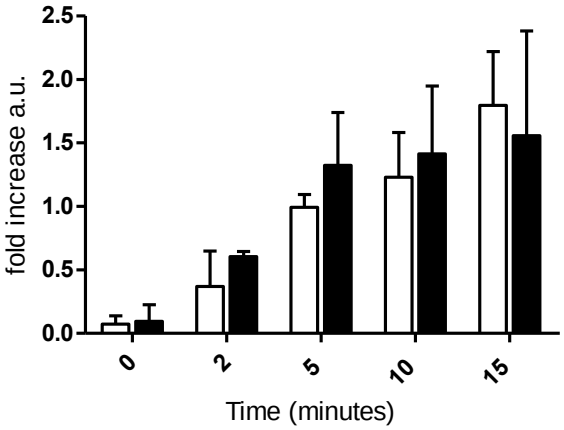

i) p-mTOR

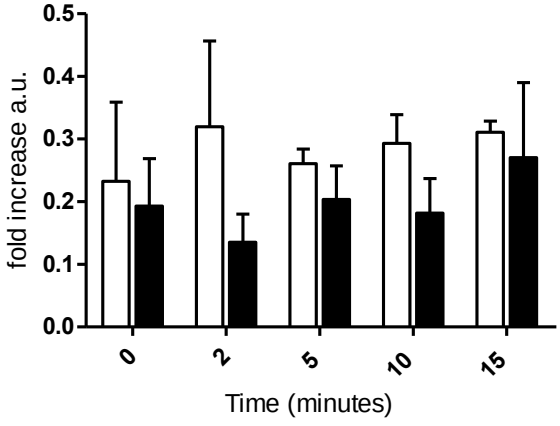

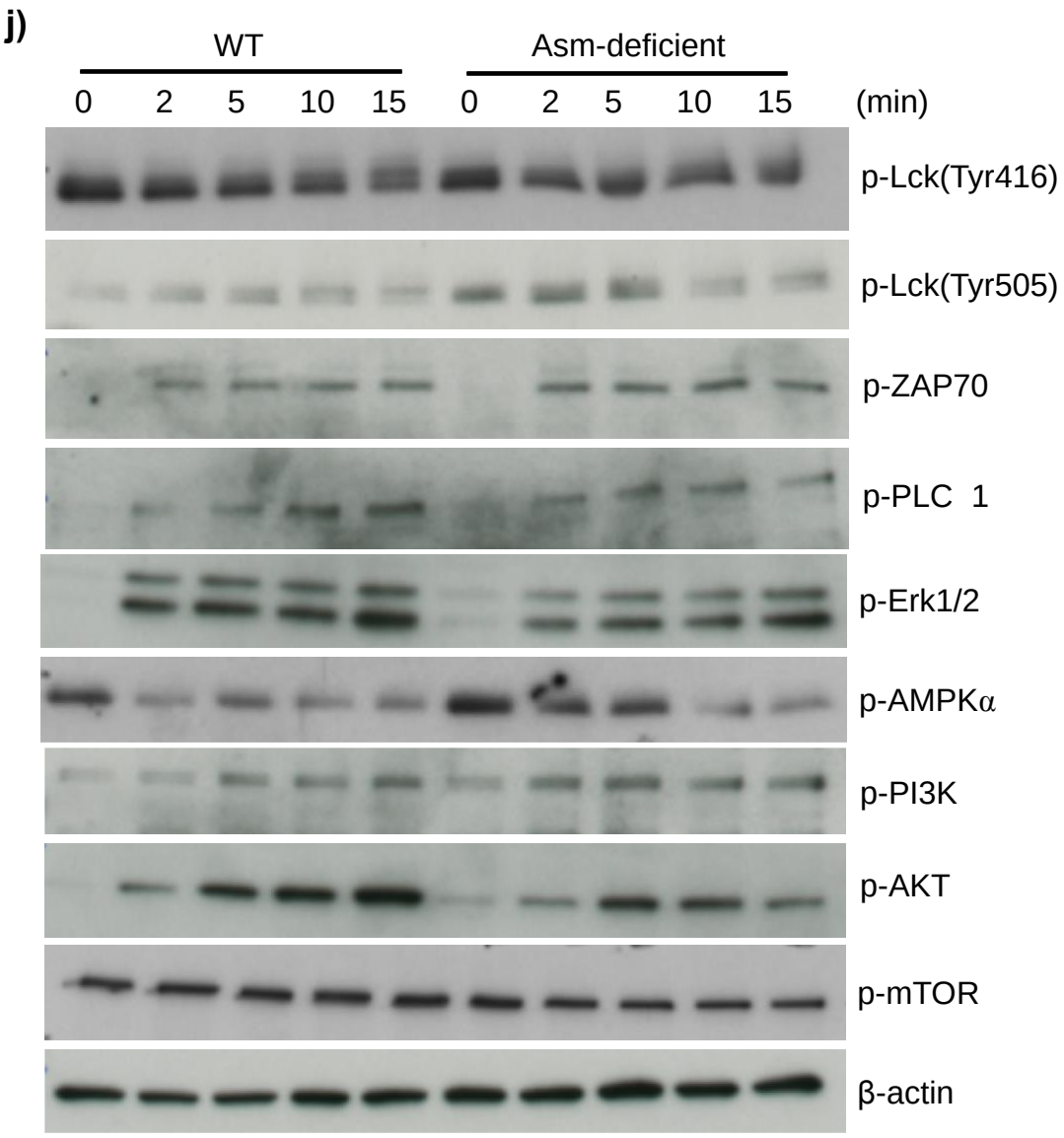

Figure 4.2: The negligible role of Asm in physiologically activated naïve CD4+ T cells. Lymphocytes isolated from LNs of WT and Asm-deficient mice were activated with plate-bound anti-CD3 and soluble anti-CD28, cross-linked with anti-mouse IgG for indicated durations and activation of signaling pathways was determined using Western blotting. Tested kinases are mentioned as the title of the bar graphs. Densitometry signals were quantified by ImageStudioLite software. β-actin was used as loading control. Expression of proteins is represented as 'fold increase a.u.' (a-i). Scanned pictures of representative Western blot films are also shown (j). Data are representative of 3 independent experiments. Error bars represent mean ± SD. * ($p<0.05$), ** ($p<0.01$) as assessed by two-way ANOVA followed Bonferroni posttest.

4.3 Imipramine has inhibitory effects on signaling pathways of Jurkat cells

Imipramine was used as a functional inhibitor of ASM and its effect on the activation of Jurkat cells was tested. Imipramine treated and untreated cells were stimulated with OKT3 antibody for 1, 2, 5, 10, 20 and 30 min or left unstimulated. Results showed that activation of ZAP70 (c), Ras (i), Erk1/2 (j) and JNK (k) happened quickly after stimulation (1 min). Phosphorylation of ZAP70 was reduced by Imipramine in a dose-dependent manner. 5 μM Imipramine did not affect the phosphorylation, but higher dosage (10 and 25 μM) caused considerable reduction.

There are 3 different kinds of mammalian Ras: N-, H- and K-Ras. Ras activation was determined by pull-down assay followed by Western blotting with mouse anti-Ras antibody which can detect all the 3 forms of Ras. There was an upregulation of the active form of Ras (GTP bound) at 1 min, which went down quickly after 2 min of stimulation. Imipramine strongly diminished Ras activation at 1 and 2 min, although there was no dose dependency of the effect.

Erk1/2 was strongly activated at 1 min after stimulation, then started to decline after 10 min. The phosphorylation of Erk1/2 was significantly abrogated by Imipramine during almost the whole period of the experiment (1 to 20 min). All doses of Imipramine (5, 10 and 25 μM) showed comparable inhibition. Activation of JNK was also reduced by Imipramine treatment, although any dose-dependent effect could not be detected. Despite the fact that there was activation of JNK after stimulation, there was no phosphorylation of its substrate cJun (l). Imipramine showed no effect as well.

No increase in the phosphorylation of Lck(Tyr416) was noticed after stimulation in untreated control cells (a). However, Imipramine treatment reduced the basal (0 min) phosphorylation of Lck(Tyr416) in a dose-dependent manner, which was significant at the dose of 25 μM. A similar reduction was observed for basal p-Lck (Tyr 505) level as well (b). Moreover, stimulation caused de-phosphorylation of inactive p-Lck (Tyr 505), which was further facilitated by Imipramine.

There was no activation of PI3K/ AKT/ mTOR pathways after OKT3 stimulation. Imipramine significantly inhibited the phosphorylation of PI3K (e) at 1, 2, 5 and 10 min. Similarly, mTOR (g) phosphorylation was reduced after 1, 2 and 20 min of stimulation. The effect of different concentrations of Imipramine was very variable and it was difficult to draw any conclusion.

Phosphorylation of AKT (f) was significantly inhibited at 2 min by Imipramine at a concentration of 10μM. No activation of PLCγ1 (d) could be detected upon stimulation. Moreover, after 5 min, the phosphorylation of PLCγ1 was even lower than unstimulated control, probably due to de-phosphorylation by phosphatases. Imipramine significantly reduced the phosphorylation in both unstimulated controls and stimulated samples.

AMPKα works as an energy sensor for T lymphocytes and its increased phosphorylation indicates energy stress and depletion of adenosine triphosphate (ATP) (Tamás et al. 2006). Present data showed reduced phosphorylation of AMPKα (h) upon stimulation. Imipramine at 5 and 25 μM concentration, further reduced the phosphorylation at 5, 20 and 30 min, although, this was not statistically significant. Exceptionally, 5 μM Imipramine significantly reduced the level of p-AMPKα at 10 min. However, 10 μM Imipramine was found to induce phosphorylation of AMPKα from 2 to 30 min of stimulation.

Present data suggest that OKT3 stimulation of Jurkat cells leads to the activation of ZAP70, Erk1/2, Ras and JNK pathways. Short term pre-incubation with Imipramine inhibits the phosphorylation of Lck(Tyr505), ZAP70, PLCγ1, Erk1/2, PI3K and JNK; and reduces the expression of active Ras as well.

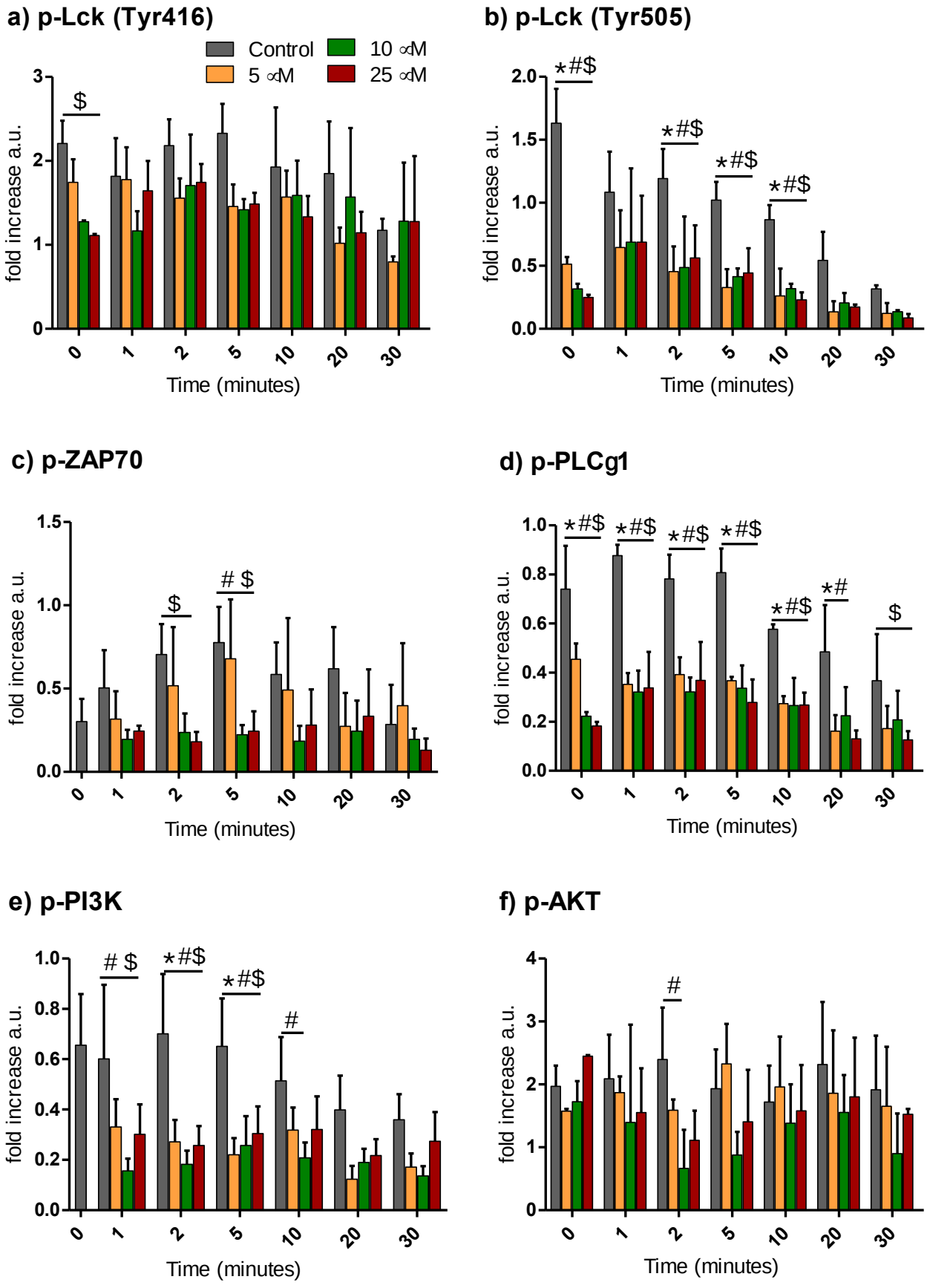
a) p-Lck (Tyr416)
Control
5 ∝M
10 ∝M
25 ∝M
fold increase a.u.
Time (minutes)
b) p-Lck (Tyr505)
c) p-ZAP70
d) p-PLCg1
e) p-PI3K
f) p-AKT

g) p-mTOR

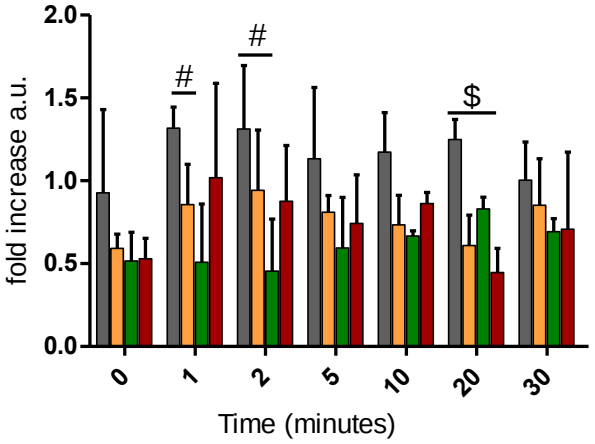

h) p-AMPKa

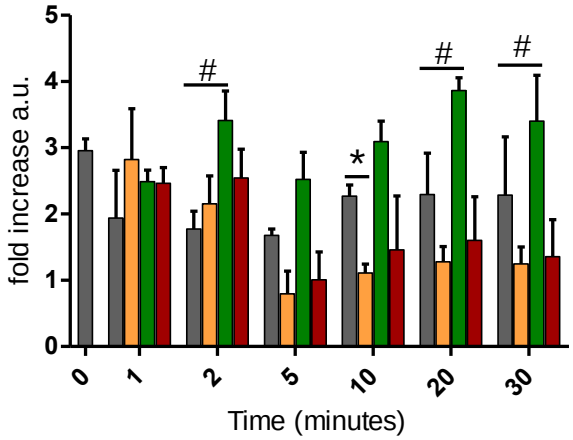

i) Ras-GTP

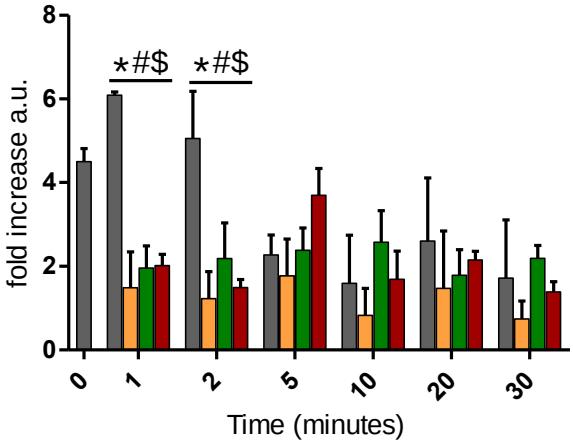

j) p-Erk1/2

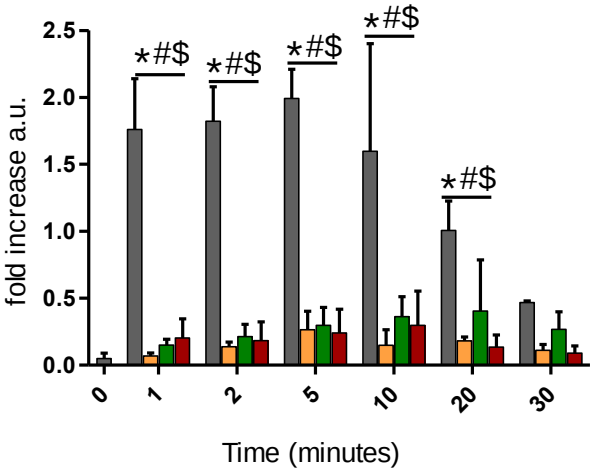

k) p-JNK

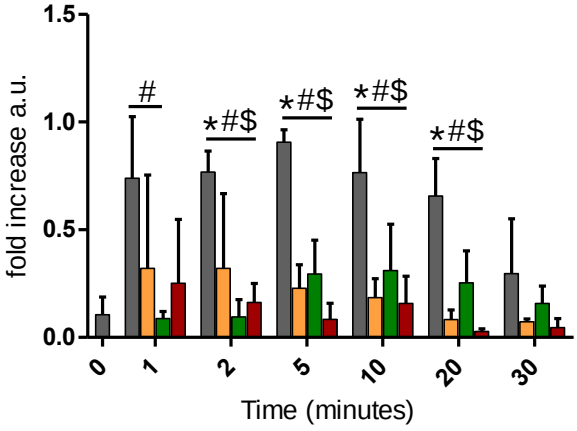

l) p-cJun

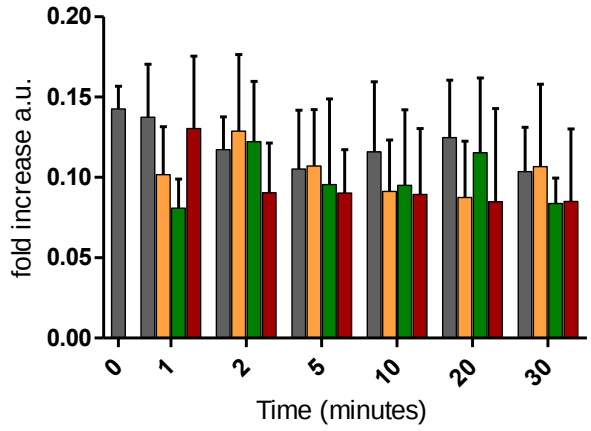

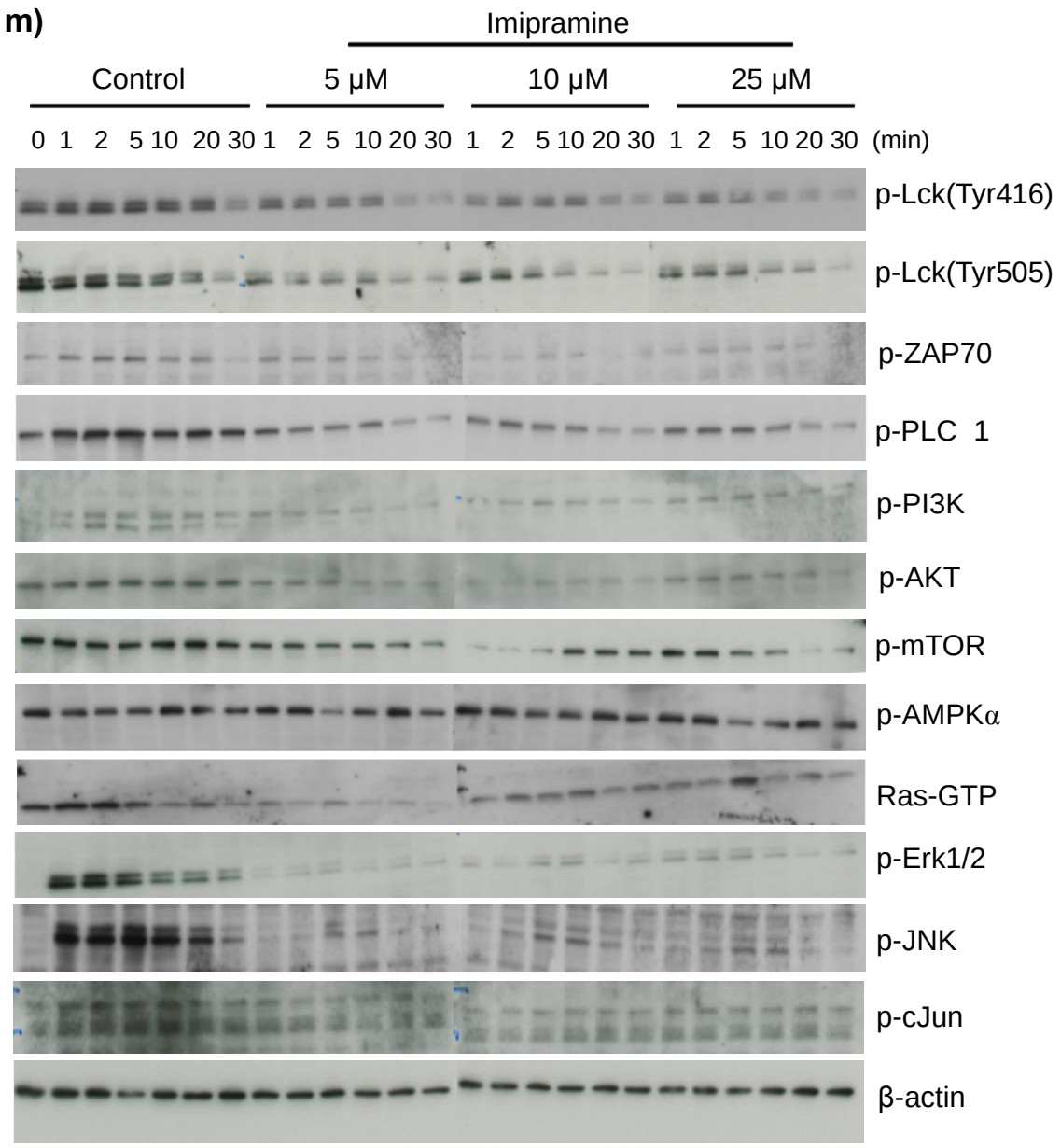

Figure 4.3: Imipramine inhibits several signaling pathways of Jurkat cells.
Cells were pre-treated with Imipramine (5, 10 and 25 μM) or left untreated prior stimulation with OKT3 antibody for indicated durations. 0 min represents untreated unstimulated control. Phosphorylated kinases were detected by immunoblotting using specific antibodies (mentioned as graph-title). Ras activation was measured by affinity-based pull-down assay. Densitometry signals were quantified by ImageStudioLite software. β-actin was used as loading control. Expression of proteins is represented as 'fold increase a.u.' (a-l). Scanned pictures of representative Western blot films are also shown (m). Error bars represent mean ± SD. * ($p < 0.05$, control vs. 5 μM Imipramine), # ($p < 0.05$, control vs. 10 μM Imipramine), $ ($p < 0.05$, control vs 25 μM Imipramine) as assessed by two-way ANOVA followed Bonferroni posttest. Data represent 3 independent experiments.

4.4 Imipramine and Asm deficiency have different effects on activation-induced calcium influx in T cells

Increase in the $[Ca^{2+}]_i$ level following TCR activation is one of the earliest and important events. Upon activation of T cells, there is the production of IP_3 which releases calcium from the ER. This rise in the $[Ca^{2+}]_i$ opens the CRAC channels at the PM and leads to calcium influx and a further increase in the $[Ca^{2+}]_i$ level.

To measure the calcium response in T lymphocytes, cell-permeant calcium indicator dye Fluo-4 AM was used, which can be detected in BL1 channel in Attune NxT flow cytometer. Fluorescence intensity of Fluo-4 depends on the $[Ca^{2+}]_i$. Cells were loaded with the indicator according to manufacturer's instruction. Data were acquired in a dot plot by setting the time in X-axis and BL1 in Y-axis. Events were collected continuously for 300 seconds. The analysis was done with FlowJo software by using the ''kinetics'' tool. Data are shown as histograms where the X-axis represents time and Y-axis represents the mean fluorescence intensity (MFI) of Fluo-4 (a, b).

To determine the role of Asm in anti-CD3/CD28 co-stimulation-induced calcium response, primary lymphocytes were collected from LNs of WT and Asm-deficient mice. Following loading with Fluo-4, cells were also co-stained for the CD4 surface marker to distinguish them in the whole population. After adding anti-CD3, anti-CD28 and anti-mouse IgG to the cells, $[Ca^{2+}]_i$ started to rise very quickly and stayed high till the end of acquisition (300 seconds). The changes in the $[Ca^{2+}]_i$ upon activation was compared between WT and Asm-deficient cells (a). There was no difference between these two groups regarding the calcium response after anti-CD3/CD28 co-stimulation.

Similarly, the effect of Imipramine pre-treatment in OKT3-induced calcium response in Jurkat cells was tested (b). Imipramine was used at 5, 10 and 25 μM concentration. Control (without Imipramine) and test samples (treated with Imipramine), all showed a basal calcium level of ~4.5K (a.u. produced by FlowJo software). After addition of OKT3, $[Ca^{2+}]_i$ started to go up. Control cells showed a single sharp peak at ~100 seconds, then went downhill. Test samples showed multiple peaks at ~50 seconds; then

the intensity started to go down after ~100 seconds. Although Imipramine treated cells showed reduced $[Ca^{2+}]_i$ after stimulation, there was no difference between different doses of Imipramine.

The data led to the assumption that Asm is not necessary for anti-CD3/CD28 co-stimulation-induced calcium response in murine primary CD4+ T cells and Imipramine inhibits the OKT3-induced calcium rise in Jurkat cells.

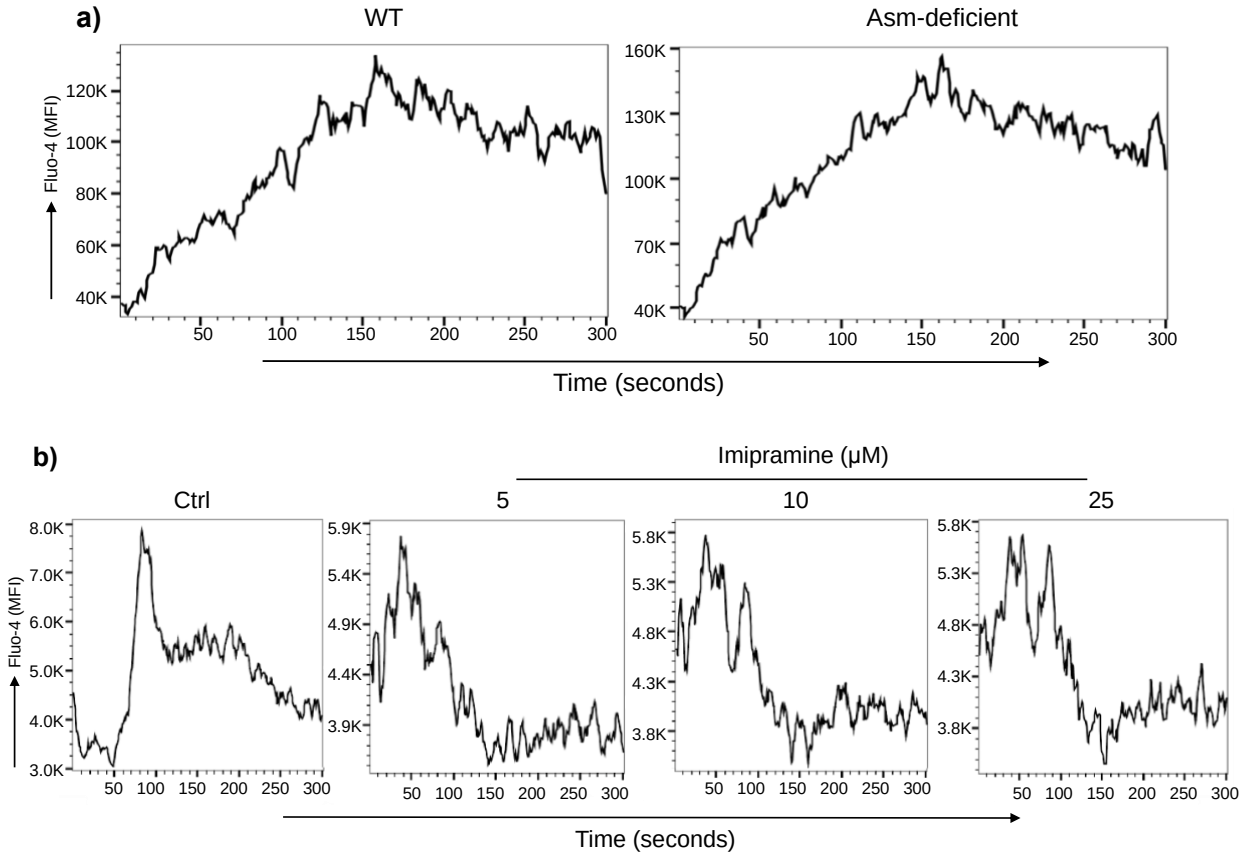

Figure 4.4: Imipramine and Asm deficiency have different effects on activation induced-calcium influx in T cells.

Fluo-4 loaded T cells from WT and Asm-deficient mice were stimulated with anti-CD3 and anti-CD28 (a). Jurkat cells were incubated with 5, 10 and 25 µM Imipramine and stimulated with OKT3 antibody (b). Following the addition of respective stimulus, cells were immediately acquired by flow cytometer. Changes in $[Ca^{2+}]_i$ level was measured as changes in the MFI of Fluo-4 by Attune NxT flow cytometer and analyzed with FlowJo software. Data are representative of 3 independent experiments. “Ctrl” indicates Imipramine untreated control.

4.5 Imipramine inhibits peptide25-induced activation of Tg CD4+ T cells

In the experiments described above, the effects of Asm deficiency in peptide25-induced activation of the signaling cascade in TCR Tg CD4+ T cells have been tested. Next, the studies were extended by investigating the effect of Asm inhibition by Imipramine on late events of T cell activation such as proliferation, surface markers expression, cytokine production and secretion.

Cell proliferation was tested by Alamar blue and CFSE dye dilution methods. Freshly isolated splenocytes from P25/Asm$^{+/+}$ mice were pre-treated with Imipramine (25 μM) or left untreated. Cells were activated with peptide25 and anti-CD28 and cultured for 24, 48, 72 and 96 h depending on the individual experiments. To determine the cell division pattern, cells were loaded with CFSE prior activation and cultured for 48 and 96 h, followed by determination of CFSE intensity by flow cytometer. In this method, the intensity of CFSE is reduced by half in each cell division. After 48 and 96 h of activation, the number of cell divisions in the untreated control group were 2-3 and 6-7, respectively. At both time points, Imipramine treated cells showed impaired cell division (a). For Alamar blue assay, at 48 and 72 h, aliquots of cells were collected, re-plated in fresh 96-well plates and Alamar blue dye was added at 10% concentration or left untreated. After incubation for 2 h at 37°C, changes in the fluorescence intensity was measured with a plate reader. In this assay, fluorescence Intensity is proportional to viable, metabolically active cell number in the culture. Results showed that Imipramine significantly reduced the number of viable, active cells after 48 and 72 h of activation compared to untreated control (b).

Activation of CD4+ T cells is followed by expression of different cell surface markers. Each surface marker has its distinct expression pattern and significance for cell differentiation, proliferation, effector function and survival. In this project, the expression of three regulatory molecules, i.e., CD25, CD44 as positive regulators and PD1 as a negative regulator was checked. Considering the expression kinetics, CD25 (c) and CD44 (d) expression was measured after 48 h within the CD4+ population. As discussed earlier that PD1 negatively regulates T cell activation, the frequency of PD1

was checked in all CD4+ T cells (e) and also specifically in activated CD4+ T cells (CD4+CD44+) (f) after 24, 48 and 72 h of activation.

Results showed that expression of both CD25 and CD44 was significantly reduced with Imipramine treatment. Upon activation, PD1 expression in CD4+ cells started to rise after 24 h, reached a peak level at 48 h and slightly reduced afterwards in control cells. On the other hand, Imipramine treated cells showed a continuous rise in PD1 expression until 72 h (e). A similar pattern was found in the case of PD1 expression among the CD4+CD44+ double positive population (f). However, expression of PD1 was significantly reduced by Imipramine over the duration of the experiment.

Secretion of IL-2 (g) and INFγ (h) was determined by checking their level in the culture supernatant after 24 h and 48 h of activation, respectively. Results showed that peptide25 and anti-CD28 stimulation leads to IL-2 secretion in P25/Asm$^{+/+}$ cells, which is significantly diminished by Imipramine. Comparable inhibition was found for INFγ secretion as well. Previously, it has been documented that Asm deficiency leads to intracellular accumulation of IL-2 in murine splenocytes after stimulation with Concanavalin-A (Stoffel et al. 1998). Therefore, in the present study, the percentage of IL-2 producing cells (IL-2+) in CD4+ T cells was checked by intracellular staining for flow cytometry, after 6 h of activation (i). Moreover, the effect of Imipramine in this aspect was also investigated. Data showed the frequency of IL-2+ cells among CD4+ T cells was significantly reduced by Imipramine.

The present findings led to the conclusion that Imipramine inhibits peptide25 and anti-CD28-induced proliferation, surface molecules expression, cytokine secretion and production in P25/Asm$^{+/+}$ CD4+ T cells.

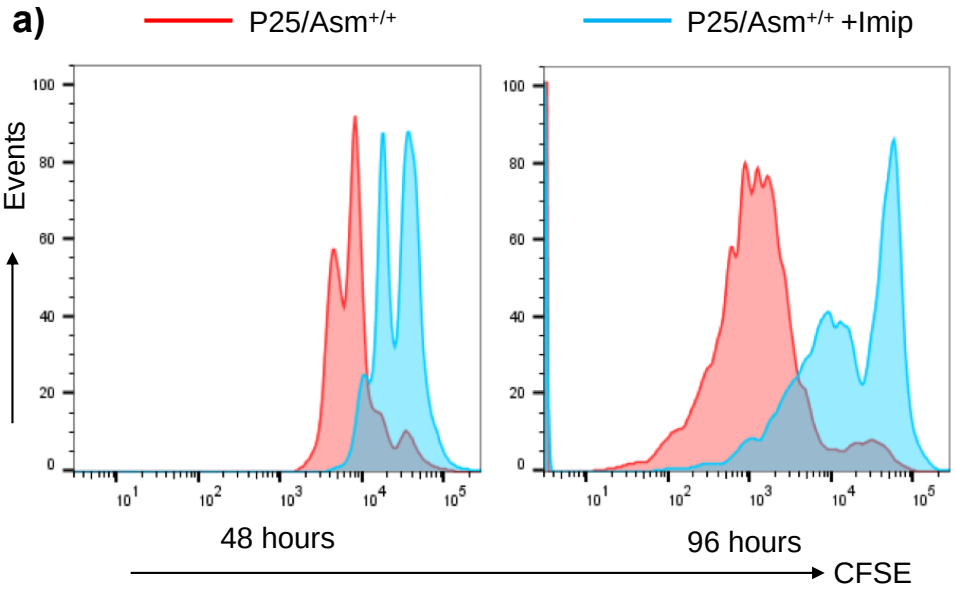
a)
P25/Asm+/+
P25/Asm+/+ +Imip
Events
48 hours
96 hours
CFSE

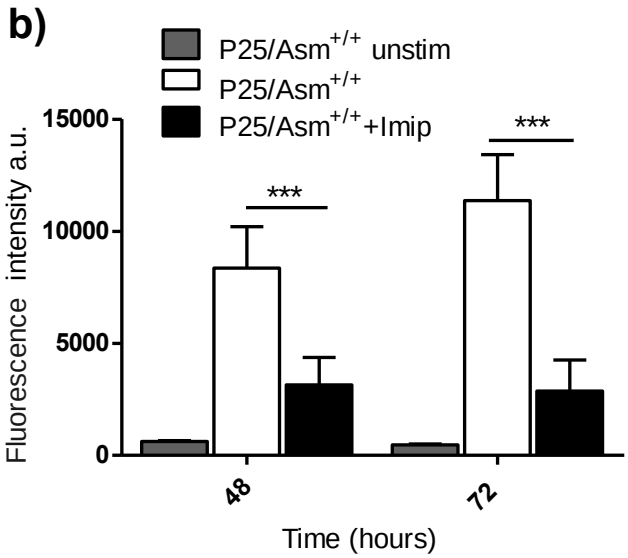
b)
P25/Asm+/+ unstim
P25/Asm+/+
P25/Asm+/+ +Imip
Fluorescence intensity a.u.
15000
10000
5000
0
***
***
48
72
Time (hours)

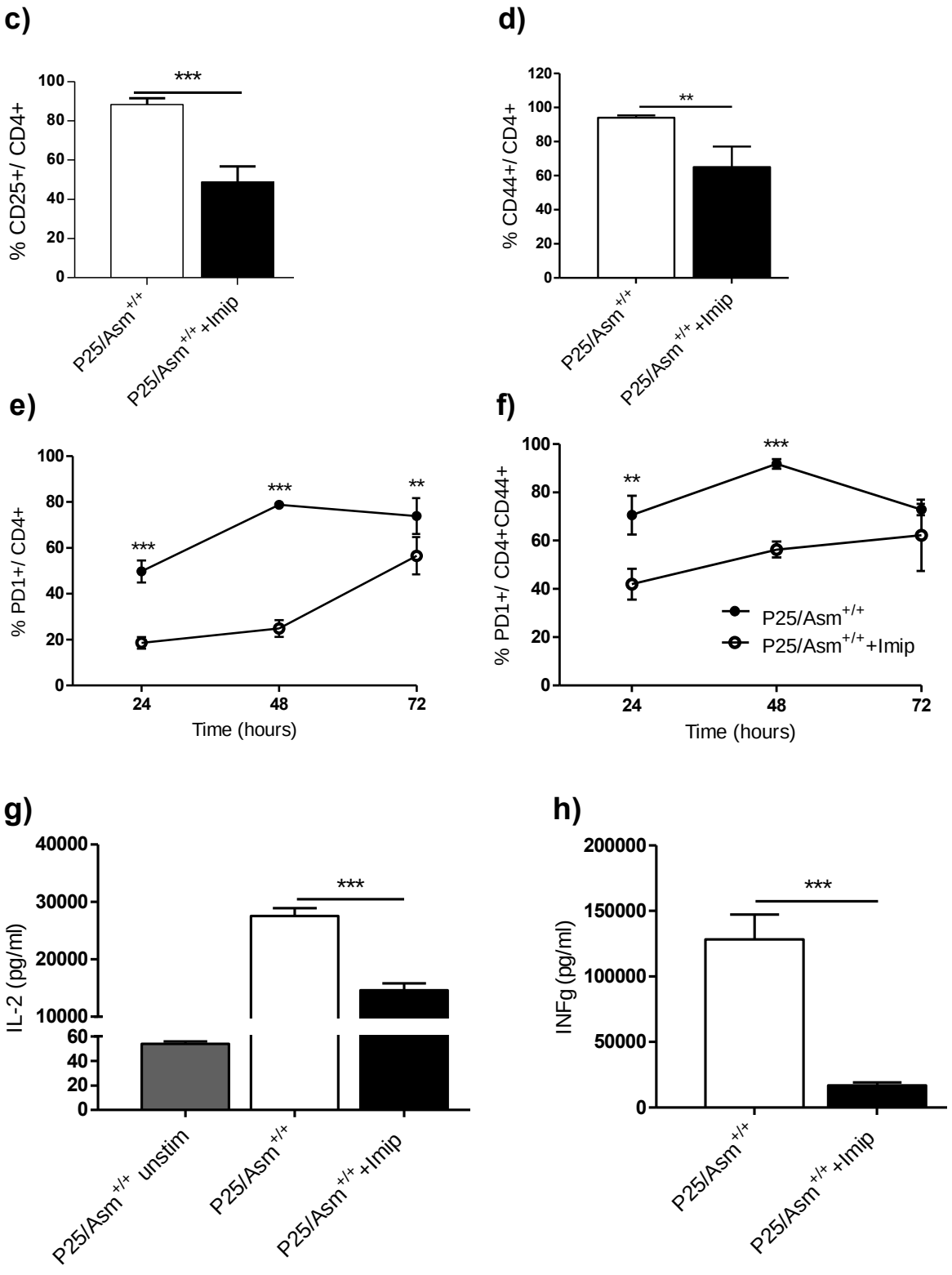
c)
% CD25+/ CD4+
***
P25/Asm+/+
P25/Asm+/+ +Imip
d)
% CD44+/ CD4+
**
P25/Asm+/+
P25/Asm+/+ +Imip
e)
% PD1+/ CD4+
***
***
**
Time (hours)
f)
% PD1+/ CD4+CD44+
**
***
P25/Asm+/+
P25/Asm+/+ +Imip
Time (hours)
g)
IL-2 (pg/ml)
***
P25/Asm+/+ unstim
P25/Asm+/+
P25/Asm+/+ +Imip
h)
INFg (pg/ml)
***
P25/Asm+/+
P25/Asm+/+ +Imip

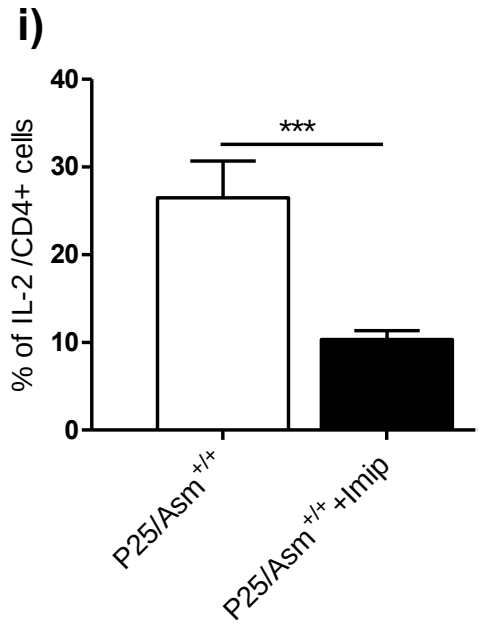

Figure 4.5: Imipramine inhibits peptide25-induced activation of Tg naïve CD4+ T cells.
Freshly isolated, RBC lysed spleen cells from P25/Asm$^{+/+}$ mice were pre-incubated with Imipramine (25 μM) or left untreated. Cells were activated with peptide25 and anti-CD28 or left inactivated. Cell division pattern was determined by measuring the intensity of CFSE in CD4+ T cells using flow cytometry after 48 and 96 h of activation (a). The proliferation of cells was also assessed by Alamar blue-based assay at 48 and 72 h (b). Frequency of CD25+ (c) and CD44+ (d) and PD1+ (e) cells in CD4+ cells was measured by flow cytometry at indicated time points. The frequency of PD1+ in CD4+CD44+ double positive cells was determined as well (f). By ELISA, secretion of IL-2 (g) and INFγ (h) was measured after 24 and 48 h of activation, respectively. The frequency of IL-2+ cells in CD4+ population was determined by flow cytometry (i). Error bars represent mean ± SD. ** ($p < 0.01$), *** ($p < 0.001$) as assessed by two-way ANOVA followed Bonferroni posttest (e, f) or unpaired t-test (b-d, g-i). Data represent 3 independent experiments. “Unstim’’ and “Imip” indicate unstimulated control and Imipramine, respectively.

4.6 Asm is partially necessary for peptide25-induced naïve T cell activation

After the experiments with Imipramine in P25/Asm$^{+/+}$ cells, similar experiments were done with P25/Asm$^{-/-}$ cells to answer the question whether negative effects produced by Imipramine are due to Asm inhibition or not.

Splenocytes from P25/Asm$^{+/+}$ and P25/Asm$^{-/-}$ mice were activated with peptide25 and anti-CD28 and cultured for different durations. Cell division kinetic was determined by CFSE dye dilution method after 48 and 96 h (a). After 48 h of activation, P25/Asm$^{-/-}$ cells showed delayed division compared to P25/Asm$^{+/+}$ cells. However, after 96 h both groups showed comparable cell divisions. Cell proliferation was also measured with Alamar blue assay after 48 and 72 h (b). At 48 h, P25/Asm$^{-/-}$ cells showed reduced cell number in culture although the difference was not statistically significant. However, after 72 h, P25/Asm$^{+/+}$ and P25/Asm$^{-/-}$ cells showed similar cell number. These data indicate that Asm is necessary only during the early stage of proliferation.

Expression of surface markers, i.e., CD25 (c), CD44 (d) in CD4+; and PD1 in CD4+ (e) and also in CD4+CD44+ double positive cells (f) was determined by flow cytometry after 48 and 72 h. P25/Asm$^{-/-}$ cells showed a significantly lower percentage of CD25+/CD4+ cells than P25/Asm$^{+/+}$ control at 48 h. AT 72 h, this difference was disappeared. Otherwise, P25/Asm$^{+/+}$ and P25/Asm$^{-/-}$ cells showed similar expression of CD44 and PD1. PD1 is known to constrict immune response and induce tolerance in peptide-activated CD4+ T cells (Konkel et al. 2010). To get a better insight into the effect of PD1 on cell proliferation/cell cycle and the role of Asm in this process; PD1 expression was also checked only among the dividing CD4+ cells (CFSE low) (g). Results showed no difference between P25/Asm$^{+/+}$ and P25/Asm$^{-/-}$ cells.

IL-2 (h) and INFγ (i) secretion were measured in culture supernatant at 24 and 48 h, respectively. P25/Asm$^{-/-}$ cells showed significantly lower secretion of both cytokines. The frequency of IL-2+ cells was determined by flow cytometry after 6 h of activation (j). The percentage of IL-2+/CD4+ cells was lower in P25/Asm$^{-/-}$ cells compared to P25/Asm$^{+/+}$ but the difference did not reach statistical significance.

The results led to the hypothesis that Asm is necessary for peptide25-induced proliferation and cytokine secretion/production in TCR Tg CD4+ T cells only during the early (till 48 h) stage of activation. Considering the late proliferative stage and the expression of surface molecules, Asm has no effect.

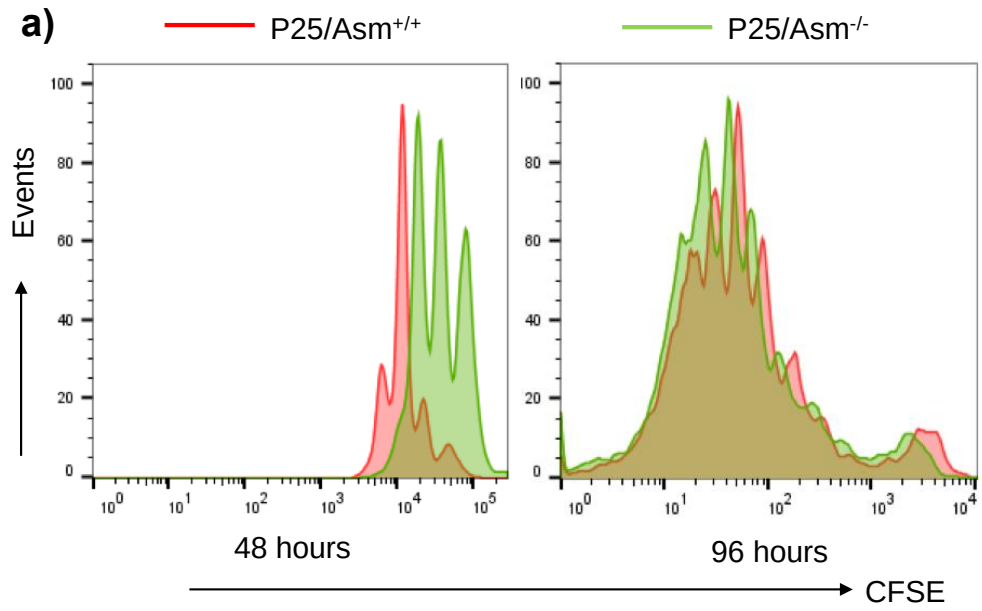

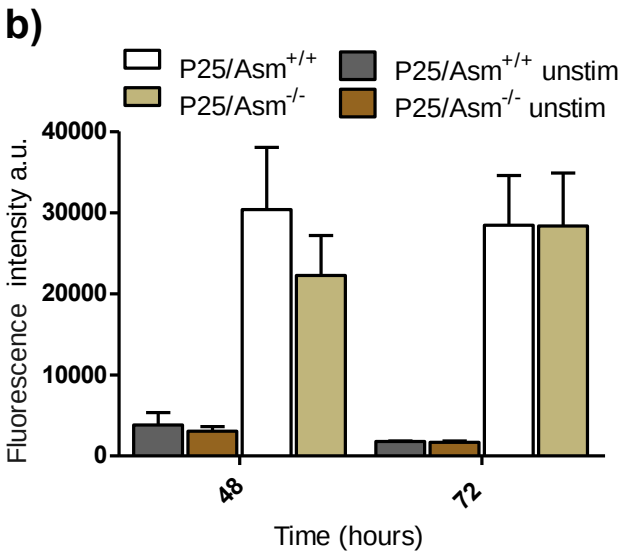

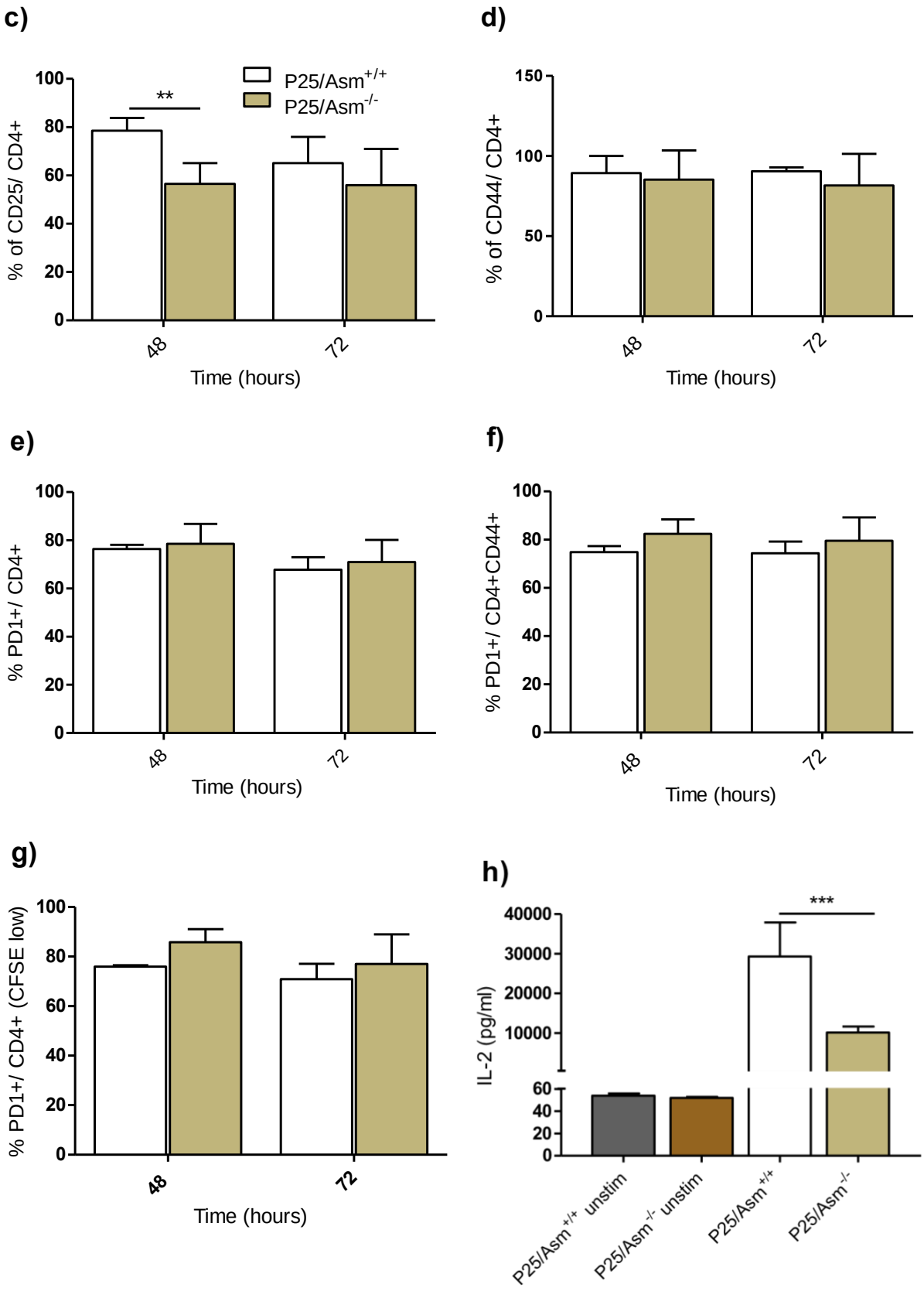
c)
P25/Asm+/+
P25/Asm-/-
**
% of CD25/ CD4+
Time (hours)
d)
% of CD44/ CD4+
Time (hours)
e)
% PD1+/ CD4+
Time (hours)
f)
% PD1+/ CD4+CD44+
Time (hours)
g)
% PD1+/ CD4+ (CFSE low)
Time (hours)
h)
***
IL-2 (pg/ml)
P25/Asm+/+ unstim
P25/Asm-/- unstim
P25/Asm+/+
P25/Asm-/-

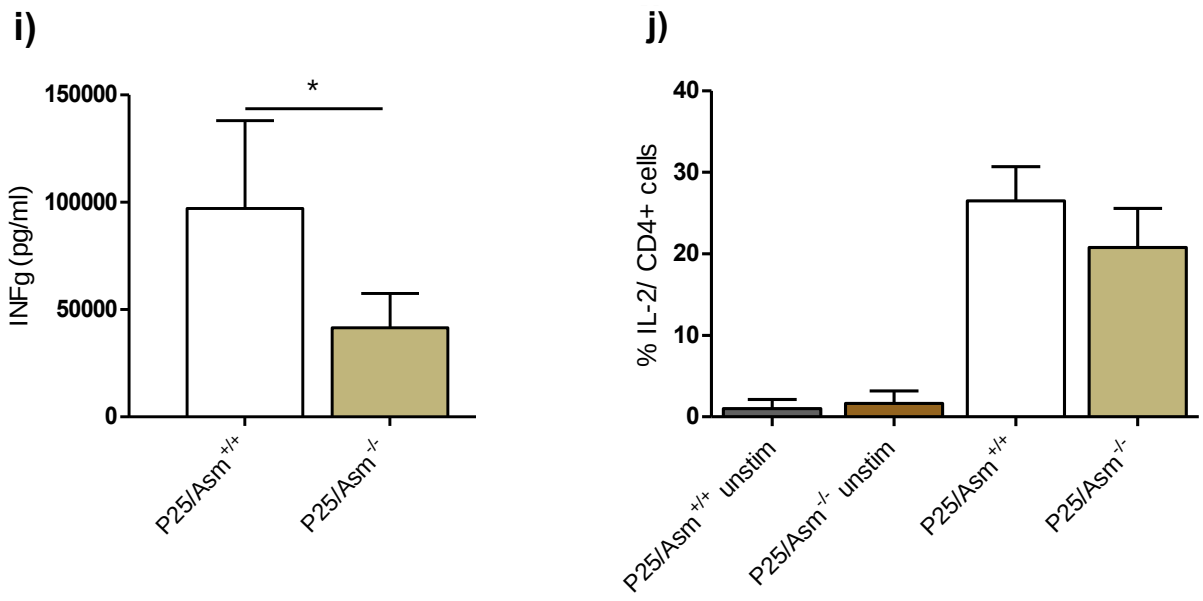

Figure 4.6: Asm is partially necessary for peptide25-induced naïve T cell activation.
Freshly isolated, RBC lysed spleen cells from P25/Asm$^{+/+}$ and P25/Asm$^{-/-}$ mice were activated with peptide25 and anti-CD28 or left inactivated. Cells were loaded with CFSE prior activation. The intensity of CFSE was measured using flow cytometry after 48 and 96 h (a). Proliferation was also assessed by the Alamar blue-based assay after 48 and 72 h (b). Frequency of CD25+ (c), CD44+ (d) and PD1+ (e) cells in CD4+ cells was measured by flow cytometry after 48 and 72 h. Similarly, the frequency of PD1+ cells in CD4+CD44+ double positive cells (f) was also determined. To evaluated if PD1+CD4+ cells belong to the dividing or non-dividing CD4+ population, frequency of PD1+ was measured in only CFSE low CD4+ cells (g). By ELISA, secretion of IL-2 (h) and INFγ (i) was measured after 24 and 48 h of activation, respectively. Frequency of IL-2+ cells in CD4+ cells were determined by flow cytometry (j). Error bars represent mean $\pm$ SD. * ($p< 0.05$), ** ($p< 0.01$) and *** ($p< 0.001$) as assessed by two-way ANOVA followed Bonferroni posttest (c) and unpaired t-test (h, i). Data represent 3-5 independent experiments. ‘’Unstim’’ indicates unstimulated control.

4.7 The negative effect of Imipramine on cell viability is not due to toxicity

Upon ligation of TCR to its specific peptide-MHC II ligand, CD4+ T cells differentiate into effector cells and undergo proliferation. After performing their effector functions, the majority of T cells dies by apoptosis. Moreover, if the activation is not successful, primary naïve T cells also undergo rapid apoptosis in culture. In several studies, it has been indicated that ASM is necessary for complete activation of murine and human T cells.

In this project, the question was asked: what is the effect of Asm inhibition on the viability of naïve CD4+ T cells upon peptide25-induced activation? To answer this question, Imipramine treated (25 μM) or untreated splenocytes from P25/Asm$^{+/+}$ mice were activated with peptide25 plus anti-CD28 and cultured for different duration. The number of viable cells in the culture was counted after 6, 12, 24, 48, 72 and 96 h using Trypan blue dye exclusion method (a). It is important to keep in mind that, the TCR Tg mice model used in this project, expresses peptide25 specific TCR only in CD4+ T cells (Tamura et al. 2004). Therefore, stimulation with peptide25 activates only CD4+ cell population.

Results showed that viable cell number was reduced till 36 h after stimulation for both Imipramine treated and untreated cells, most probably cells other than CD4+ T cells died due to the lack of survival signals for them. At later time points, the viable cell count was increased and reached a peak level at 48 h. This upregulation of viable cell number in the culture indirectly represents the activation-induced proliferation of CD4+ T cells, although cells showed a delayed proliferative response. In the present study, the reason for this delay could be that no extracellular IL-2 was added to the culture, which is known to exhilarate T cell proliferation (Kendall et al. 1988). Cells which were activated by peptide25 produced IL-2 and sent signals for further proliferation. This whole process could lengthen the entire proliferation event. Such a delay in the proliferation of murine splenocytes is also supported by previous research (Chan and Ochi et al. 1995). In the present data, both control and Imipramine treated cells showed a similar trend in the changes of viable cell count over time. However, Imipramine significantly reduced the number of viable cells in comparison to control. To determine whether the cell death is

due to apoptosis or not, cells were stained for CD4, Annexin V and PI at 24, 48 and 72 h post-activation. After acquiring data by flow cytometry, results showed that Imipramine treated CD4+ T cells express a significantly higher level of Annexin V than control cells after 48 and 72 h of activation (b). Nevertheless, at 24 h, the rate of apoptotic cells was similar between these two groups. Considering the frequency of total dead cells (PI+), Imipramine treated cells showed a slightly higher rate at 48 h, although at 24 and 72 h it was much the same as control (c).

To understand if the higher rate of apoptotic cell death by Imipramine is due to Asm inhibition or not, P25/Asm$^{-/-}$ cells were also incubated with Imipramine and compared the results to Imipramine treated P25/Asm$^{+/+}$ cells. Data showed that Imipramine significantly increased the frequency of apoptotic cells in both P25/Asm$^{+/+}$ and P25/Asm$^{-/-}$ CD4+ T cell population after 48 and 72 h of activation (d). Regarding the percentage of the total dead cells, it was slightly higher in Imipramine treated groups at 48 h but did not reach statistical significance (e).

Next question was asked: If this higher death rate with Imipramine treatment is due to toxicity or not? To test that, cells from spleens and LNs of WT mice were cultured for different durations till 48 h with or without Imipramine. Imipramine was used at 1, 5, 10 and 25 μM concentration. Cells were further divided into two groups by stimulating with anti-CD3/CD28 or left unstimulated. Aliquots of cells were collected after 2, 4, 6, 12, 24, 48 h and both viable and dead cells were counted using Trypan blue. At least 200 cells were counted per sample and percentage of dead cells was calculated. Data revealed that Imipramine treated and untreated samples showed very comparable frequency of dead cells (f-i). This data indicates that Imipramine is not directly toxic to murine primary T cells.

The conclusion was drawn that Imipramine impairs the peptide25 plus anti-CD28-induced activation of both P25/Asm$^{+/+}$ and P25/Asm$^{-/-}$ CD4+ T cells, which is followed by the apoptotic death of not activated cells. This impaired activation is probably the reason for the higher apoptotic death rate noticed in Imipramine treated cells but not direct toxicity induced by Imipramine.

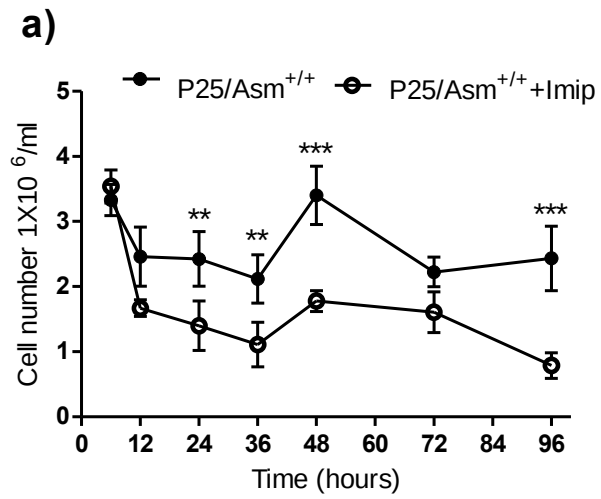
a)
P25/Asm+/+
P25/Asm+/+ +Imip
Cell number 1X10 6/ml
Time (hours)
**
**
***
***

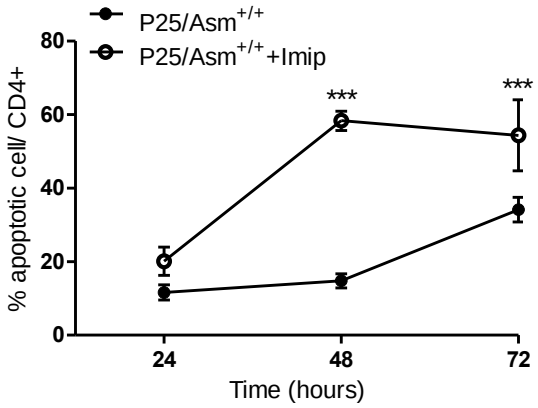
b)
P25/Asm+/+
P25/Asm+/+ +Imip
% apoptotic cell/ CD4+
Time (hours)
***
***

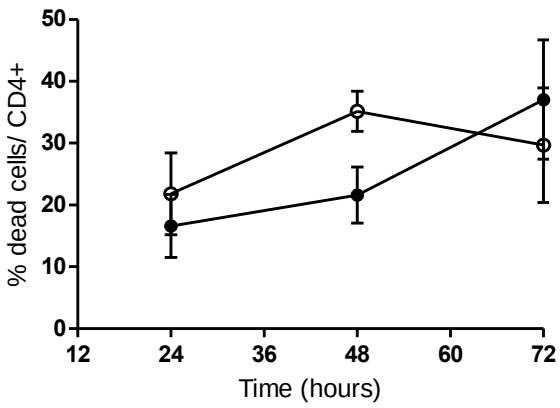
c)
% dead cells/ CD4+
Time (hours)

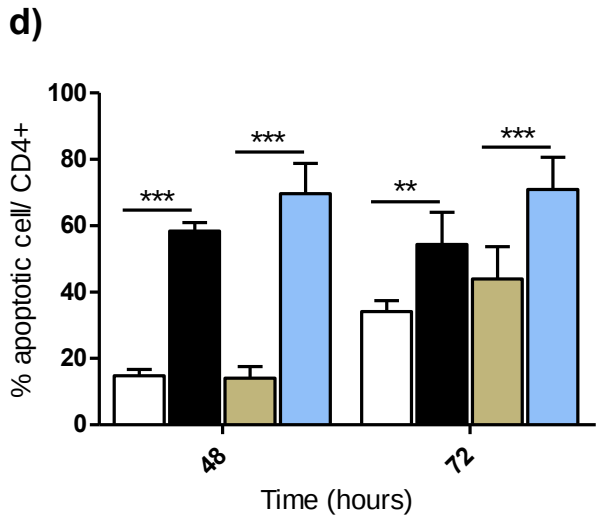
d)
% apoptotic cell/ CD4+
Time (hours)
***
***
**
***

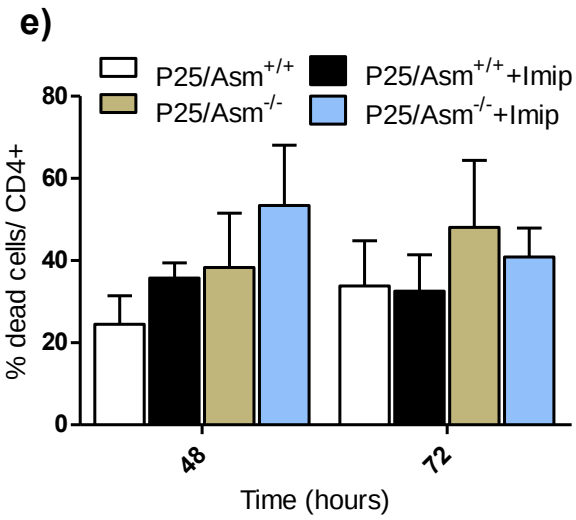
e)
P25/Asm+/+
P25/Asm+/+ +Imip
P25/Asm-/-
P25/Asm-/- +Imip
% dead cells/ CD4+
Time (hours)

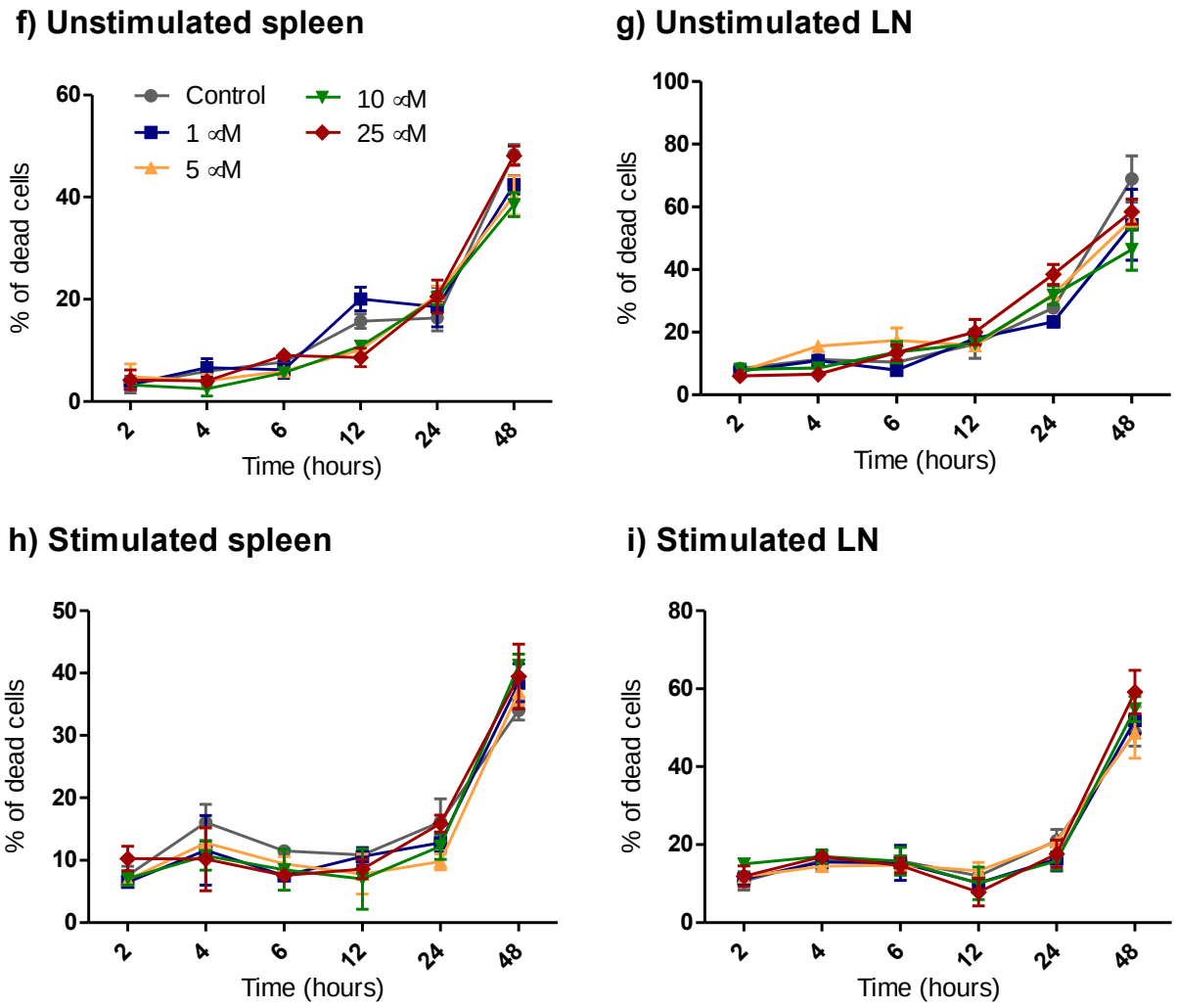

Figure 4.7: Imipramine is not toxic to murine primary T cells.
Freshly isolated splenocytes from P25/Asm$^{+/+}$ mice were treated with Imipramine or left untreated prior activation with peptide25 and anti-CD28. Change in the number of viable cells in the culture over time was determined by Trypan blue dye (a) and percentage of apoptotic (b) and dead cells (c) within CD4+ cells was determined by staining with Annexin V and PI at indicated time points. Separately, similar experiments were performed in both P25/Asm$^{+/+}$ and P25/Asm$^{-/-}$ cells together to determine the percentage of apoptotic (d) and dead cells (e) with or without Imipramine treatment. In different experiments, unstimulated cells from spleens and LNs of WT mice were cultured for indicated durations with Imipramine at 1, 5, 10 and 25 μM concentration or left untreated (f, g). Separately, cells were co-stimulated with anti-CD3 and anti-CD28 and cultured in the presence or absence of Imipramine (h, i). Aliquots of cells were collected from culture and dead cells were counted with Trypan blue at indicated time points and expressed as % of total cells (f-i). Data are representative of 3 independent experiments. Error bars represent mean ± SD. ** ($p < 0.01$), *** ($p < 0.001$) as assessed by two-way ANOVA followed Bonferroni posttest. “Imip” indicates Imipramine.

4.8 Asm deficiency does not affect cell viability after peptide25-induced activation

The data presented above show that Imipramine treatment of murine primary T cells increases the apoptotic cell death. Therefore, In the next step, the effect of Asm deficiency on the viability of naïve TCR Tg T cells was checked. Splenocytes isolated from P25/Asm$^{+/+}$ and P25/Asm$^{-/-}$ mice were activated with peptide25 plus anti-CD28 and cultured for different durations. As described earlier, the number of viable cells in the culture was counted with Trypan blue after 6, 12, 24, 48, 72 and 96 h of stimulation (a). In P25/Asm$^{+/+}$ group, after the initial death till 36 h, the cell count was increased and reached a peak at 48 h which dropped at 72 h and remained stationary till 96 h. In P25/Asm$^{-/-}$ cells, following the death of non-lymphocytes till 36 h, the number of viable cells was increased steadily till 96 h. The frequency of apoptotic (Annexin V+) and dead cells (PI+) among CD4+ T cells was determined as well (b, c). There was no difference between P25/Asm$^{+/+}$ and P25/Asm$^{-/-}$ cells. Trypan blue data showed that P25/Asm$^{-/-}$ cells have a different kinetic of proliferation than P25/Asm$^{+/+}$ cells. To have a deeper understanding, apoptotic cell death only in the dividing (CFSE low) CD4+ T cells was checked (d, e). Again, no difference between these two groups could be detected.

The results indicate that Asm does not play a role in cell viability/apoptotic death after peptide25 and anti-CD28 co-stimulation of TCR Tg CD4+ cells.

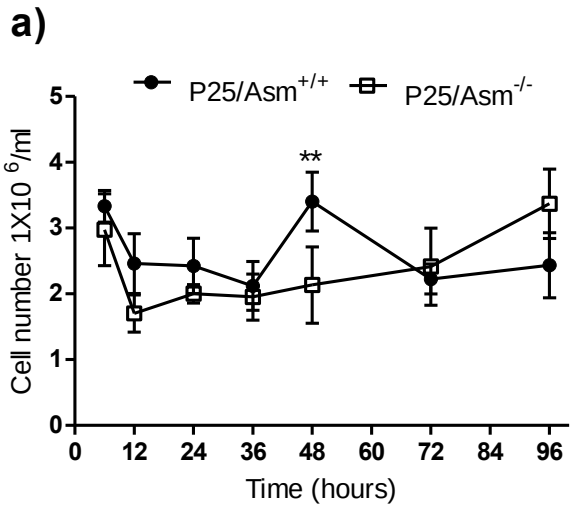

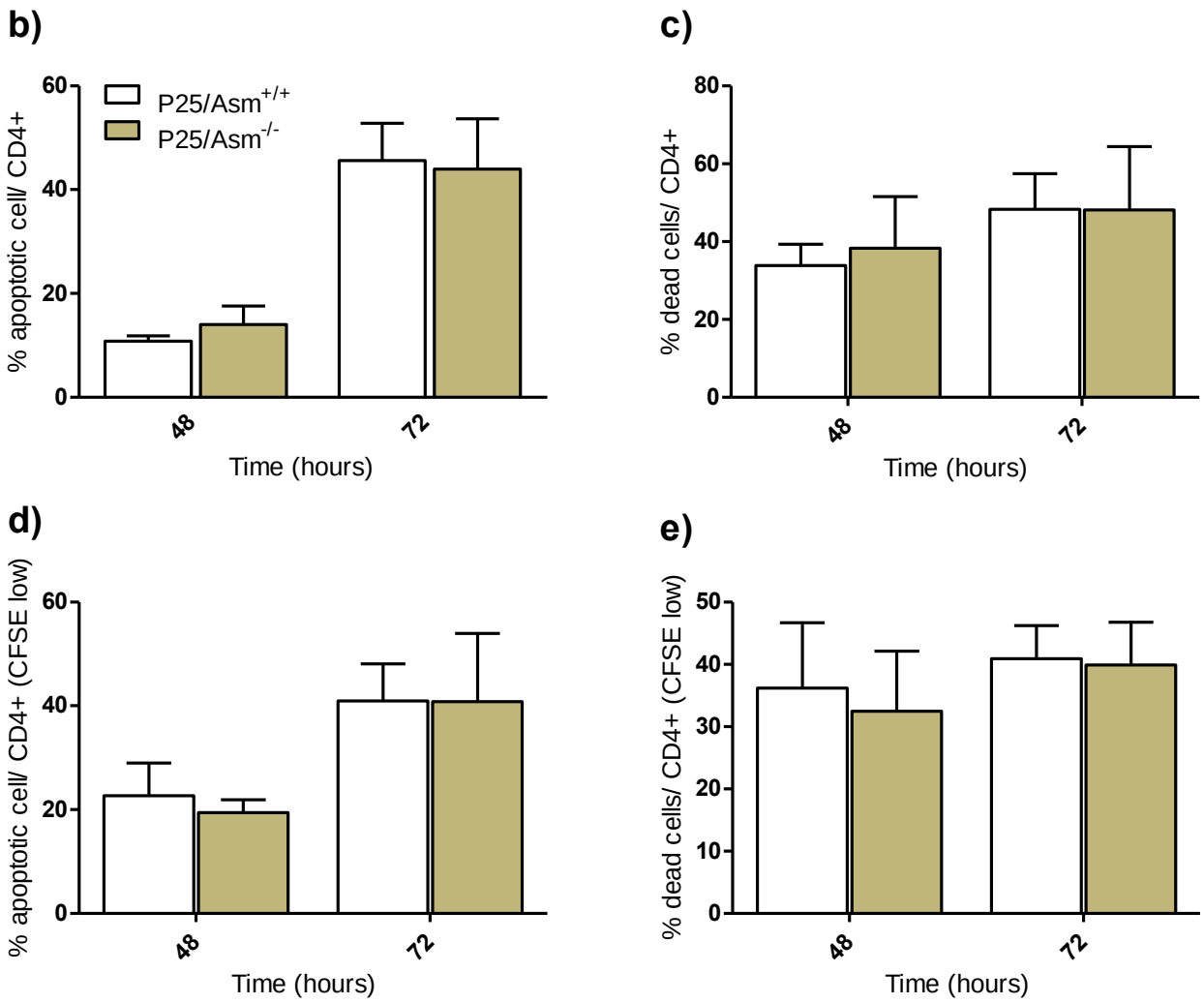

Figure 4.8: Asm is not involved in the apoptotic death of naïve CD4+ T cells after peptide25-induced activation.

Freshly isolated splenocytes from P25/Asm$^{+/+}$ and P25/Asm$^{-/-}$ mice were activated with peptide25 and anti-CD28. Change in the number of viable cells over time was determined with Trypan blue dye (a). Percentage of apoptotic and dead cells within CD4+ (b and c, respectively) and CFSE low CD4+ cells (d and e, respectively) were determined by staining with Annexin V and PI after 48 and 72 h of activation. Data are representative of 3 independent experiments. Error bars represent mean ± SD. ** ($p < 0.01$) as assessed by two-way ANOVA followed Bonferroni posttest.

4.9 Imipramine not only inhibits the activation of P25/Asm$^{+/+}$ but also of P25/Asm$^{-/-}$ CD4+ T cells

The data described above revealed that Imipramine treatment and Asm deficiency have different effects on peptide25-induced cell activation. Although, FIASMAs like Imipramine are being used as functional inhibitors of ASM in sphingolipid research, they might also inhibit AC, acid lipase and phospholipase A and C (Kornhuber et al. 2010),(Kornhuber et al. 2011). To check the specificity of Imipramine, P25/Asm$^{-/-}$ cells were also treated with Imipramine prior activation with peptide25 and investigated for the effect on proliferation, surface molecules expression and cytokine production in comparison to Imipramine treated P25/Asm$^{+/+}$ cells.

Proliferation was determined in CFSE-loaded cells by flow cytometry. After 96 h of activation, results indicated that Imipramine inhibits the proliferation of not only P25/Asm$^{+/+}$ cells but also P25/Asm$^{-/-}$ cells (a). After 48 h post-activation, the frequency of CD25+ (b) and CD44+ (c) cells among CD4+ T cells was significantly reduced with Imipramine treatment in both P25/Asm$^{+/+}$ and P25/Asm$^{-/-}$ groups. The expression of PD1 in total CD4+ population (d) and specifically in activated CD4+ cells (CD4+CD44+) (e) was determined after 48 and 72 h of activation. Imipramine significantly inhibited the expression of PD1 in CD4+ cells at both time points and also in CD4+CD44+ cells at 48 h. However, at 72 h, the reduction of PD1 expression in CD4+CD44+ cells was only significant in P25/Asm$^{-/-}$ cells. The concentration of IL-2 and INFγ in the culture supernatant was significantly low in Imipramine treated cells (f, g). Percentage of IL-2 producing CD4+ T cells was also significantly diminished by Imipramine in both P25/Asm$^{+/+}$ and P25/Asm$^{-/-}$ cells (h).

These data indicate that the Inhibitory effects of Imipramine in peptide25 and anti-CD28-activated TCR Tg CD4+ T cells are not specifically due to Asm inhibition. This also suggests the presence of additional targets for Imipramine action.

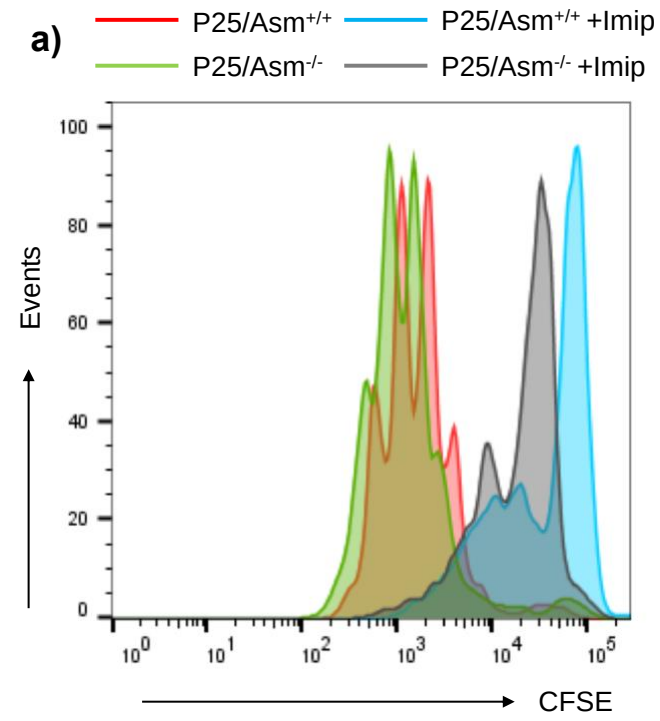
a)
P25/Asm+/+
P25/Asm+/+ +Imip
P25/Asm-/-
P25/Asm-/- +Imip
Events
CFSE

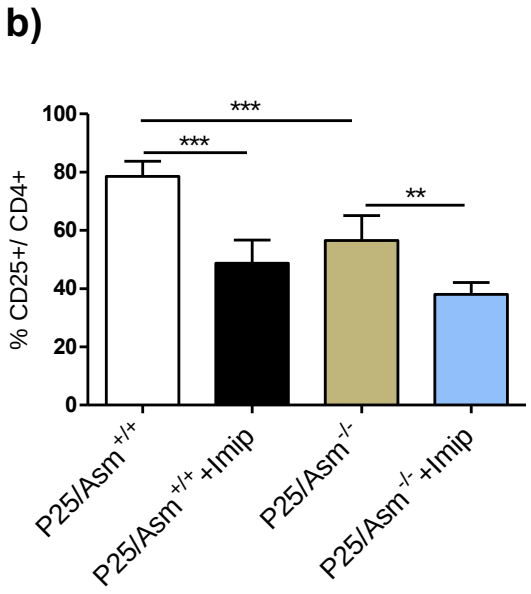
b)
% CD25+/ CD4+
P25/Asm+/+
P25/Asm+/+ +Imip
P25/Asm-/-
P25/Asm-/- +Imip

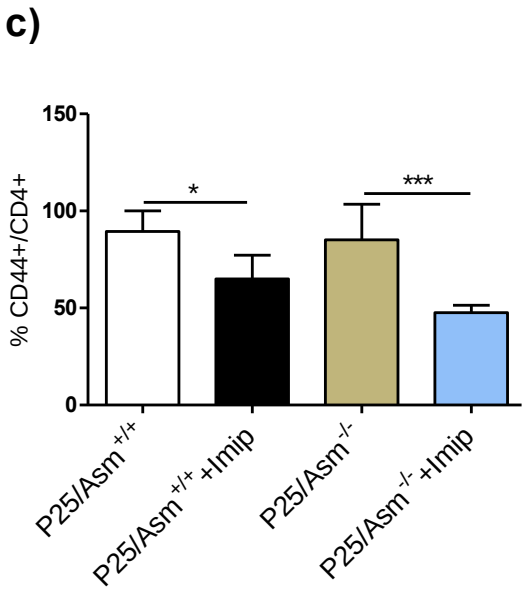
c)
% CD44+/CD4+
P25/Asm+/+
P25/Asm+/+ +Imip
P25/Asm-/-
P25/Asm-/- +Imip

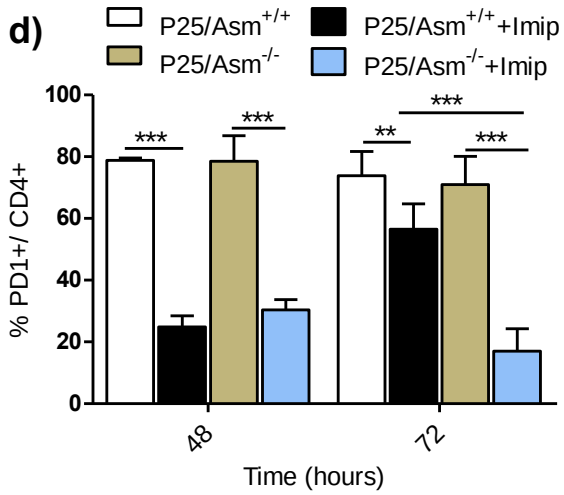
d)
P25/Asm+/+
P25/Asm+/+ +Imip
P25/Asm-/-
P25/Asm-/- +Imip
% PD1+/ CD4+
Time (hours)
48
72

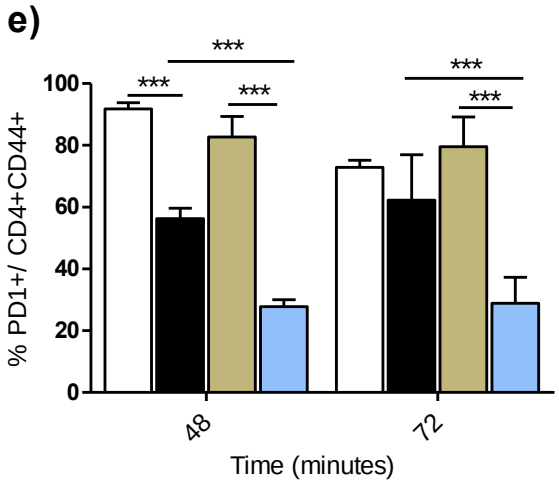
e)
% PD1+/ CD4+CD44+
Time (minutes)
48
72

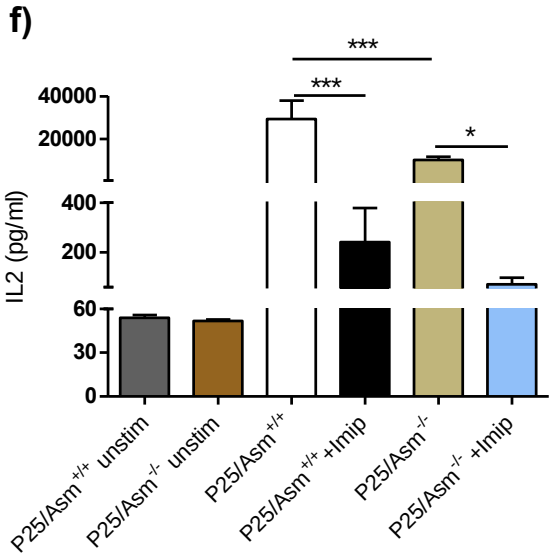
f)
IL2 (pg/ml)
P25/Asm+/+ unstim
P25/Asm-/- unstim
P25/Asm+/+
P25/Asm+/+ +Imip
P25/Asm-/-
P25/Asm-/- +Imip

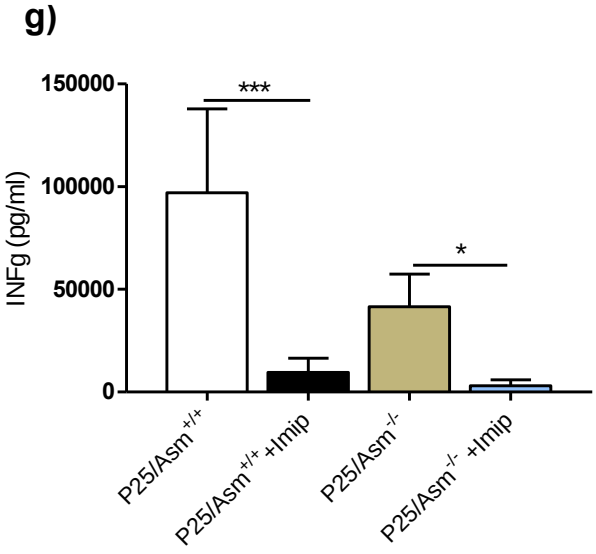
g)
INFg (pg/ml)
P25/Asm+/+
P25/Asm+/+ +Imip
P25/Asm-/-
P25/Asm-/- +Imip

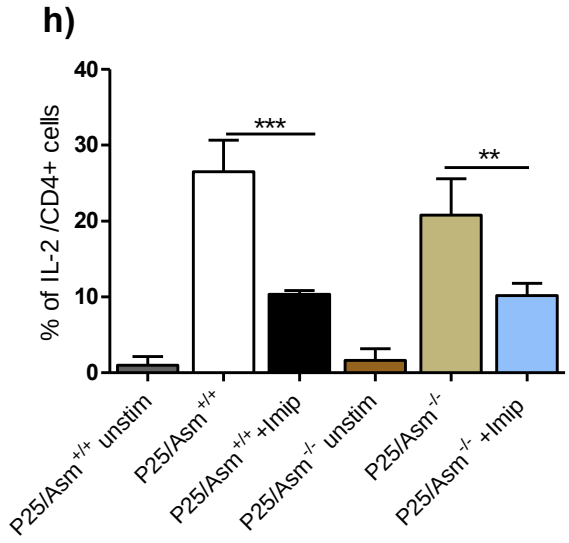
h)
% of IL-2 /CD4+ cells
P25/Asm+/+ unstim
P25/Asm+/+
P25/Asm+/+ +Imip
P25/Asm-/- unstim
P25/Asm-/-
P25/Asm-/- +Imip

Figure 4.9: Imipramine inhibits the activation of both P25/Asm$^{+/+}$ and P25/Asm$^{-/-}$ T cells
Freshly isolated, RBC lysed spleen cells from P25/Asm$^{+/+}$ and P25/Asm$^{-/-}$ mice were shortly pre-incubated with 25 μM Imipramine or left untreated. Both treated and untreated cells were activated with peptide25 and anti-CD28 or left inactivated. Proliferation kinetics was measured by CFSE method. The intensity of CFSE was measured using flow cytometry after 96 hours of activation (a). Frequency of CD25+ (b), CD44+ (c) and PD1+ (d) in CD4+ cells were measured by flow cytometry at indicated time points. Similarly, the frequency of PD1+ in CD4+CD44+ double positive cells was also determined (e). By ELISA, secretion of IL-2 (f) and INFγ (g) were measured after 24 and 48 h of activation, respectively. Frequency of IL-2+CD4+ cells was counted with flow cytometry after 6 h of activation (h). Data are representative of 3-5 independent experiments. Error bars represent mean ± SD. * ($p< 0.05$), ** ($p< 0.01$) and *** ($p< 0.001$) as assessed by one-way ANOVA followed Tukey's multiple comparison test (b-c; f-h) and two-way ANOVA followed Bonferroni posttest (d-e). "Imip" indicates Imipramine.

4.10 ASM activity is cell-type and stimulant-type dependent

In the next step, the effect of stimulation in Asm activity of murine primary lymphocytes was determined. To do that, freshly isolated cells from LNs of WT mice were activated with plate-bound anti-CD3 and soluble anti-CD28 cross-linked with anti-mouse IgG for 2, 5, 10, 20 and 30 min or left inactivated (a). Asm activity was measured using BODIPY FL-C12 SM as described in the method section. The results showed that Asm activity starts to increase soon after stimulation and reached a peak level at 10 min and then starts to decrease after 20 min. Similarly, the ASM activity in Jurkat cells after OKT3 stimulation for 1, 2, 5, 10, 20 and 30 min was measured (b). Results showed that OKT3 stimulation does not increase ASM activity in Jurkat cells.

The data are suggestive of that activation of ASM upon stimulation of T cells, varies depending on the types of cells and stimuli.

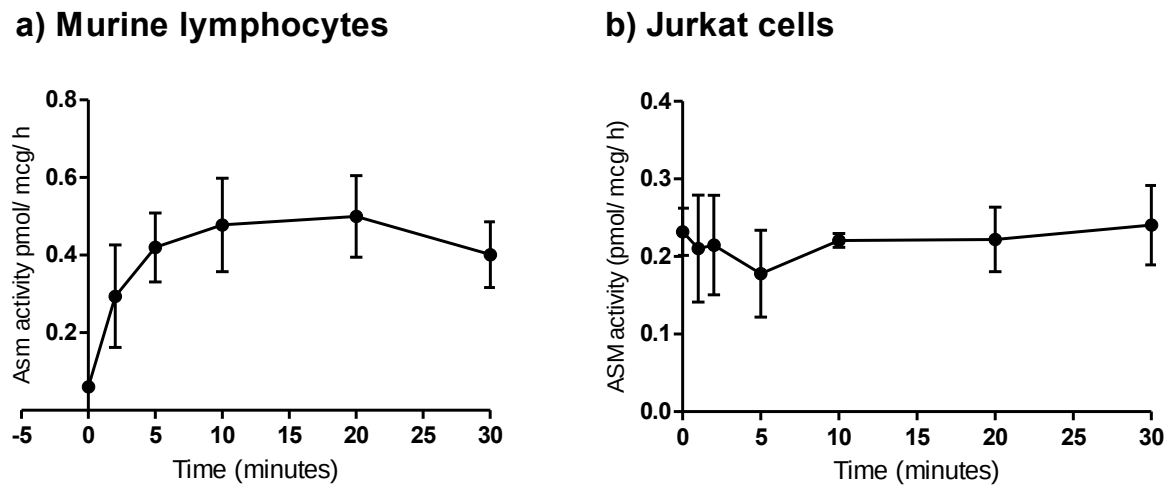

Figure 4.10: ASM activity is cell-type and stimulant-type dependent.
Primary lymphocytes from WT mice were co-stimulated with anti-CD3/CD28 or left unstimulated. Asm activity was measured in whole cell lysates using BODIPY FL-C12 SM at indicated time points (a). ASM activity in Jurkat cells was measured after OKT3 stimulation for indicated time points (b). 0 min represents unstimulated sample for both (a) and (b). Data are representative of 3 independent experiments. Error bars represent mean ± SD. “mcg” indicates microgram of protein.

4.11 Imipramine inhibits not only ASM activity but also AC activity

The present study showed that Imipramine severely abrogates the phosphorylation of multiple kinases in Jurkat cells after OKT3 stimulation, although no upregulation of ASM activity upon stimulation was detected. This indicates that Imipramine induces its negative effects on signal transduction by acting on some targets other than ASM.

To investigate this argument, Asm activity was measured in murine primary cells isolated from LNs of WT mice. Cells were incubated with 15, 25 and 40 μM Imipramine for 1 h at 37°C. Whole cell lysates were used to determine Asm activity (a). Results showed that Imipramine treatment reduced Asm activity by ~50% at 15 and 25 μM concentration compared to control. With 40 μM there was a reduction of activity by ~70% of control. Additionally, the effect of Imipramine in ASM activity in Jurkat cells was also checked (c). There was a ~40% reduction of activity with 5 μM of Imipramine and no further reduction with higher doses (10 and 25 μM) could be detected.

Subsequently, the effect of Imipramine in Ac activity was evaluated. Same as before, freshly isolated cells form LNs of WT mice were incubated with 15, 25 and 40 μM of Imipramine and Ac activity was determined using C12-NBD ceramide as a substrate (b). With 15 μM imipramine there was a ~20% reduction of Ac activity, with higher dosage (25 and 40 μM) there was a ~50% reduction in comparison to untreated control.

Data showed that Imipramine inhibits both Asm and Ac activity in unstimulated primary murine lymphocytes and also inhibits ASM activity in unstimulated Jurkat cells .

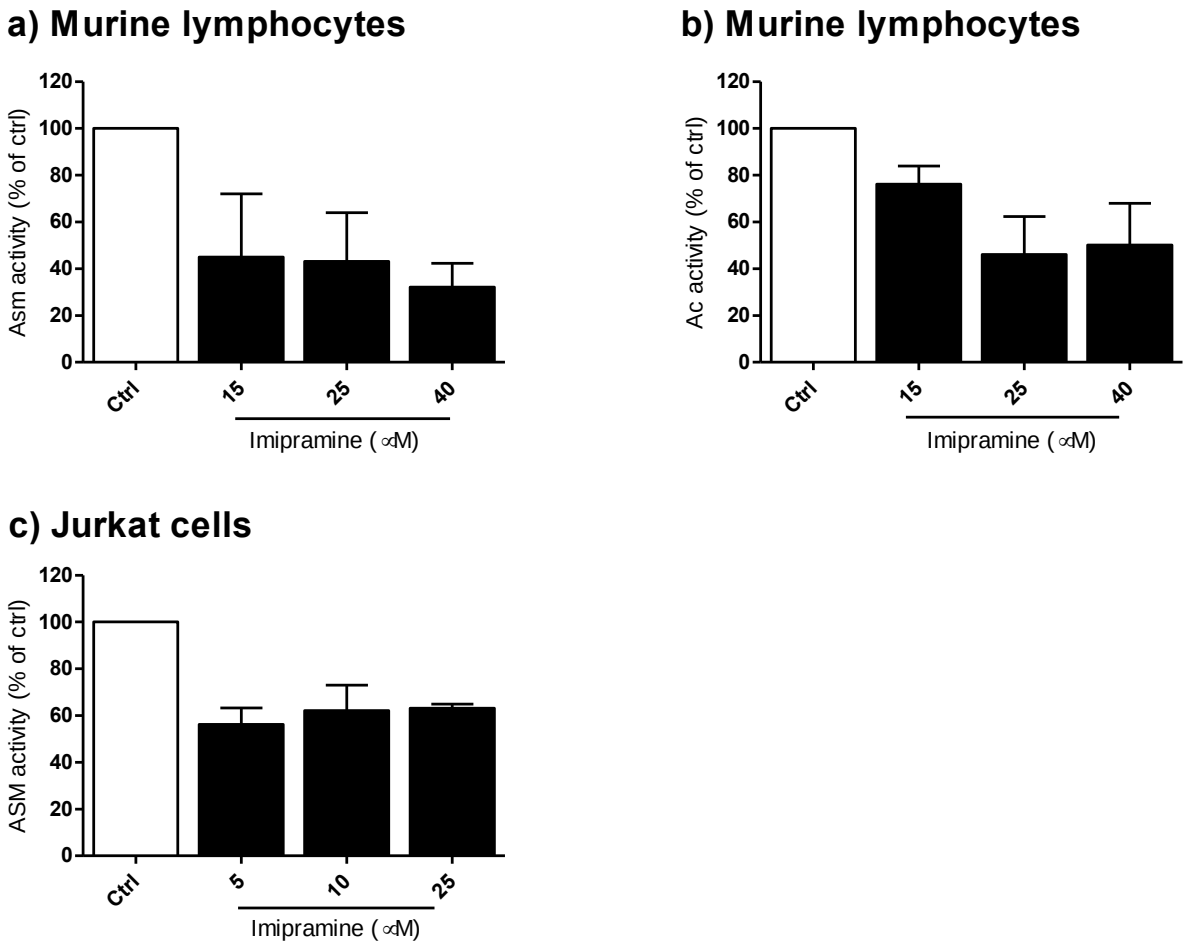

Figure 4.11: Imipramine inhibits both ASM and AC activity.
Cells were isolated from LNs of WT mice and incubated with 15, 25 and 40 μM concentration of Imipramine for 1 hour. Asm and Ac activity were determined in whole cell lysates and expressed as the percentage of untreated control (a, b). In the same way, Jurkat cells were treated with 5, 10 and 25 μM of Imipramine for 1 h and ASM activity was measured in unstimulated cells (c) Data are representative of 3 independent experiments. Error bars represent mean ± SD.

4.12 Asm has limited effects on BCG-induced activation of kinases in CD4+ and CD8 T+ cells in spleen

BCG has been used as a safe alternative to Mtb in infection biology for many years (Mustafa et al. 2000), (Grace and Ernst et al. 2016). In this project, peptide25 and TCR Tg mice specific to this peptide were used for experiments. Peptide25 is derived from the Ag85B protein of BCG and Mtb. Earlier results in this project demonstrated that P25/Asm$^{-/-}$ cells show reduced activation of PLCγ1, Erk1/2 and AKT upon peptide25 stimulation during the early stage (2 to 5 min post-stimulation) compared to P25/Asm$^{+/+}$ cells. To evaluate the activation of signaling kinases *in vivo*, WT and Asm-deficient mice were infected with BCG by intravenous injection. After 3 days, mice were sacrificed and spleens were collected. Frozen sections of spleen were co-stained with CD4/ CD8 and p-ZAP70/ p-AKT/ p-Erk/ p-JNK for confocal microscopy.

Initial interest was to check the phosphorylation of kinases specifically in CD4+ and CD8+ T cells. However, due to the generalized pattern of phosphorylation in the sections, the areas of the tissue containing CD4+ or CD8+ T cells were evaluated and compared between WT and Asm-deficient mice.

Firstly, sections were co-stained for CD4 and phospho-kinases. In WT non-infected mice there was higher phosphorylation of ZAP70 in CD4+ T cells than Asm-deficient mice. In both WT and Asm-deficient infected mice, p-ZAP70 could be detected in a comparable pattern. However, phosphorylation was not specific for CD4+ cells (a). AKT was scarcely phosphorylated in few CD4+ T cells in both WT and Asm-deficient non-infected mice. After infection, AKT was strongly phosphorylated in CD4+ cells in WT but not in Asm-deficient mice (b). In non-infected Asm-deficient mice, staining for p-JNK was slightly higher than WT control. After infection, any further elevation of p-JNK positive staining could be noticed in neither WT nor Asm-deficient mice (c). Phosphorylation of Erk1/2 was comparable in both WT and Asm-deficient mice with or without BCG infection. However, these cells were not positive for CD4 staining (d).

Next, staining was done for phospho-proteins in CD8+ cells. Asm-deficient non-infected mice showed relatively increased staining for p-ZAP70 than WT mice. However, phosphorylation of ZAP70 was not specifically detectable in CD8+ T cells. After infection, WT mice showed stronger staining for p-ZAP70 than Asm-deficient mice (e). There was no evident p-AKT staining in CD8+ T cells in both WT and Asm-deficient mice (f). Regarding the phosphorylation of JNK and Erk1/2, no positively stained CD8+ cells could be observed in both WT and Asm-deficient mice and moreover, there was no correlation with BCG infection as well (g, h).

These findings drive to the conclusion that 3 days after BCG infection, there is increased phosphorylation of AKT in CD4+ cells and ZAP70 in CD8+ cells in WT mice compared to Asm-deficient mice. This indicates a possible role of Asm on activation of these kinases *in vivo.*

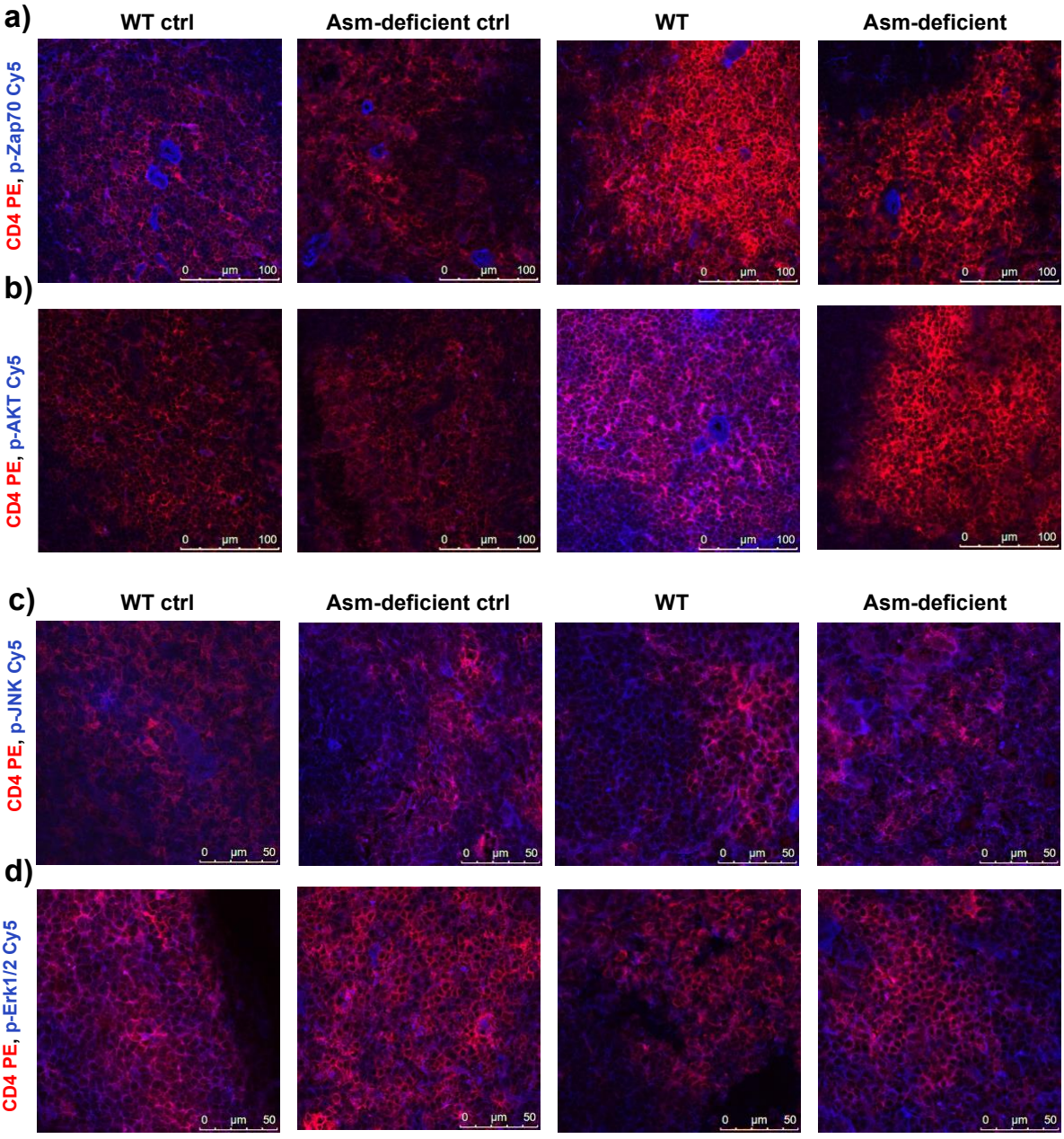
a)
WT ctrl
Asm-deficient ctrl
WT
Asm-deficient
CD4 PE, p-Zap70 Cy5
b)
CD4 PE, p-AKT Cy5
c)
CD4 PE, p-JNK Cy5
d)
CD4 PE, p-Erk1/2 Cy5
0 µm 100
0 µm 50

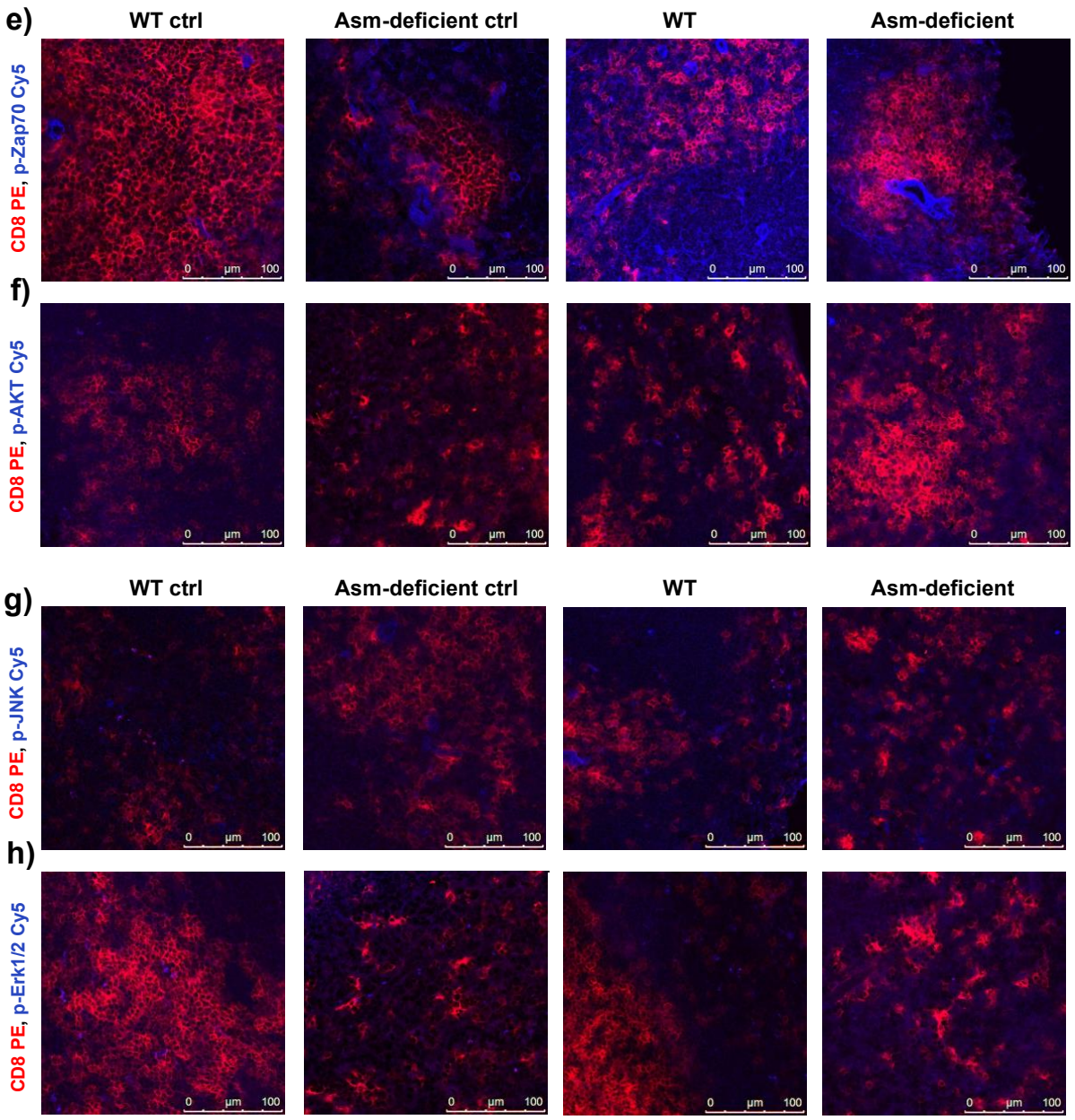

Figure 4.12: Asm has limited effects on BCG-induced activation of kinases in CD4+ and CD8+ T cells in the spleen.

WT and Asm-deficient mice were infected with BCG. After 3 days of infection, mice were sacrificed and spleens were cryo-preserved for immunohistochemistry. Frozen tissue sections were co-stained for either CD4 (a-d) or CD8 (e-h) and phospho-proteins. CD4/ CD8 and phospho-protein antibodies are PE (red) and Cy5 (blue) conjugated, respectively. Scale bars are shown at the lower right corner. “Ctrl” indicates uninfected mice. Data represent 3 mice in each group.

4.13 Effect of Imipramine on sphingolipid content of Jurkat cells following OKT3 stimulation

To understand the changes in the lipid composition of Jurkat cells, after OKT3 stimulation in the presence or absence of Imipramine, mass spectrometry analysis was performed. Total SM and ceramide including their different subspecies (C16, C18, C20, C22, C24, C24:1), total sphingosine and S1P levels were measured in $0.5x10^6$ cells/samples. Main ceramide and SM species were C16 and C24:1. The data showed no significant change of total levels of ceramide (a) and SM (b) neither after stimulation nor after Imipramine treatment. However, random reduction of some SM species, namely, C18, C22 and C24 was observed after Imipramine incubation. In addition, after Imipramine treatment sphingosine and S1P levels were reduced in both unstimulated (0 min) and stimulated (1 to 20 min) cells in comparison to untreated controls (c, d).

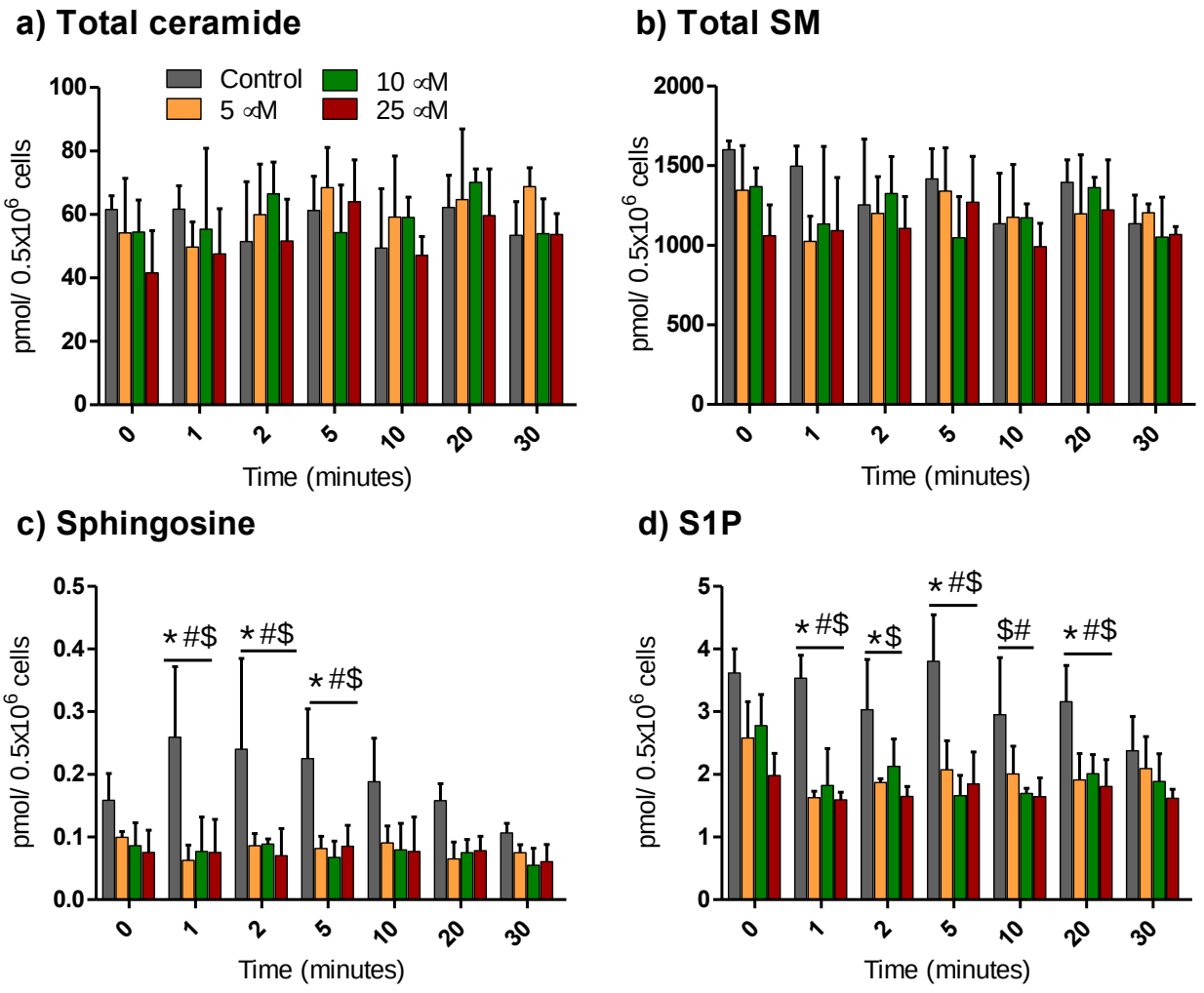

e) Ceramide C16

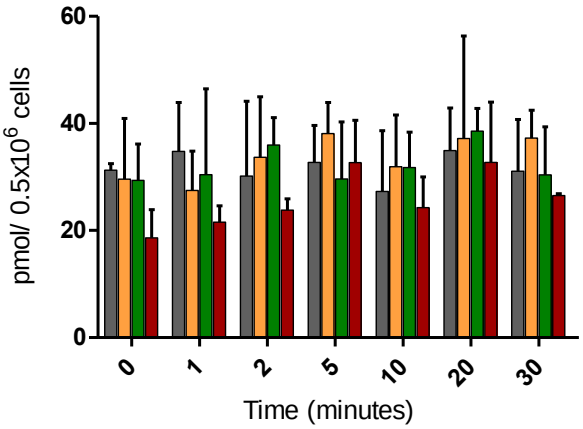

f) Ceramide C18

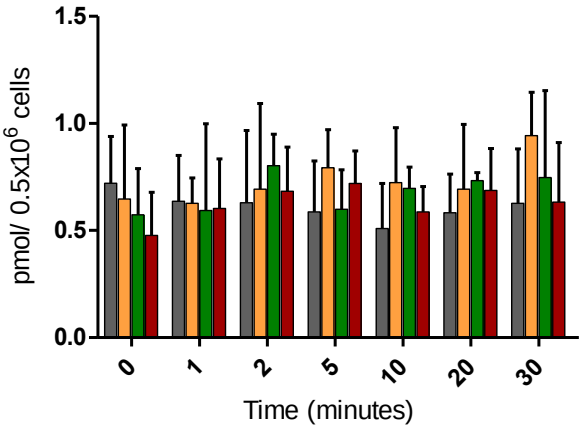

g) Ceramide C20

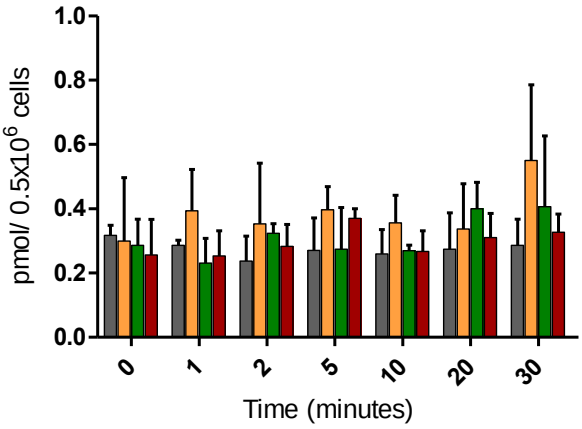

h) Ceramide C22

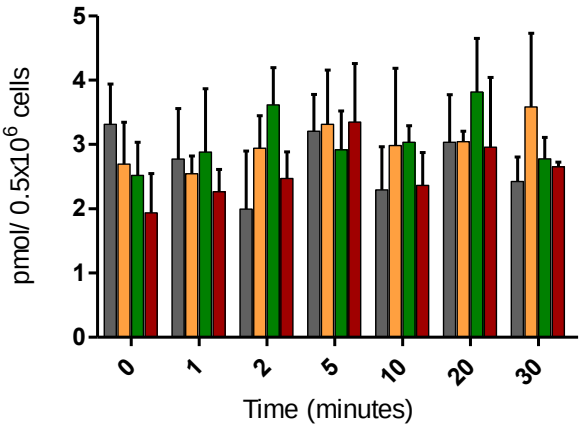

i) Ceramide C24

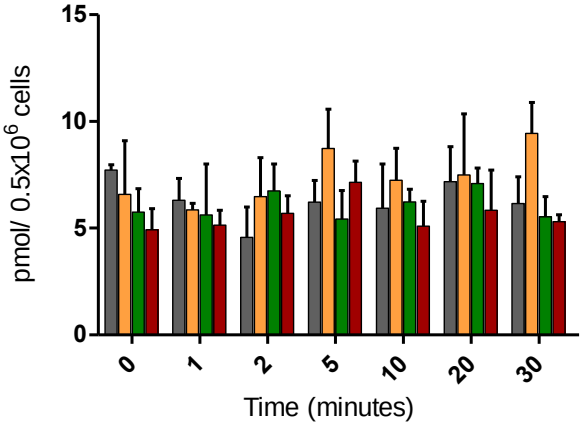

j) Ceramide C24:1

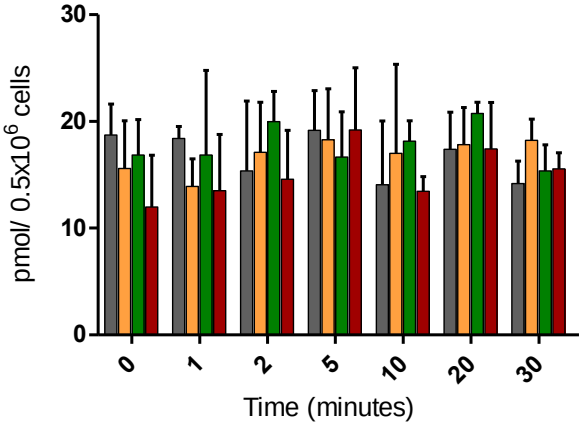

k) SM C16

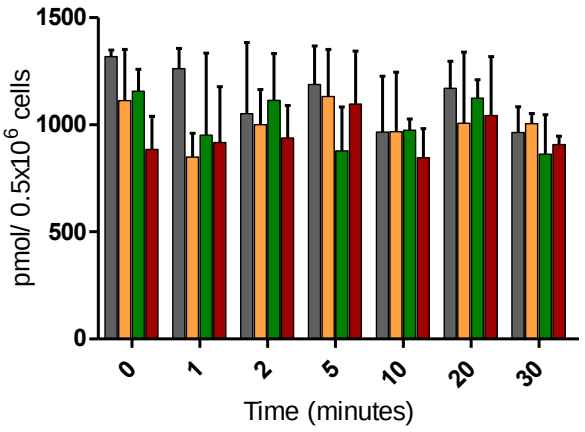

l) SM C18

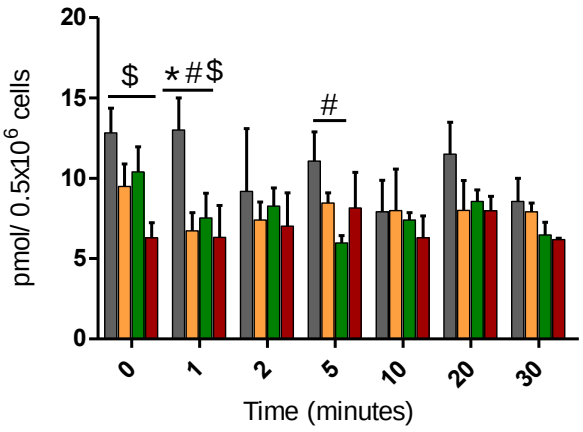

m) SM C20

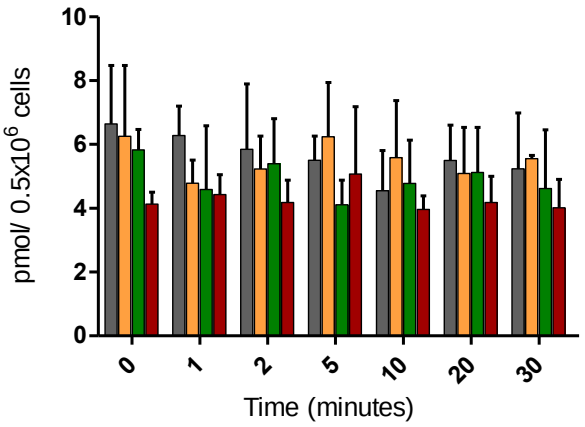

n) SMC22

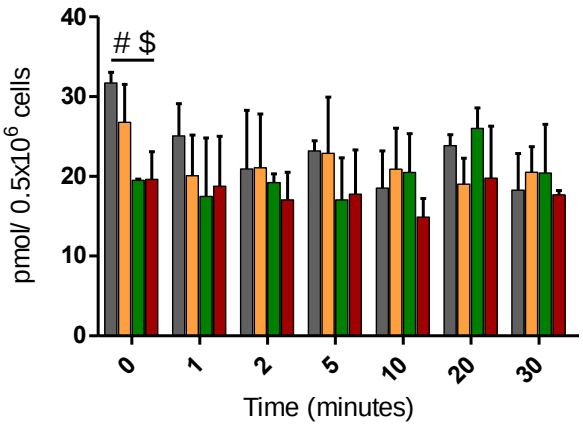

o) SM C24

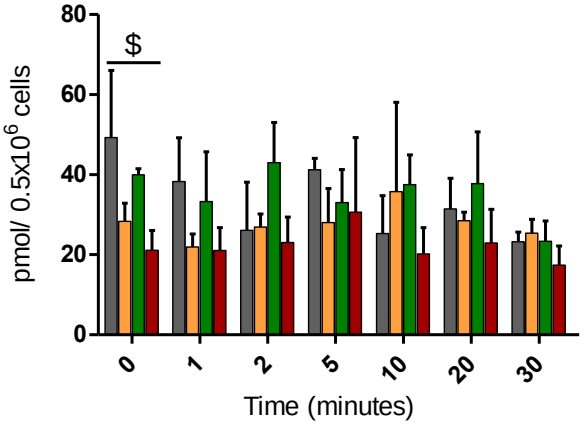

p) SM C24:1

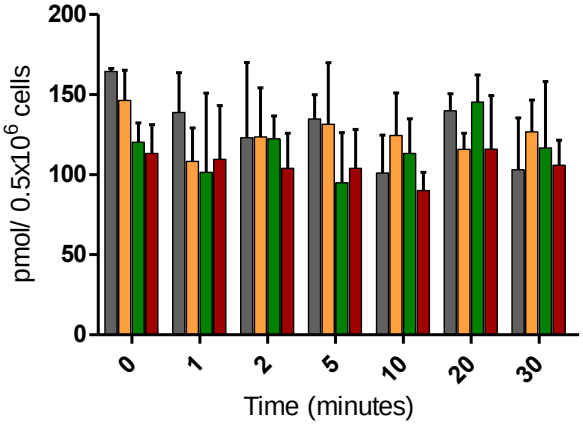

Figure 4.13: Effect of Imipramine on sphingolipid composition of Jurkat cell.
Cells were pre-incubated with Imipramine or left untreated prior stimulation with OKT3 antibody Lipid composition was measured by mass spectrometry. Total levels of ceramide, SM, sphingosine and S1P were determined (a-d). Moreover, different subspecies of ceramide (e-j) and SM (k-p) were also measured. * ($p < 0.05$, control vs. 5 μM Imipramine), # ($p < 0.05$, control vs. 10 μM Imipramine), $ ($p < 0.05$, control vs 25 μM Imipramine) as assessed by two-way ANOVA followed Bonferroni posttest. Data are representative of 3 independent experiments. Error bars represent mean ± SD. "Control" indicates Imipramine untreated cells.

5 Discussion

Many studies have been conducted to understand the link between the ASM system and activation of T cells. Still, there are gaps to be filled in this topic. Hence, the present project targeted to explore the effects of ASM in 3 completely different models/systems, i.e., peptide25-induced stimulation of TCR Tg CD4+ T cells, physiological anti-CD3/CD28 activation of murine primary naïve T lymphocytes and OKT3 stimulation of Jurkat cells.

The present study demonstrated that stimulation of Tg CD4+ T cells with peptide25 in the presence of anti-CD28 leads to the activation of PLCγ1, AKT and Erk1/2 kinases within 2-5 min of stimulation in both P25/Asm$^{+/+}$ and P25/Asm$^{-/-}$ cells. The phosphorylation of ZAP70 in P25/Asm$^{+/+}$ cells was very low after stimulation. Moreover, there was no increase in the phosphorylation of ZAP70 in P25/Asm$^{-/-}$ cells. This finding contradicts the robust phosphorylation of PLCγ1, which is the substrate of kinase ZAP70. The explanation could be that Zap70 remains associated with the ς-chains of CD3 molecules of the TCR-CD3 complex. It undergoes rapid phosphorylation and subsequent de-phosphorylation upon TCR ligation. The kinetics of this important event is finely controlled in both human and murine T cells. It has been reported that stimulation of murine thymocytes with anti-CD3 antibody leads to a rapid rise of p-ZAP70 at 1 min, peaked at 3 min and rapidly reduced afterwards (van Oers et al. 1994). Another group showed that in Jurkat E6.1 human leukemic cell line, after stimulation with anti-CD3, ZAP70 was phosphorylated within 10 seconds, reached its maximum level by 30 seconds. Almost 50% of p-ZAP70 was de-phosphorylated in next 120 seconds (Houtman et al. 2005). In the present study, such a sharp time-dependent change of p-ZAP70 upon stimulation could not be detected. Probably because the phosphorylation reached its peak level and went back to the basal level within 2 min, which is the shortest stimulation time point tested in the current project. Checking the p-ZAP70 level in shorter duration by improving the stimulation protocol might resolve this issue.

In the second model, anti-CD3/CD28 co-stimulation-induced activation of signaling cascades in T lymphocytes was investigated in both WT and Asm-deficient cells. Data showed that stimulation leads to the activation of ZAP70, AKT and Erk1/2 kinases in both groups and Asm deficiency does not have any substantial effect in these processes. However, PLCγ1 and PI3K phosphorylation were considerably inhibited in Asm-deficient cells. Additionally, phosphorylation of mTOR, AMPKα, Lck(Tyr416) and Lck(Tyr505) was checked. Results did not reveal any activation of mTOR and AMPKα. Moreover, there was de-phosphorylation of the latter kinase upon stimulation. These findings contradict the previous data which described activation of mTOR and AMPKα upon TCR ligation (Pearce et al. 2010).

mTOR is a serine/threonine kinase which integrates immune signals and metabolic cues from the environment to regulate the differentiation of naïve T cells into effector cells (Maciolek et al. 2014),(Chi et al. 2012). A major stimulatory input for mTOR activation comes from the PI3K-AKT pathways, while activated AMPK inhibits mTOR signaling (Ma et al. 2017),(Chi et al. 2012). Recently it has been reported that PI3K-AKT-mTOR is not a straightforward connection as it thought to be. PI3K can regulate activation of T cells in both mTOR dependent and independent way (Gamper and Powell et al. 2012). It could be that the stimulation method used in the present study directed PI3K into the mTOR-independent direction. On the other hand, AMPKα, which is another serine/threonine kinase, involved in the regulation of cellular metabolism, energy consumption and cell cycle. It can be activated in two ways: increased $[Ca^{2+}]_i$ or increased intracellular AMP/ATP ratio. It has been shown that TCR triggering induces phosphorylation of AMPKα in a calcium-dependent manner (Tamás et al. 2006). However, research done in T lymphocytes from AMPKα1-deficient mice exhibited similar immune-competency to WT cells upon antigenic stimulation (Mayer et al. 2008). This suggests that classically induced immune response does not impose metabolic stress upon T cells. This might be the reason why no upregulation of p-AMPKα could be observed after classic anti-CD3/CD28 stimulation for short duration (2-15 min) in the present study. In addition to this, there was no noticeable difference in phosphorylation of AMPKα between WT and Asm-deficient cells, which is comparable to the similar

activation-induced calcium response observed in these two groups, considering activation of AMPKα in a calcium-dependent manner.

Lck is a tyrosine kinase which belongs to the Src family kinases. TCR triggering causes activation of Lck which phosphorylates and activates ZAP70. The latter is well known for transferring activation signals from membrane-associated signalosome towards the nucleus. Both activity and inactivity of Lck are tightly controlled by tyrosine phosphorylation at different sites. Phosphorylation at Tyr416 (active) in the activation loop of the kinase domain upregulates its activity (Hunter et al. 1987), while the phosphorylation of the carboxy-terminal Tyr505 (inactive) downregulates Lck activity (Chow et al. 1993). It has been shown that ~40% of the Lck is consecutively active in resting T cells (Nika et al. 2010). This high level of pre-activated Lck is needed for the CD3-ς chain phosphorylation after TCR ligation. Once activated, if there is further increase in the p-Lck(Tyr416) level or not, is still controversial. Moreover, it has been shown that the overall phosphorylation of Lck does not differ between activated and resting T cells (Brownlie and Zamoyska et al. 2013a). In accordance to this, present study reported a high level of p-Lck(Tyr416) in unstimulated control cells, although in stimulated samples there was de-phosphorylation of Lck(Tyr416) (active Lck) and increased phosphorylation of the LckTyr505 (inactive Lck). The present study could not provide an answer to explain this discrepancy. Moreover, Asm-deficient cells did not show any changes in the phosphorylation level of neither active nor inactive form of Lck. This difference between WT and Asm-deficient cells suggest a role of Asm in the activation of Lck in activated T cells and maintenance of a threshold level of active Lck in resting T cells. However, further studies are needed to identify the involved mechanisms.

Previously Nix and colleagues showed that after anti-CD3 and anti-CD3/CD28 stimulation of murine splenocytes for 2 to 8 min, the overall tyrosine phosphorylation was delayed and severely impaired in Asm-deficient cells (Nix and Stoffel et al. 2000). Likewise, here in the present experiments, reduced phosphorylation of some tyrosine kinases was detected in Asm-deficient cells. However as mentioned earlier, the negligible reduction was limited to 2 to 5 min post-activation. It is speculated that

stimulation for a longer duration, e.g., 15 min in the referred study would abolish the observed dramatic difference in tyrosine phosphorylation between WT and Asm-deficient cells. Taking together, in this project it has been shown that Asm is partially needed for the phosphorylation of selected kinases in murine primary T cells which further depends on the stimulant type and duration of stimulation.

Imipramine which is a tricyclic antidepressant belongs to the group of biologically active molecules, FIASMAs. Imipramine has been used to study the effect of functional inhibition of ASM for many years (Beckmann et al. 2014),(Kornhuber et al. 2010). In T cell research it has been shown that Imipramine (20 μM) treatment of human peripheral blood-derived CD4+ T cells diminishes the signal transduction after activation with anti-CD3 or anti-CD28 alone and with anti-CD3/CD28 co-stimulation as well (Bai et al. 2015). This experiment was extended here into Jurkat cells by stimulating them with OKT3 antibody. Moreover, a wider range of Imipramine (1-25 μM) was used for ASM inhibition. Results demonstrated that OKT3 stimulation of Jurkat cells leads to the activation of ZAP70, Erk1/2, Ras and JNK; which also supports the previous studies (Perez de Castro et al. 2004),(Bai et al. 2015). However, in contrary to the literature, present results did not show any increased level of phosphorylation of PLCγ1 and PI3K/AKT/mTOR pathways after stimulation. It has been documented that ligation of CD28 is the primary initiator of downstream PI3K/AKT/mTOR signals. p85α, the regulatory subunit of PI3K, is recruited to the TCR-CD3 complex by CD3ς or CD28, or via TCR-interacting molecules (Alcázar et al. 2007). In the present stimulation protocol, anti-CD28 was not used as a co-stimulatory molecule. This might be the explanation behind the non-activation of PI3K/AKT/mTOR pathways in Jurkat cells after OKT3 stimulation.

In addition, PI3K is a lipid kinase which produces PIP3 and PIP2. These lipids recruit PH domain-containing proteins (e.g., ITK) to the cell membrane and help the initiation of different signaling pathways (e.g., AKT/mTOR). Membrane localization of ITK is regulated by the cellular level of PIP3 and PIP2. On the other hand, the production of PIP3 and PIP2 is positively and negatively regulated by PI3K and PTEN, respectively.

Jurkat cells do not express PTEN. Which leads to the accumulation of PIP3 and PIP2 and ultimately constitutively high activation of AKT (Alcázar et al. 2007),(Shan et al. 2000). Which might explain the observation of a high basal level of p-PI3K, p-AKT and p-mTOR in unstimulated samples in the present study. Probably AKT was maximally phosphorylated in the unstimulated cells, that is why it could not be further increased by OKT3 cross-linking. Even though there was no increased phosphorylation of mTOR and PI3K upon stimulation, Imipramine treatment further reduced their phosphorylation in stimulated cells. However, Imipramine did not have any inhibitory effect on AKT phosphorylation.

Correspondingly, Imipramine severely abrogated the phosphorylation of PLCγ1, Erk1/2 and JNK in Jurkat cells, which is in accordance to the work of Bai and colleagues (Bai et al. 2015). Moreover, the data appeared that stimulation resulted in increased Ras-GTPase activity which was inhibited by Imipramine, although the effect was limited to the very early time points (1-2 min) of stimulation. After that, the activity of Ras-GTPase and the inhibitory effect of Imipramine, both diminished over time. This was very comparable to the kinetics of phosphorylation of PLCγ1, which was also sharply reduced after 5 min. Studies have shown that stimulation of Jurkat cells with low grade (1 μg/ml) anti-CD3 and anti-CD28 causes expression of N-Ras, exclusively on Golgi apparatus in a PLCγ-dependent manner (Perez de Castro et al. 2004). Possibly, in the present model of Jurkat cell stimulation, impaired activation of PLCγ1 affected the activation of Ras-GTPase as well.

As already discussed the mechanism of Lck activation in T cells, the phosphorylation of both Lck(Tyr416) and Lck(Tyr505) upon OKT3 stimulation was examined. The data revealed that the stimulation induces de-phosphorylation of the inactive form of Lck which was further augmented by Imipramine treatment. However, there was no increased phosphorylation of the active site within Lck, although the substrate of this enzyme, ZAP70 showed increased phosphorylation upon stimulation.

As mentioned earlier, TCR ligation leads to the phosphorylation of AMPKα in a calcium-dependent manner. Although the present data showed increased $[Ca^{2+}]_i$ upon OKT3

ligation, there was no enhanced phosphorylation of AMPKα in the present setup. This contradicts the previously published work (Tamás et al. 2006). One probable reason for this contradiction might be that in the referred study, Jurkat cells were activated with UCHT1 antibody. On the other hand, OKT3 antibody was used in the present study. There is evidence that OKT3, but not UCHT1, triggers mitogenesis via an IL-2-dependent mechanism in Jurkat cells (Van Wauwe et al. 1984). Therefore, these two antibodies might have different effects on the activation of AMPKα as well. In addition to this, results demonstrated attenuated calcium response by Imipramine treatment yet no inhibition of AMPKα. Furthermore, Imipramine enhanced AMPKα phosphorylation in stimulated cells. Studies showed that Increased AMP/ATP during metabolic stress in T cells leads to AMPKα activation (Mayer et al. 2008). Enhanced phosphorylation of AMPKα with Imipramine treatment in the present study, may indicate such a metabolic crisis imposed by Imipramine. However, to understand the involved mechanisms, further investigations are necessary. In summary, Imipramine abolishes the activation of several kinases in Jurkat cells upon stimulation with OKT3 antibody.

Elevation of $[Ca^{2+}]_i$ in T cells is one of the earliest responses upon TCR ligation. Formation of immunological synapse between APC and T cell is a calcium-dependent process. Sustained elevated level of calcium is necessary for the successful transcription of calcium-dependent genes, most importantly IL-2 and other cytokines. This process is primarily important for T cell differentiation into effector cells (Oh-Hora et al. 2009),(Lewis et al. 2001). Several studies described the involvement of ASM in T cell calcium responses induced by different stimuli. Ligation of CD95 exhibited inhibition of calcium influx in Jurkat cells by activating ASM and production of ceramide (Lepple-Wienhues et al. 1999). Comparable inhibition of calcium influx in ASM/ceramide dependent manner was reported after binding of TNFα to TNFR1 in Jurkat cells (Church et al. 2005). However, the role of ceramide in TCR-induced calcium response is still controversial. It has been demonstrated that application of extracellular C2-ceramide blocks the anti-CD3 mediated calcium signals in murine helper T cells (Detre et al. 2006). In contrary, another group suggested that addition of ceramide increases the $[Ca^{2+}]_i$ and subsequent calcium entry in Jurkat cells both in the presence and absence

of extracellular calcium. Moreover, their comparison of OKT3 and ceramide-mediated calcium response indicated that these two molecules follow the same mechanism as well (Colina et al. 2005). In this project, the role of Asm deficiency in calcium influx was investigated in murine primary lymphocytes after anti-CD3/CD28 stimulation by flow cytometry. Results showed a rapid increase of $[Ca^{2+}]_i$ after the stimulation. Nonetheless, Asm deficiency did not exhibit any effect in this event. Similarly, the calcium influx in Jurkat cells after the addition of OKT3 antibody was measured as well. As reported, OKT3 activates PLCγ1 producing IP_3, which leads to the release of calcium from ER (Lewis et al. 2001), the present study also recorded increased $[Ca^{2+}]_i$ upon OKT3 stimulation. Imipramine has been shown to reduce the slow inward calcium current in bovine cardiac myocytes and murine neuroblastoma cells (Ogata et al. 1989),(Isenberg and Tamargo et al. 1985). Likewise, the current data showed the inhibitory effect of Imipramine in OKT3-induced calcium influx in Jurkat cells.

This project elaborately tested the signaling cascades in three different types of T cells and the effect of ASM and variable doses of Imipramine on them. Afterwards, the later events of T cell activation such as proliferation, differentiation and cytokine production were investigated in peptide25 TCR Tg CD4+ T cells in the context of Asm deficiency and Imipramine treatment. Data showed that Imipramine (25 μM) treatment significantly impaired the cell division and proliferation in P25/Asm$^{+/+}$ CD4+ T cells, which is supported by its inhibitory effects in human CD4+ T cells described by Bai and colleagues (Bai et al. 2015). Peptide25-induced activation led to the increased expression of several surface molecules such as CD25, CD44 and PD1 following the kinetics described in the literature (Stoffel et al. 1998),(Konkel et al. 2010). Expression of all the tested surface molecules was reduced by Imipramine. It has been demonstrated that several tricyclic antidepressants including Imipramine inhibit the release of IL-2 and INFγ in human peripheral T cells (Xia et al. 1996). Likewise, in the present experiments, the secretion of signature cytokines of CD4+ T cells, e.g., IL-2 and INFγ was significantly inhibited in Imipramine treated cells. Moreover, the percentage of IL2+CD4+ T cells was reduced by Imipramine. The negative effects of Imipramine in

late activation events of murine CD4+ T cells described here are in accordance with the published data on human CD4+ T cells (Bai et al. 2015).

To evaluate if the compelling inhibitory effects of Imipramine on peptide25-induced activation of Tg CD4+ T cells is due to the reduction of Asm activity or not, similar late activation parameters were compared between CD4+ T cells from P25/Asm$^{+/+}$ and P25/Asm$^{-/-}$ mice. Previously it has been shown that anti-CD3/CD28 co-stimulation led to the impaired proliferation of splenocytes from Asm-deficient mice (Stoffel et al. 1998). In contrary to this, present results showed that Asm deficiency delays the proliferation at the beginning of activation, although later, P25/Asm$^{-/-}$ cells displayed very similar cell division pattern and proliferation to P25/Asm$^{+/+}$ cells. This suggests that Asm is not needed for the late proliferative response or it could be the involvement of mechanisms compensating for the gene defect as well. Moreover, the reason behind this discrepancy could be that in the present experiments TCR Tg CD4+ cells were activated with peptide25 instead of anti-CD3/CD28. It has been suggested that the outcome of activation of T cells depends on the strength and kind of initial stimulation. Considering the expression of surface molecules, present results indicated that Asm is not involved in the upregulation of CD44 and PD1 following peptide25-induced stimulation. Nevertheless, CD25 expression was significantly reduced by Asm deficiency at 48 h post-stimulation. This correlates to the significant reduction of IL-2 secretion in P25/Asm$^{-/-}$ cells at 24 h because CD25 is a component of the IL-2 receptor. Asm deficiency also significantly reduced the secretion of INFγ, checked at 48 h post-stimulation. Discussed earlier that Asm-deficient cells showed reduced secretion but increased intracellular accumulation of IL-2 (Stoffel et al. 1998). In contrary to this, the present data reported that P25/Asm$^{-/-}$ CD4+ T cells showed reduced frequency of IL-2+ cells. The probable interpretation could be that in the mentioned study, IL-2+ cells were counted from whole splenocytes population, not specifically in CD4+ T cells. To be noted, researchers documented secretion of IL-2 in DCs and CD8+ T cells as well, which are abundant in murine spleen (Malek and Castro et al. 2010),(Cheng et al. 2002). On the other hand, the present data show IL-2+ cells specifically within the CD4+ population.

To address the inconsistency in peptide25-induced activation of Imipramine treated and P25/Asm$^{-/-}$ CD4+ T cells, it was speculated that action of Imipramine is not Asm specific. Therefore, P25/Asm$^{-/-}$ cells were also treated with Imipramine and investigated for the same activation parameters. Findings revealed comparable inhibitory effects of Imipramine in P25/Asm$^{-/-}$ cells. Results suggest that the negative effects of Imipramine in CD4+ T cell activation are not mediated by Asm inhibition alone. In conclusion, the present project showed Asm is needed for initial IL-2 production, IL-2 and INFγ secretion and proliferation of peptide25 TCR Tg CD4+ cells. However, subsequent proliferative stage and expression of surface molecules are Asm independent.

When CD4+ T cells are activated with specific peptide-MHC II, they undergo differentiation, proliferation and contraction phases. During the contraction phase, most of the activated cells die by apoptosis. Additionally, when the stimulation is not optimum, cells also die due to the absence of survival signals (Brenner et al. 2008). Serotonin reuptake inhibitors and tricyclic antidepressants are widely used functional inhibitors of ASM. It has been shown that both types of molecules induce apoptosis of both resting and proliferating human lymphocytes (Karlsson et al. 1998),(Na et al. 1996),(Gobin et al. 2014). Several plausible mechanisms are proposed to explain their pro-apoptotic effects. One study suggested that Inhibition of ASM leads to lysosomal accumulation of SM and induces lipid stress followed by ER stress and apoptotic death of cells (Klutzny et al. 2017). Additionally, ASM inhibitors may induce T cell death by blocking several signaling pathways, interfering with calcium response, down regulating anti-apoptotic Bcl-2 and producing ROS (Gobin et al. 2013),(Karlsson et al. 1998). In accordance with these, the present data also showed increased cell death in Imipramine treated peptide25-activated TCR Tg CD4+ T cells. Data revealed that the percentage of apoptotic CD4+ T cells were very similar to untreated control cells till 24 h post-activation. Afterwards, the apoptosis rate raised significantly in the Imipramine treated cells. Parallel to this, the frequency of total dead cells was also increased by imipramine. However, the difference was not that striking. Despite congruent results, it is believed that in the present model, the cell death was due to impaired initial activation of T cells by Imipramine which leads to the death of inactivated cells. Because it has

been documented that the optimum concentration of Imipramine to induce apoptosis is 50 μM or even 100 μM, which is much higher than the concentration used in this project (Karlsson et al. 1998),(Na at al. 1996),(Koch et al. 2003). Nevertheless, to exclude the chance of direct toxicity of Imipramine in the present setup, primary cells isolated from spleens and LNs of WT mice were treated with Imipramine. Both activated or inactivated cells were incubated with Imipramine (1, 5, 10 and 25 μM) or left untreated for 2 to 48 h. Regarding the percentage of dead cells, results showed that Imipramine was not toxic to primary murine cells at any dose ranging from 1 to 25 μM. This is in accordance with many other previous studies where Imipramine was used in similar or higher dose than used here and without any evidence of toxicity (Rotolo et al. 2005),(Brenner et al. 1998),(Verdurmen et al. 2010),(Dumitru et al. 2009),(Bauer et al. 2009),(Hauck et al. 2000).

The effect of ASM deficiency in AICD in T cells is controversial. Nix and co-workers showed that after anti-CD3, anti-CD3/CD28 and PMA/ionomycin stimulation of splenocytes from Asm-deficient mice, they were more susceptible to anti-CD95 antibody induced apoptosis (Nix and Stoffel et al. 2000). In contrast to this, it has also been reported that Concanavalin-A activated splenocytes from Asm-deficient mice showed similar sensitivity to CD95-mediated cell death (Xuan et al. 2010). In the same direction, the present study also showed a similar frequency of apoptotic and dead cells among total CD4+ cells in P25/Asm$^{+/+}$ and P25/Asm$^{-/-}$ group after 48 and 72 h of activation. It has been reported that activated human T cells are more sensitive towards ASM inhibition-induced apoptosis (Karlsson et al. 1998). To investigate specifically activated CD4+ T cells, cells were loaded with CFSE dye prior stimulation. Afterwards the frequency of apoptotic and dead cells among CFSE low CD4+ T cells (indicating CD4+T cells undergoing proliferation after activation) was determined. There was no apparent difference between P25/Asm$^{+/+}$ and P25/Asm$^{-/-}$ cells.

In the peptide25-induced model of T cell activation, peptide25 was used to stimulate CD4+ T cells isolated from TCR Tg mice. Peptide25 is derived from the Ag85B of BCG and Mtb. Peptide25 specific TCR Tg mice is a widely-used model to study the role of T cells in tuberculosis (Tamura et al. 2004), (Shafiani et al. 2010), (Wolf et al. 2007). To

extend the *in vitro* peptide25 results to *in vivo* level, WT and Asm-deficient mice were infected intravenously with BCG and examined for early T cell activation. It has been shown that, in systemic BCG infection of mice, T cell activity could be detected as delayed type hypersensitivity induced by immunogenic challenge soon after 4 days of infection (Mackaness et al. 1974). As in this project the primary interest was in early activation of TCR signaling, the mice were sacrificed following 3 days of infection. Activation of different TCR signaling kinases was checked in spleens by immunohistology. Both CD4+ and CD8+ T cells were investigated for p-ZAP70, p-Erk1/2, p-AKT and p-JNK staining. Comparable to *in vitro* findings the *in vivo* data revealed that WT and Asm-deficient mice have similar phosphorylation pattern of tested kinases, except that the phosphorylation of AKT in CD4+ cells and phosphorylation of ZAP70 in CD8+ cells were higher in WT mice than Asm-deficient mice. The results further support the idea that Asm deficiency has limited impact on T cell activation in both *in vitro* and *in vivo.*

Krönke and co-workers showed that CD28 cross-linking of Jurkat cells and human resting T cells activates ASM in a rapid and transient manner. They also showed that anti-CD3 cross-linking of human resting T cells does not exert any ASM activity (Boucher et al. 1995). Bai and collogues demonstrated that stimulation of human CD4+T cells with anti-CD3 or anti-CD28 antibodies or anti-CD3/CD28-coated beads activates ASM (Bai et al. 2015). Müller and Avota reported that in primary human CD4+ T cells, anti-CD28-induced upregulation of ASM activity is completely abrogated by anti-CD3/CD28 co-stimulation (Mueller et al. 2014). However, results from the present project showed that OKT3 stimulation does not increase ASM activity in Jurkat cells. Effect of stimulation in T cell-Asm activity in mice is also controversial. Chan and colleagues showed that stimulation of purified CD3+ T cells from BALB/c mice, with anti-CD28 but not with anti-CD3 led to increased Asm activity (Chan and Ochi et al. 1995). However, both Krönke and Chan and their groups did not show the effect of anti-CD3/CD28 co-stimulation in ASM activity in respective cells. In contrast to this, the present study reported that there is increased Asm activity upon anti-CD3/CD28 co-stimulation of primary lymphocyte of C57BL/6 mice. All these data indicate that changes

in the ASM activity upon stimulation of mice or human T cells are largely variable and depends on the cell types and approaches of stimulation.

As discussed above, present data reported the absence of increased ASM activity upon OKT3 simulation of Jurkat cells, yet ASM inhibitor Imipramine dampened the signal transductions at various levels. This finding indicates the non-specific mode of action by Imipramine at least in the present setup. It has been suggested that FIASMAs can inhibit other lysosomal enzymes as well, such as AC (Kornhuber et al. 2010). Therefore, in the next step, the effect of Imipramine in both ASM and AC activity was measured. Data showed that Imipramine inhibits both of the enzymes. Moreover, lipid analysis findings from mass spectrometry revealed that there are no significant changes in total ceramide and SM levels in Jurkat cells neither due to OKT3 stimulation nor due to Imipramine treatment. Nevertheless, there was a reduced level of sphingosine and S1P after stimulation which was further reduced by Imipramine. AC hydrolyses ceramide to produce sphingosine which is immediately phosphorylated to S1P in the physiological situation. Thus, the reduction of sphingosine and S1P in treated cells indirectly indicates the inhibition of AC by Imipramine in Jurkat cells.

6 Summary

In summary, the present study showed a restricted function of Asm in peptide25-induced and physiologically activated murine primary lymphocytes. Activation of only a limited set of kinases of TCR signaling cascade is Asm dependent. The Asm inhibitor Imipramine completely abrogates Tg CD4+ T cell responses after peptide25-induced activation, but P25/Asm$^{-/-}$ cells compensate some of the effects and show even better survival and proliferation than P25/Asm$^{+/+}$ cells. Similar to murine cells, Imipramine significantly inhibits the activation of several signaling pathways in human Jurkat cells. In addition, activity assays and mass spectrometry data also suggested that besides ASM, Imipramine also inhibits AC activity, which may explain the discrepancies in T cell responses between Imipramine treated and Asm-deficient P25/Asm$^{-/-}$ cells. Thus, This project provides new insights into the role of ASM in early and late aspects of T cell activation.

7 References

Adam, D., Heinrich, M., Kabelitz, D., and Schütze, S. (2002). Ceramide: Does it matter for T cells? Trends Immunol. *23*, 1–4.

Agata, Y., Kawasaki, A., Nishimura, H., Ishida, Y., Tsubata, T., Yagita, H., and Honjo, T. (1996). Expression of the PD-1 antigen on the surface of stimulated mouse T and B lymphocytes. Int. Immunol. *8*, 765–772.

Ahmed, S.A., Gogal, R.M., and Walsh, J.E. (1994). A new rapid and simple non-radioactive assay to monitor and determine the proliferation of lymphocytes: an alternative to [3H]thymidine incorporation assay. J. Immunol. MethodsJournal Immunol. Methods *170*, 211–224.

Airola, M. V, and Hannun, Y.A. (2013). Sphingolipid metabolism and neutral sphingomyelinases. Handb. Exp. Pharmacol. *215*, 57–76.

Alcázar, I., Marqués, M., Kumar, A., Hirsch, E., Wymann, M., Carrera, A.C., and Barber, D.F. (2007). Phosphoinositide 3-kinase gamma participates in T cell receptor-induced T cell activation. J. Exp. Med. *204*, 2977–2987.

Altman, A., and Villalba, M. (2003). Protein kinase C-theta (PKCtheta): it's all about location, location, location. Immunol. Rev. *192*, 53–63.

Anes, E., Kühnel, M.P., Bos, E., Moniz-Pereira, J., Habermann, A., and Griffiths, G. (2003). Selected lipids activate phagosome actin assembly and maturation resulting in killing of pathogenic mycobacteria. Nat. Cell Biol. *5*, 793–802.

Armstrong B, J.A., and Hart, A. (1975). Phagosome-lysosome interactions in cultured macrophages infected with virulent tubercle bacilli Reversal of the usual nonfusion pattern and observations on bacterial survival. J. Exp. Med. *142*.

Avota, E., Gulbins, E., and Schneider-Schaulies, S. (2011). DC-SIGN mediated sphingomyelinase-activation and ceramide generation is essential for enhancement of viral uptake in dendritic cells. PLoS Pathog. *7*, e1001290.

Baaten, B.J.G., Li, C.R., and Bradley, L.M. (2010). Multifaceted regulation of T cells by CD44. Commun. Integr. Biol. *3*, 508–512.

Bai, A., and Guo, Y. (2017). Acid sphingomyelinase mediates human CD4(+) T-cell signaling: potential roles in T-cell responses and diseases. Cell Death Dis. *8*, e2963.

Bai, A., Kokkotou, E., Zheng, Y., and Robson, S.C. (2015). Role of acid sphingomyelinase bioactivity in human CD4+ T-cell activation and immune responses. Cell Death Dis. *6*, e1828–e1828.

Baier-Bitterlich, G., Uberall, F., Bauer, B., Fresser, F., Wachter, H., Grunicke, H., Utermann, G., Altman, A., and Baier, G. (1996). Protein kinase C-theta isoenzyme selective stimulation of the transcription factor complex AP-1 in T lymphocytes. Mol. Cell. Biol. *16*, 1842–1850.

Bartke, N., and Hannun, Y.A. (2009). Bioactive sphingolipids: metabolism and function. J. Lipid Res. *50*, S91–S96.

Bauer, J., Liebisch, G., Hofmann, C., Huy, C., Schmitz, G., Obermeier, F., and Bock, J. (2009). Lipid alterations in experimental murine colitis: Role of ceramide and imipramine for matrix metalloproteinase-1 expression. PLoS One *4*, e7197.

Beckmann, N., Sharma, D., Gulbins, E., Becker, K.A., and Edelmann, B. (2014). Inhibition of acid sphingomyelinase by tricyclic antidepressants and analogons. Front. Physiol. *5 AUG*, 331.

Belkaid, Y., and Tarbell, K. (2009). Regulatory T Cells in the Control of Host-

Microorganism Interactions. Annu. Rev. Immunol. *27*, 551–589.
Berridge, M.J., and Taylor, C.W. (1988). Inositol trisphosphate and calcium signaling. In Cold Spring Harbor Symposia on Quantitative Biology, pp. 927–933.
Blanco, F.C., Bianco, M.V., Meikle, V., Garbaccio, S., Vagnoni, L., Forrellad, M., Klepp, L.I., Cataldi, A.A., and Bigi, F. (2011). Increased IL-17 expression is associated with pathology in a bovine model of tuberculosis. Tuberculosis *91*, 57–63.
Bock, J., and Gulbins, E. (2003). The transmembranous domain of CD40 determines CD40 partitioning into lipid rafts. FEBS Lett. *534*, 169–174.
Boomer, J.S., and Green, J.M. (2010). An enigmatic tail of CD28 signaling. Cold Spring Harb. Perspect. Biol. *2*, a002436.
Bossi, G., Griffiths, G.M., William, S., and Road, S.P. (1999). Degranulation plays an essential part in regulating cell surface expression of Fas ligand in T cells and natural killer cells. Nat. Med. *5*, 90–96.
Boucher, L.M., Wiegmann, K., Fütterer, A., Pfeffer, K., Machleidt, T., Schütze, S., Mak, T.W., and Krönke, M. (1995). CD28 signals through acidic sphingomyelinase. J. Exp. Med. *181*, 2059–2068.
Brenner, B., Ferlinz, K., Grassmé, H., Weller, M., Koppenhoefer, U., Dichgans, J., Sandhoff, K., Lang, F., and Gulbins, E. (1998). Fas/CD95/Apo-I activates the acidic sphingomyelinase via caspases. Cell Death Differ. *5*, 29–37.
Brenner, D., Krammer, P.H., and Arnold, R. (2008). Concepts of activated T cell death. Crit. Rev. Oncol. *66*, 52–64.
Brown, D.A., and London, E. (1998). Functions of lipid rafts in biological membranes. Annu. Rev. Cell Dev. Biol. *14*, 111–136.
Brownlie, R.J., and Zamoyska, R. (2013a). T cell receptor signalling networks: Branched, diversified and bounded. Nat. Rev. Immunol. *13*, 257–269.
Brownlie, R.J., and Zamoyska, R. (2013b). T cell receptor signalling networks: Branched, diversified and bounded. Nat. Rev. Immunol. *13*, 257–269.
Chan, G., and Ochi, A. (1995). Sphingomyelin-ceramide turnover in CD28 costimulatory signaling. Eur. J. Immunol. *25*, 1999–2004.
Chemnitz, J.M., Parry, R. V, Nichols, K.E., June, C.H., and Riley, J.L. (2004). SHP-1 and SHP-2 Associate with Immunoreceptor Tyrosine-Based Switch Motif of Programmed Death 1 upon Primary Human T Cell Stimulation, but Only Receptor Ligation Prevents T Cell Activation. J. Immunol. *173*, 945–954.
Chen, L., and Flies, D.B. (2013). Molecular mechanisms of T cell co-stimulation and co-inhibition. Nat. Rev. Immunol. *13*, 227–242.
Chen, W., Jin, W., Hardegen, N., Lei, K., Li, L., Marinos, N., McGrady, G., and Wahl, S.M. (2003). Conversion of Peripheral CD4 + CD25 − Naive T Cells to CD4 + CD25 + Regulatory T Cells by TGF-β Induction of Transcription Factor Foxp3. J. Exp. Med. *198*, 1875–1886.
Chen, X., Zhou, B., Li, M., Deng, Q., Wu, X., Le, X., Wu, C., Larmonier, N., Zhang, W., Zhang, H., et al. (2007). CD4+CD25+FoxP3+regulatory T cells suppress Mycobacterium tuberculosis immunity in patients with active disease. Clin. Immunol. *123*, 50–59.
Cheng, L.E., Ohlén, C., Nelson, B.H., and Greenberg, P.D. (2002). Enhanced signaling through the IL-2 receptor in CD8+ T cells regulated by antigen recognition results in preferential proliferation and expansion of responding CD8+ T cells rather than

promotion of cell death. Proc. Natl. Acad. Sci. U. S. A. *99*, 3001–3006.
Chentouf, M., Rigo, M., Ghannam, S., Navarro-Teulon, I., Mongrand, S., Pèlegrin, A., and Chardès, T. (2010). The lipid-modulating effects of a CD4-specific recombinant antibody correlate with ZAP-70 segregation outside membrane rafts. Immunol. Lett. *133*, 62–69.
Chi, H. (2012). Regulation and function of mTOR signalling in T cell fate decisions. Nat. Rev. Immunol. *12*, 325–338.
Cho, J.-H., Kim, H.-O., Surh, C.D., and Sprent, J. (2010). T Cell Receptor-Dependent Regulation of Lipid Rafts Controls Naive CD8+ T Cell Homeostasis. Immunity *32*, 214–226.
Chow, L.M., Fournel, M., Davidson, D., and Veillette, A. (1993). Negative regulation of T-cell receptor signalling by tyrosine protein kinase p50_csk_. Nature *365*, 156–160.
Church, L.D. (2005). TNFR1-induced sphingomyelinase activation modulates TCR signaling by impairing store-operated Ca2+ influx. J. Leukoc. Biol. *78*, 266–278.
Colina, C., Flores, A., Rojas, H., Acosta, A., Castillo, C., Garrido, M.D.R., Israel, A., DiPolo, R., and Benaim, G. (2005). Ceramide increase cytoplasmic Ca2+concentration in Jurkat T cells by liberation of calcium from intracellular stores and activation of a store-operated calcium channel. Arch. Biochem. Biophys. *436*, 333–345.
Contreras, F.X., Villar, A.V., Alonso, A., Kolesnick, R.N., and Goñi, F.M. (2003). Sphingomyelinase activity causes transbilayer lipid translocation in model and cell membranes. J. Biol. Chem. *278*, 37169–37174.
Da, L., Pereira, V., Desnick, R. 1, Adler, D.A., Disteche, C.M., and Schuchman, E.H. (1991). Regional Assignment of the Human Acid Sphingomyelinase Gene (SMPD1) by PCR Analysis of Somatic Cell Hybrids and in Situ Hybridization to 11 p15.1 -11pl5.4. Genomics *9*, 229–234.
Davis, J.M., and Ramakrishnan, L. (2009). The Role of the Granuloma in Expansion and Dissemination of Early Tuberculous Infection. Cell *136*, 37–49.
Davis, J.M., Clay, H., Lewis, J.L., Ghori, N., Herbomel, P., and Ramakrishnan, L. (2002). Real-Time Visualization of Mycobacterium-Macrophage Interactions Leading to Initiation of Granuloma Formation in Zebrafish Embryos. Immunity *17*, 693–702.
DeGrendele, H.C., Estess, P., and Siegelman, M.H. (1997). Requirement for CD44 in activated T cell extravasation into an inflammatory site. Science (80-.). *278*, 672–675.
Desvignes, L., and Ernst, J.D. (2009). Interferon-γ-Responsive Nonhematopoietic Cells Regulate the Immune Response to Mycobacterium tuberculosis. Immunity *31*, 974–985.
Detre, C., Kiss, E., Varga, Z., Ludányi, K., Pászty, K., Enyedi, Á., Kövesdi, D., Panyi, G., Rajnavölgyi, É., and Matkó, J. (2006). Death or survival: Membrane ceramide controls the fate and activation of antigen-specific T-cells depending on signal strength and duration. Cell. Signal. *18*, 294–306.
Divangahi, M., Desjardins, D., Nunes-Alves, C., Remold, H.G., and Behar, S.M. (2010). Eicosanoid pathways regulate adaptive immunity to Mycobacterium tuberculosis. Nat. Immunol. *11*, 751–758.
Do, Y., Nagarkatti, P.S., and Nagarkatti, M. (2004). Role of CD44 and Hyaluronic Acid (HA) in Activation of Alloreactive and Antigen-Specific T Cells by Bone Marrow-Derived Dendritic Cells. J. Immunother. *27*, 1–12.
Dobrowsky, R.T., and Hannun, Y.A. (1993). Ceramide-activated protein phosphatase: partial purification and relationship to protein phosphatase 2A. Adv. Lipid Res. *25*, 91–

104.
Dolmetsch, R.E., Lewis, R.S., Goodnow, C.C., and Healy, J.I. (1997). Differential activation of transcription factors induced by Ca2+ response amplitude and duration. Nature *386*, 855–858.
Donnadieu, E., Cefai, D., Tan, Y.P., Paresys, G., Bismuth, G., and Trautmann, A. (1992). Imaging early steps of human T cell activation by antigen-presenting cells. J. Immunol. *148*, 2643–2653.
Duke, R., P. M.Persechini, Chang, S., Liu, C., J. Cohen, and J. Youngi (1989). Purified perforin induces target cell lysis but not DNA fragmentation. *170*, 1451–1456.
Dumitru, C.A., and Gulbins, E. (2006). TRAIL activates acid sphingomyelinase via a redox mechanism and releases ceramide to trigger apoptosis. Oncogene *25*, 5612–5625.
Dumitru, C.A., Sandalcioglu, I.E., Wagner, M., Weller, M., and Gulbins, E. (2009). Lysosomal ceramide mediates gemcitabine-induced death of glioma cells. J. Mol. Med. *87*, 1123–1132.
Dustin, M.L., Chakraborty, A.K., and Shaw, A.S. (2010). Understanding the structure and function of the immunological synapse. Cold Spring Harb. Perspect. Biol. *2*, a002311.
Eckle, S., Turner, S.J., Rossjohn, J., and Mccluskey, J. (2013). Predisposed ab T cell antigen receptor recognition of MHC and MHC-I like molecules? Curr. Opin. Immunol. *25*, 653–659.
Edelmann, B., Bertsch, U., Tchikov, V., Winoto-Morbach, S., Perrotta, C., Jakob, M., Adam-Klages, S., Kabelitz, D., and Schütze, S. (2011). Caspase-8 and caspase-7 sequentially mediate proteolytic activation of acid sphingomyelinase in TNF-R1 receptosomes. EMBO J. *30*, 379–394.
Elojeimy, S., Holman, D.H., Liu, X., El-Zawahry, A., Villani, M., Cheng, J.C., Mahdy, A., Zeidan, Y., Bielwaska, A., Hannun, Y.A., et al. (2006). New insights on the use of desipramine as an inhibitor for acid ceramidase. FEBS Lett. *580*, 4751–4756.
Esen, M., Schreiner, B., Jendrossek, V., Lang, F., Fassbender, K., Grassmé, H., and Gulbins, E. (2001). Mechanisms of Staphylococcus aureus induced apoptosis of human endothelial cells. Apoptosis *6*, 431–439.
Ferlinz, K., Hurwitz, R., Vielhaber, G., Suzuki, K., and Sandhoff, K. (1994). Occurrence of two molecular forms of human acid sphingomyelinase. Biochem. J. *301 (Pt 3*, 855–862.
Flesch, I., and Kaufmann, S. (1990). Activation of Tuberculostatic Macrophage Functions By Gamma-Interferon, Interleukin-4, and Tumor-Necrosis-Factor. Infect. Immun. *58*, 2675–2677.
Flores, I., Jones, D.R., and Mérida, I. (2000). Changes in the balance between mitogenic and antimitogenic lipid second messengers during proliferation, cell arrest, and apoptosis in T-lymphocytes. FASEB J. doi:10.1096/fj.99-1066fje.
Fowler, S. (1969). Lysosomal localization of sphingomyelinase in rat liver. BBA - Enzymol. *191*, 481–484.
Freeman, G.J., Long, A.J., Iwai, Y., Bourque, K., Chernova, T., Nishimura, H., Fitz, L.J., Malenkovich, N., Okazaki, T., Byrne, M.C., et al. (2000). Engagement of the Pd-1 Immunoinhibitory Receptor by a Novel B7 Family Member Leads to Negative Regulation of Lymphocyte Activation. J. Exp. Med. *192*, 1027–1034.

Gamper, C.J., and Powell, J.D. (2012). All PI3Kinase signaling is not mTOR: dissecting mTOR-dependent and independent signaling pathways in T cells. Front. Immunol. *3*, 312.
Gatfield J, and Pieters J (1997). Essential Role for Cholesterol in Entry of Mycobacteria into Macrophages. Science *277*, 2007–2011.
Gault, C.R., Obeid, L.M., and Hannun, Y.A. (2010). An overview of sphingolipid metabolism: From synthesis to breakdown. Adv. Exp. Med. Biol. *688*, 1–23.
Gobin, V., Van Steendam, K., Fevery, S., Tilleman, K., Billiau, A.D., Denys, D., and Deforce, D.L. (2013). Fluoxetine Reduces Murine Graft-Versus-Host Disease by Induction of T cell Immunosuppression. J. Neuroimmune Pharmacol. *8*, 934–943.
Gobin, V., Van Steendam, K., Denys, D., and Deforce, D. (2014). Selective serotonin reuptake inhibitors as a novel class of immunosuppressants. Int. Immunopharmacol. *20*, 148–156.
Goldstein, G. (1987). Monoclonal antibody specificity: Orthoclone OKT3 T-cell blocker. Nephron *46 Suppl 1*, 5–11.
Golubovskaya, V., and Wu, L. (2016). Different subsets of T cells, memory, effector functions, and CAR-T immunotherapy. Cancers (Basel). *8*.
Gorelik A, Illes K, Heinz LX, Superti-Furga G, and Nagar B (2016). Crystal structure of mammalian acid sphingomyelinase. Nat. Commun. *7*, 12196.
Grace, P.S., and Ernst, J.D. (2016). Suboptimal Antigen Presentation Contributes to Virulence of Mycobacterium tuberculosis In vivo. J. Immunol. *196*, 357–364.
Grassme, H., Jendrossek, V., Bock, J., Riehle, A., and Gulbins, E. (2002). Ceramide-Rich Membrane Rafts Mediate CD40 Clustering. J. Immunol. *168*, 298–307.
Grassmé, H., Gulbins, E., Brenner, B., Ferlinz, K., Sandhoff, K., Harzer, K., Lang, F., and Meyer, T.F. (1997). Acidic sphingomyelinase mediates entry of N. gonorrhoeae into Nonphagocytic cells. Cell *91*, 605–615.
Grassmé, H., Jekle, A., Riehle, A., Schwarz, H., Berger, J., Sandhoff, K., Kolesnick, R., and Gulbins, E. (2001). CD95 Signaling via Ceramide-rich Membrane Rafts. J. Biol. Chem. *276*, 20589–20596.
Grassmé, H., Cremesti, A., Kolesnick, R., and Gulbins, E. (2003). Ceramide-mediated clustering is required for CD95-DISC formation. Oncogene *22*, 5457–5470.
Grassmé, H., Riehle, A., Wilker, B., and Gulbins, E. (2005a). Rhinoviruses infect human epithelial cells via ceramide-enriched membrane platforms. J. Biol. Chem. *280*, 26256–26262.
Grassmé, H., Riehle, A., Wilker, B., and Gulbins, E. (2005b). Rhinoviruses infect human epithelial cells via ceramide-enriched membrane platforms. J. Biol. Chem. *280*, 26256–26262.
Gulbins, E., Palmada, M., Reichel, M., Lüth, A., Böhmer, C., Amato, D., Müller, C.P., Tischbirek, C.H., Groemer, T.W., Tabatabai, G., et al. (2013). Acid sphingomyelinase-ceramide system mediates effects of antidepressant drugs. Nat. Med. *19*, 934–938.
Haimovitz-Friedman, A. (1994). Ionizing radiation acts on cellular membranes to generate ceramide and initiate apoptosis. J. Exp. Med. *180*, 525–535.
Hannun, Y.A., and Bell, R.M. (1989). Functions of sphingolipids and their breakdown products in cellular regulation. Am. Assoc. Adv. Sci. *243*, 500–507.
Hauck, C.R., Grassmé, H., Bock, J., Jendrossek, V., Ferlinz, K., Meyer, T.F., and Gulbins, E. (2000). Acid sphingomyelinase is involved in CEACAM receptor-mediated

phagocytosis of Neisseria gonorrhoeae. FEBS Lett. *478*, 260–266.
Heinrich, M., Wickel, M., Schneider-Brachert, W., Sandberg, C., Gahr, J., Schwandner, R., Weber, T., Brunner, J., Krönke, M., and Schütze, S. (1999). Cathepsin D targeted by acid sphingomyelinase-derived ceramide. EMBO J. *18*, 5252–5263.
Hémar, A., and Dautry-Varsat, A. (1990). Cyclosporin A inhibits the interleukin 2 receptor α chain gene transcription but not its cell surface expression: the α chain stability can explain this discrepancy. Eur. J. Immunol. *20*, 2629–2635.
Hémar, A., Subtil, A., Lieb, M., Morelon, E., Hellio, R., and Dautry-Varsat, A. (1995). Endocytosis of interleukin 2 receptors in human T lymphocytes: distinct intracellular localization and fate of the receptor alpha, beta, and gamma chains. J. Cell Biol. *129*, 55–64.
Hendricks, O., Butterworth, T.S., and Kristiansen, J.E. (2003). The in-vitro antimicrobial effect of non-antibiotics and putative inhibitors of efflux pumps on Pseudomonas aeruginosa and Staphylococcus aureus. Int. J. Antimicrob. Agents *22*, 262–264.
Henry, B., Ziobro, R., Becker, K.A., Kolesnick, R., and Gulbins, E. (2013). Acid Sphingomyelinase. (Springer, Vienna), pp. 77–88.
Heusel, J.W., Wesselschmidt, R.L., Shresta, S., Russell, J.H., and Ley, T.J. (1994). Cytotoxic lymphocytes require granzyme B for the rapid induction of DNA fragmentation and apoptosis in allogeneic target cells. Cell *76*, 977–987.
Horinouchi, K., Erlich, S., Perl, D.P., Ferlinz, K., Bisgaier, C.L., Sandhoff, K., Desnick, R.J., Stewart, C.L., and Schuchman, E.H. (1995). Acid sphingomyelinase deficient mice: a model of types A and B Niemann-Pick disease. Nat. Genet. *10*, 288–293.
Houtman, J.C.D., Houghtling, R.A., Barda-Saad, M., Toda, Y., and Samelson, L.E. (2005). Early Phosphorylation Kinetics of Proteins Involved in Proximal TCR-Mediated Signaling Pathways. J. Immunol. *175*, 2449–2458.
Hudig, D., Fraser, S.A., Karimi, R., and Michalak, M. (2018). Perforin Lytic Activity Is Controlled by Calreticulin. J Immunol Ref. J. Immunol. *164*, 4150–4155.
Hueber, A.O. (2000). CD95: More than just a death factor? Nat. Cell Biol. *2*.
Humphreys, I.R., Stewart, G.R., Turner, D.J., Patel, J., Karamanou, D., Snelgrove, R.J., and Young, D.B. (2006). A role for dendritic cells in the dissemination of mycobacterial infection. Microbes Infect. *8*, 1339–1346.
Hunter, T. (1987). A tail of two src's: Mutatis mutandis. Cell *49*, 1–4.
Hurwitz, R., Ferlinz, K., Vielhaber, G., Moczall, H., and Sandhoff, K. (1994). Processing of human acid sphingomyelinase in normal and I-cell fibroblasts. J. Biol. Chem. *269*, 5440–5445.
Huwiler, A., Kolter, T., Pfeilschifter, J., and Sandhoff, K. (2000). Physiology and pathophysiology of sphingolipid metabolism and signaling. Biochim. Biophys. Acta - Mol. Cell Biol. Lipids *1485*, 63–99.
Huwiler, A., Johansen, B., Skarstad, A., and Pfeilschifter, J. (2001). Ceramide binds to the CaLB domain of cytosolic phospholipase A2 and facilitates its membrane docking and arachidonic acid release. FASEB J. *15*, 7–9.
Isenberg, G., and Tamargo, J. (1985). Effect of Imipramine on calcium and potassium currents in isolated bovine ventricular myocytes. Eur. J. Pharmacol. *108*, 121–131.
Janardhan, S. V., Praveen, K., Marks, R., and Gajewski, T.F. (2011). Evidence implicating the Ras pathway in multiple CD28 costimulatory functions in CD4 + T cells. PLoS One *6*, e24931.

Kagina, B.M.N., Abel, B., Scriba, T.J., Hughes, E.J., Keyser, A., Soares, A., Gamieldien, H., Sidibana, M., Hatherill, M., Gelderbloem, S., et al. (2010). Specific T cell frequency and cytokine expression profile do not correlate with protection against tuberculosis after bacillus Calmette-Guérin vaccination of newborns. Am. J. Respir. Crit. Care Med. *182*, 1073–1079.
Kang, P.B., Azad, A.K., Torrelles, J.B., Kaufman, T.M., Beharka, A., Tibesar, E., DesJardin, L.E., and Schlesinger, L.S. (2005). The human macrophage mannose receptor directs Mycobacterium tuberculosis lipoarabinomannan-mediated phagosome biogenesis. J. Exp. Med. *202*, 987–999.
Karlsson, H. (1998). Induction of apoptosis in proliferating lymphocytes by tricyclic antidepressants. Apoptosis *3*, 255–260.
Keir, M.E., Butte, M.J., Freeman, G.J., and Sharpe, A.H. (2008). PD-1 and Its Ligands in Tolerance and Immunity. Annu. Rev. Immunol. *26*, 677–704.
Kendall, S. (1988). Interleukin-2: inception, impact and implications. Am. Assoc. Adv. Sci. *240*, 1169–1176.
Kim, Y.H., Buchholz, M.J., and Nordin, A.A. (1993). Murine T-lymphocyte proliferation induced by interleukin 2 correlates with a transient increase in p56lck kinase activity and the tyrosine phosphorylation of a 97-kDa protein. Proc. Natl. Acad. Sci. U. S. A. *90*, 3187–3191.
Kitatani, K., Idkowiak-Baldys, J., and Hannun, Y.A. (2008). The sphingolipid salvage pathway in ceramide metabolism and signaling. Cell. Signal. *20*, 1010–1018.
Klutzny, S., Lesche, R., Keck, M., Kaulfuss, S., Schlicker, A., Christian, S., Sperl, C., Neuhaus, R., Mowat, J., Steckel, M., et al. (2017). Functional inhibition of acid sphingomyelinase by Fluphenazine triggers hypoxia-specific tumor cell death. Cell Death Dis. *8*, 1–15.
Kobayashi, N., Kono, T., Hatakeyama, M., Minami, Y., Miyazaki, T., Perlmutter, R.M., and Taniguchi, T. (1993). Functional coupling of the src-family protein tyrosine kinases p59fyn and p53/56lyn with the interleukin 2 receptor: implications for redundancy and pleiotropism in cytokine signal transduction. Proc. Natl. Acad. Sci. U. S. A. *90*, 4201–4205.
Koch, J.M., Kell, S., and Aldenhoff, J.B. (2003). Differential effects of fluoxetine and imipramine on the phosphorylation of the transcription factor CREB and cell-viability. J. Psychiatr. Res. *37*, 53–59.
Kolzer, M., Arenz, C., Ferlinz, K., Werth, N., Schulze, H., Klingenstein, R., and Sandhoff, K. (2003). Phosphatidylinositol-3,5-Bisphosphate is a potent and selective inhibitor of acid sphingomyelinase. Biol Chem *384*, 1293–1298.
Kölzer, M., Werth, N., and Sandhoff, K. (2004). Interactions of acid sphingomyelinase and lipid bilayers in the presence of the tricyclic antidepressant desipramine. FEBS Lett. *559*, 96–98.
Konkel, J.E., Frommer, F., Leech, M.D., Yagita, H., Waisman, A., and Anderton, S.M. (2010). PD-1 signalling in CD4+ T cells restrains their clonal expansion to an immunogenic stimulus, but is not critically required for peptide-induced tolerance. Immunology *130*, 92–102.
Kornhuber, J., Medlin, A., Bleich, S., Jendrossek, V., Henkel, A.W., Wiltfang, J., and Gulbins, E. (2005). High activity of acid sphingomyelinase in major depression. J. Neural Transm. *112*, 1583–1590.

Kornhuber, J., Tripal, P., Reichel, M., Mühle, C., Rhein, C., Muehlbacher, M., and Groemer, T.W. (2010). Functional Inhibitors of Acid Sphingomyelinase (FIASMAs): A Novel Pharmacological Group of Drugs with Broad Clinical Applications. Cell Physiol Biochem *26*, 9–20.
Kornhuber, J., Muehlbacher, M., Trapp, S., Pechmann, S., Friedl, A., Reichel, M., Mü Hle, C., Terfloth, L., Groemer, T.W., Spitzer, G.M., et al. (2011). Identification of Novel Functional Inhibitors of Acid Sphingomyelinase. PLoS One *6*.
Kursar, M., Koch, M., Mittrucker, H.-W., Nouailles, G., Bonhagen, K., Kamradt, T., and Kaufmann, S.H.E. (2007). Cutting Edge: Regulatory T Cells Prevent Efficient Clearance of Mycobacterium tuberculosis. J. Immunol. *178*, 2661–2665.
Kwan, C., and Ernst, J.D. (2011). HIV and tuberculosis: A deadly human syndemic. Clin. Microbiol. Rev. *24*, 351–376.
Lang, P.A., Schenck, M., Nicolay, J.P., Becker, J.U., Kempe, D.S., Lupescu, A., Koka, S., Eisele, K., Klarl, B.A., Rübben, H., et al. (2007). Liver cell death and anemia in Wilson disease involve acid sphingomyelinase and ceramide. Nat. Med. *13*, 164–170.
Larkin, J., Renukaradhya, G.J., Sriram, V., Du, W., Gervay-Hague, J., and Brutkiewicz, R.R. (2006). CD44 Differentially Activates Mouse NK T Cells and Conventional T Cells. J. Immunol. *177*, 268–279.
Latchman, Y., Wood, C.R., Chernova, T., Chaudhary, D., Borde, M., Chernova, I., Iwai, Y., Long, A.J., Brown, J.A., Nunes, R., et al. (2001). PD-L2 is a second ligand for PD-1 and inhibits T cell activation. Nat. Immunol. *2*, 261–268.
Lepple-Wienhues, A., Belka, C., Laun, T., Jekle, A., Walter, B., Wieland, U., Welz, M., Heil, L., Kun, J., Busch, G., et al. (1999). Stimulation of CD95 (Fas) blocks T lymphocyte calcium channels through sphingomyelinase and sphingolipids. Proc. Natl. Acad. Sci. U. S. A. *96*, 13795–13800.
Lewis, R.S. (2001). Calcium signaling mechanisms in T lymphocytes. Annu. Rev. Immunol. *19*, 497–521.
Li, X., Becker, K.A., and Zhang, Y. (2010). Ceramide in Redox Signaling and Cardiovascular Diseases. *150081*, 41–48.
Lieberman, J. (2003). The ABCs of granule-mediated cytotoxicity: New weapons in the arsenal. Nat. Rev. Immunol. *3*, 361–370.
Lin, X., O'Mahony, A., Mu, Y., Geleziunas, R., and Greene, W.C. (2000). Protein kinase C-theta participates in NF-kappaB activation induced by CD3-CD28 costimulation through selective activation of IkappaB kinase beta. Mol. Cell. Biol. *20*, 2933–2940.
Lovat, P.E., Di Sano, F., Corazzari, M., Fazi, B., Donnorso, R.P., Pearson, A.D.J., Hall, A.G., Redfern, C.P.F., and Piacentini, M. (2004). Gangliosides link the acidic sphingomyelinase-mediated induction of ceramide to 12-lipoxygenase-dependent apoptosis of neuroblastoma in response to fenretinide. J. Natl. Cancer Inst. *96*, 1288–1299.
Lozano, J., Morales, A., Cremesti, A., Fuks, Z., Tilly, J.L., Schuchman, E., Gulbins, E., and Kolesnick, R. (2001). Niemann-Pick Disease versus acid sphingomyelinase deficiency. Cell Death Differ *8*, 100–103.
Ma, E.H., Poffenberger, M.C., Wong, A.H.T., and Jones, R.G. (2017). The role of AMPK in T cell metabolism and function. Curr. Opin. Immunol. *46*, 45–52.
Maciolek, J.A., Alex Pasternak, J., and Wilson, H.L. (2014). Metabolism of activated T lymphocytes. Curr. Opin. Immunol. *27*, 60–74.

Mackaness, G.B., Lagrange, P.H., and Ishibashi, T. (1974). The Modifying Effect of BCG on the Immunological Induction of T Cells. J. Exp. Med. *139*, 1540–1552.
Makgoba, M.W., Martin, E., and Shaw, S. (1989). The CD2-LFA-3 and LFA- 1 -ICAM palhways : relevance to T-cel recognition. *10*, 417–422.
Malaplate-Armand, C., Florent-Béchard, S., Youssef, I., Koziel, V., Sponne, I., Kriem, B., Leininger-Muller, B., Olivier, J.L., Oster, T., and Pillot, T. (2006). Soluble oligomers of amyloid-β peptide induce neuronal apoptosis by activating a cPLA2-dependent sphingomyelinase-ceramide pathway. Neurobiol. Dis. *23*, 178–189.
Malek, T.R., and Castro, I. (2010). Interleukin-2 Receptor Signaling: At the Interface between Tolerance and Immunity. Immunity *33*, 153–165.
Mayer, A., Denanglaire, S., Viollet, B., Leo, O., and Andris, F. (2008). AMP-activated protein kinase regulates lymphocyte responses to metabolic stress but is largely dispensable for immune cell development and function. Eur. J. Immunol. *38*, 948–956.
Menne, C., Lauritsen, J.P.H., Dietrich, J., Kastrup, J., Wegener, A.-M.K., Andersen, P.S., Odum, N., and Geisler, C. (2001). T-Cell Receptor Downregulation by Ceramide-Induced Caspase Activation and Cleavage of the zeta Chain. Scand. J. Immunol. *53*, 176–183.
Mérida, I., Flores, C., Martinez-A, Y.A., Hannun, I., Flores, I., Martinez-A, C., Hannun, Y.A., and Mérida, I. (2018). Dual Role of Ceramide in the Control of Apoptosis Following IL-2 Withdrawal. J Immunol Ref. J. Immunol. *160*, 3528–3533.
Miller, M.E., Adhikary, S., Kolokoltsov, A.A., and Davey, R.A. (2012). Ebolavirus Requires Acid Sphingomyelinase Activity and Plasma Membrane Sphingomyelin for Infection. J. Virol. *86*, 7473–7483.
Mintzer, R.J., Appell, K.C., Cole, A., Johns, A., Pagila, R., Polokoff, M.A., Tabas, I., Snider, R.M., and Meurer-Ogden, J.A. (2005). A novel high-throughput screening format to identify inhibitors of secreted acid sphingomyelinase. J. Biomol. Screen. *10*, 225–234.
Mogues, T., Goodrich, M.E., Ryan, L., Lacourse, R., and North, R.J. (2001). The Relative Importance of T Cell Subsets in Immunity and Immunopathology of Airborne Mycobacterium tuberculosis Infection in Mice. J. Exp. Med *022711000*, 271–280.
Molnár, J., Mucsi, I., and Kása, P. (1983). Inhibition of the adhesion of E. coli on cultured human epitheliel cells in the presence of promethazine or imipramine. Zentralblatt Für Bakteriol. Mikrobiol. Und Hyg. 1. Abt. Orig. A, Medizinische Mikrobiol. Infekt. Und Parasitol. *254*, 388–396.
Mueller, N., Avota, E., Collenburg, L., Grassmé, H., and Schneider-Schaulies, S. (2014). Neutral Sphingomyelinase in Physiological and Measles Virus Induced T Cell Suppression. PLoS Pathog *10*.
Mustafa, A.S., Shaban, F.A., Abal, A.T., Al-Attiyah, R., Wiker, H.G., Lundin, K.E.A., Oftung, F., and Huygen, K. (2000). Identification and HLA Restriction of Naturally Derived Th1-Cell Epitopes from the Secreted Mycobacterium tuberculosis Antigen 85B Recognized by Antigen-Specific Human CD4 T-Cell Lines. Infect. Immun. *68*, 3933–3940.
Na, L. (1996). Tricyclic antidepressants induce apoptosis in human T lymphocytes. Int. J. Immunopharmacol. *08*, 534–543.
Naval, A.M., Krensky, A., Anel, S., Gamen, D.A., Hanson, A., Kaspar, J., Gamen, S., Hanson, D.A., Kaspar, A., Naval, J., et al. (2018). Granulysin-Induced Apoptosis. I. Involvement of at Least Two Distinct Pathways. J Immunol Ref. *161*, 1758–1764.

Nelson, B., and Willerford, D. (1998). Biology of the interleukin-2 receptor. Adv. Immunol. *70*.
Newrzella, D., and Stoffel, W. (1996). Functional Analysis of the Glycosylation of Murine Acid Sphingomyelinase. J. Biol. Chem. *271*, 32089–32095.
Ni, X., and Morales, C.R. (2006). The lysosomal trafficking of acid sphingomyelinase is mediated by sortilin and mannose 6-phosphate receptor. Traffic *7*, 889–902.
Nika, K., Soldani, C., Salek, M., Paster, W., Gray, A., Etzensperger, R., Fugger, L., Polzella, P., Cerundolo, V., Dushek, O., et al. (2010). Constitutively active lck kinase in T cells drives antigen receptor signal transduction. Immunity *32*, 766–777.
Nishizuka, Y. (1995). Protein kinase C and lipid signaling for sustained cellular responses. FASEB J. *9*, 484–496.
Nix, M., and Stoffel, W. (2000). Perturbation of membrane microdomains reduces mitogenic signaling and increases susceptibility to apoptosis after T cell receptor stimulation. Cell Death Differ. *7*, 413–424.
O'Byrne, D., and Sansom, D. (2000). Lack of costimulation by both sphingomyelinase and C2 ceramide in resting human T cells. Immunology *100*, 225–230.
van Oers, N.S.C., Killeen, N., and Weiss, A. (1994). ZAP-70 is constitutively associated with tyrosine-phosphoryated TCR z in murine thymocytes and lymph node cells. Immunity *1*, 675–685.
Ogata, N., Yoshii, M., and Narahashi, T. (1989). Psychotropic drugs block voltage-gated ion channels in neuroblastoma cells. *476*, 140–144.
Oh-Hora, M. (2009). Calcium signaling in the development and function of T-lineage cells. Immunol. Rev. *231*, 210–224.
Park, H., Li, Z., Yang, X.O., Chang, S.H., Nurieva, R., Wang, Y.H., Wang, Y., Hood, L., Zhu, Z., Tian, Q., et al. (2005). A distinct lineage of CD4 T cells regulates tissue inflammation by producing interleukin 17. Nat. Immunol. *6*, 1133–1141.
Pearce, E.L. (2010). Metabolism in T cell activation and differentiation. Curr. Opin. Immunol. *22*, 314–320.
Perez de Castro, I., Bivona, T.G., Philips, M.R., and Pellicer, A. (2004). Ras Activation in Jurkat T cells following Low-Grade Stimulation of the T-Cell Receptor Is Specific to N-Ras and Occurs Only on the Golgi Apparatus. Mol. Cell. Biol. *24*, 3485–3496.
Perrotta, C., Bizzozero, L., Falcone, S., Rovere-Querini, P., Prinetti, A., Schuchman, E.H., Sonnino, S., Manfredi, A.A., and Clementi, E. (2007). Nitric oxide boosts chemoimmunotherapy via inhibition of acid sphingomyelinase in a mouse model of melanoma. Cancer Res. *67*, 7559–7564.
Philips, J.A., and Ernst, J.D. (2012). Tuberculosis Pathogenesis and Immunity. Annu. Rev. Pathol. Mech. Dis. *7*, 353–384.
Pike, L.J. (2003). Lipid rafts. J. Lipid Res. *44*, 655–667.
Ponta, H., Sherman, L., and Herrlich, P.A. (2003). CD44: From adhesion molecules to signalling regulators. Nat. Rev. Mol. Cell Biol.
Puissegur, M.P., Botanch, C., Duteyrat, J.L., Delsol, G., Caratero, C., and Altare, F. (2004). An in vitro dual model of mycobacterial granulomas to investigate the molecular interactions between mycobacteria and human host cells. Cell. Microbiol. *6*, 423–433.
Qureshi, O.S., Zheng, Y., Nakamura, K., Attridge, K., Manzotti, C., Schmidt, E.M., Baker, J., Jeffery, L.E., Kaur, S., Briggs, Z., et al. (2011). Trans-endocytosis of CD80 and CD86: A molecular basis for the cell-extrinsic function of CTLA-4. Science (80-.).

332, 600–603.
Rhee, S.G., Suh, P.G., Ryu, S.H., and Lee, S.Y. (1989). Studies of inositol phospholipid - Specific phospholipase C. Science (80-.). *244*, 546–550.
Rhein, C., Tripal, P., Seebahn, A., Konrad, A., Kramer, M., Nagel, C., Kemper, J., Bode, J., Mühle, C., Gulbins, E., et al. (2012). Functional implications of novel human acid sphingomyelinase splice variants. PLoS One *7*, e35467.
Riethmüller, J., J Anthonysamy, E Serra, M Schwab, G Döring, and E Gulbins (2009). Therapeutic Efficacy and Safety of Amitriptyline in Patients with Cystic Fibrosis. Cell. Physiol. Biochem. *24*, 65–72.
Rotolo, J.A., Zhang, J., Donepudi, M., Lee, H., Fuks, Z., and Kolesnick, R. (2005). Caspase-dependent and -independent activation of acid sphingomyelinase signaling. J. Biol. Chem. *280*, 26425–26434.
Rudd, C.E., Taylor, A., and Schneider, H. (2009). CD28 and CTLA-4 coreceptor expression and signal transduction. Immunol. Rev. *229*, 12–26.
Rudolph, M.G., Stanfield, R.L., and Wilson, I.A. (2006). How TCRs bind MHCs, peptides, and coreceptors. Annu. Rev. Immunol. *24*, 419–466.
Russell, D.G. (2001). Mycobacterium tuberculosis: here today, and here tomorrow. Nat. Rev. Mol. Cell Biol *2*, 569–577.
Russell, J.H., and Ley, T.J. (2002). Lymphocyte-mediated cytotoxicity. Annu. Rev. Immunol *05*, 323–370.
Schissel, S.L., Jiang, X.-C., Tweedie-Hardmanţ, J., Jeong, T.-S., Camejo, E.H., Najib, J., Rappţ, J.H., Williams, K.J., and Tabas, I. (1998a). Secretory Sphingomyelinase, a Product of the Acid Sphingomyelinase Gene, Can Hydrolyze Atherogenic Lipoproteins at Neutral pH. J. Biol. Chem. *273*, 2738–2746.
Schissel, S.L., Keesler, G.A., Schuchman, E.H., Williams, K.J., and Tabas, I. (1998b). The cellular trafficking and zinc dependence of secretory and lysosomal sphingomyelinase, two products of the acid sphingomyelinase gene. J. Biol. Chem. *273*, 18250–18259.
Schramm, M., Herz, J., Haas, A., Krönke, M., and Utermöhlen, O. (2008). Acid sphingomyelinase is required for efficient phago-lysosomal fusion. Cell. Microbiol. *10*, 1839–1853.
Schuchman, E.H. (1992). Structural Organization and Complete Nucleotide Sequence of the Gene Encoding Human Acid Sphingomyelinase (SMPD1). Genomics *205*, 197–205.
Schuchman, E.H. (2010). Acid sphingomyelinase, cell membranes and human disease: Lessons from Niemann-Pick disease. FEBS Lett. *584*, 1895–1900.
Schuchman, E.H., Suchi, M., Takahashi, T., Sandhoff, K., and Desnick, R.J. (1991). Human acid sphingomyelinase: Isolation, nucleotide sequence, and expression of the full-length and alternatively spliced cDNAs. J. Biol. Chem. *266*, 8531–8539.
Shafiani, S., Tucker-Heard, G., Kariyone, A., Takatsu, K., and Urdahl, K.B. (2010). Pathogen-specific regulatory T cells delay the arrival of effector T cells in the lung during early tuberculosis. J. Exp. Med. *207*, 1409–1420.
Shakor, A.B.A., Kwiatkowska, K., and Sobota, A. (2004). Cell surface ceramide generation precedes and controls Fc gammaRII clustering and phosphorylation in rafts. J. Biol. Chem. *279*, 36778–36787.
Shan, X., Czar, M.J., Bunnell, S.C., Liu, P., Liu, Y., Schwartzberg, P.L., and Wange,

R.L. (2000). Deficiency of PTEN in Jurkat T cells causes constitutive localization of Itk to the plasma membrane and hyperresponsiveness to CD3 stimulation. Mol. Cell. Biol. *20*, 6945–6957.
Sharpe, A.H., Wherry, E.J., Ahmed, R., and Freeman, G.J. (2007). The function of programmed cell death 1 and its ligands in regulating autoimmunity and infection. Nat. Immunol. *8*, 239–245.
Sheppard, K.A., Fitz, L.J., Lee, J.M., Benander, C., George, J.A., Wooters, J., Qiu, Y., Jussif, J.M., Carter, L.L., Wood, C.R., et al. (2004). PD-1 inhibits T-cell receptor induced phosphorylation of the ZAP70/CD3ζ signalosome and downstream signaling to PKCθ. FEBS Lett. *574*, 37–41.
Singer, S.J., and Nicolson, G.L. (1972). The Fluid Mosaic Model of the Structure of Cell Membrane. Science *175*, 720–731.
Stancevic, B., and Kolesnick, R. (2010). Ceramide-rich platforms in transmembrane signaling. FEBS Lett. *584*, 1728–1740.
Stoffel, B., Bauer, P., Nix, M., Deres, K., and Stoffel, W. (1998). Ceramide-independent CD28 and TCR signaling but reduced IL-2 secretion in T cells of acid sphingomyelinase-deficient mice. Eur. J. Immunol. *28*, 874–880.
Swain, S.L., Weinberg, A.D., English, M., and Huston, G. (1990). IL-4 directs the development of Th2-like helper effectors. J Immunol *145*, 3796–3806.
Takatori, H., Nakajima, H., Kagami, S. i, Hirose, K., Suto, A., Suzuki, K., Kubo, M., Yoshimura, A., Saito, Y., and Iwamoto, I. (2005). Stat5a Inhibits IL-12-Induced Th1 Cell Differentiation through the Induction of Suppressor of Cytokine Signaling 3 Expression. J. Immunol. *174*, 4105–4112.
Tamás, P., Hawley, S.A., Clarke, R.G., Mustard, K.J., Green, K., Hardie, D.G., and Cantrell, D.A. (2006). Regulation of the energy sensor AMP-activated protein kinase by antigen receptor and Ca2+ in T lymphocytes. J. Exp. Med. *203*, 1665–1670.
Tamura, T., Ariga, H., Kinashi, T., Uehara, S., Kikuchi, T., Nakada, M., Tokunaga, T., Xu, W., Kariyone, A., Saito, T., et al. (2004). The role of antigenic peptide in CD4+ T helper phenotype development in a T cell receptor transgenic model. Int. Immunol. *16*, 1691–1699.
Tonnetti, L., Verí, M.C., Bonvini, E., and D'Adamio, L. (1999). A role for neutral sphingomyelinase-mediated ceramide production in T cell receptor-induced apoptosis and mitogen-activated protein kinase-mediated signal transduction. J. Exp. Med. *189*, 1581–1589.
Tsai, M.C., Chakravarty, S., Zhu, G., Xu, J., Tanaka, K., Koch, C., Tufariello, J.A., Flynn, J.A., and Chan, J. (2006). Characterization of the tuberculous granuloma in murine and human lungs: Cellular composition and relative tissue oxygen tension. Cell. Microbiol. *8*, 218–232.
Utermöhlen, O., Herz, J., Schramm, M., and Krönke, M. (2008). Fusogenicity of membranes: The impact of acid sphingomyelinase on innate immune responses. Immunobiology *213*, 307–314.
Varma, R., Campi, G., Yokosuka, T., Saito, T., and Dustin, M.L. (2006). T Cell Receptor-Proximal Signals Are Sustained in Peripheral Microclusters and Terminated in the Central Supramolecular Activation Cluster. Immunity *25*, 117–127.
Veiga, M.P., Arrondo, J.L.R., Goñi, F.M., and Alonso, A. (1999). Ceramides in phospholipid membranes: Effects on bilayer stability and transition to nonlamellar

phases. Biophys. J. *76*, 342–350.
Veldhoen, M., Hocking, R.J., Atkins, C.J., Locksley, R.M., and Stockinger, B. (2006). TGFβ in the context of an inflammatory cytokine milieu supports de novo differentiation of IL-17-producing T cells. Immunity *24*, 179–189.
Verdurmen, W.P.R., Thanos, M., Ruttekolk, I.R., Gulbins, E., and Brock, R. (2010). Cationic cell-penetrating peptides induce ceramide formation via acid sphingomyelinase: Implications for uptake. J. Control. Release *147*, 171–179.
Villalba, M., Coudronniere, N., Deckert, M., Teixeiro, E., Mas, P., and Altman, A. (2000). A novel functional interaction between Vav and PKCtheta is required for TCR-induced T cell activation. Immunity *12*, 151–160.
Van Wauwe, J.P., Goossens, J.G., and Beverley, P.C. (1984). Human T lymphocyte activation by monoclonal antibodies; OKT3, but not UCHT1, triggers mitogenesis via an interleukin 2-dependent mechanism. J. Immunol. *133*, 129–132.
Wolf, A.J., Linas, B., Trevejo-Nunez, G.J., Kincaid, E., Tamura, T., Takatsu, K., and Ernst, J.D. (2007). Mycobacterium tuberculosis Infects Dendritic Cells with High Frequency and Impairs Their Function In Vivo. J. Immunol. *179*, 2509–2519.
Wolf, A.J., Desvignes, L., Linas, B., Banaiee, N., Tamura, T., Takatsu, K., and Ernst, J.D. (2008). Initiation of the adaptive immune response to *Mycobacterium tuberculosis* depends on antigen production in the local lymph node, not the lungs. J. Exp. Med.
Wucherpfennig, K.W., Gagnon, E., Call, M.J., Huseby, E.S., and Call, M.E. (2010). Structural biology of the T-cell receptor: insights into receptor assembly, ligand recognition, and initiation of signaling. Cold Spring Harb. Perspect. Biol. *2*, a005140.
Xia, Z., DePierre, J.W., and Nässberger, L. (1996). Tricyclic antidepressants inhibit IL-6, IL-1β and TNF-α release in human blood monocytes and IL-2 and interferon-γ in T cells. Immunopharmacology *34*, 27–37.
Xiong, Z.J., Huang, J., Poda, G., Pomès, R., and Privé, G.G. (2016). Structure of Human Acid Sphingomyelinase Reveals the Role of the Saposin Domain in Activating Substrate Hydrolysis. J. Mol. Biol. *428*, 3026–3042.
Xuan, N.T., Shumilina, E., Schmid, E., Bhavsar, S.K., Rexhepaj, R., Götz, F., Gulbins, E., and Lang, F. (2010). Role of acidic sphingomyelinase in thymol-mediated dendritic cell death. Mol. Nutr. Food Res. *54*, 1833–1841.
Zeidan, Y.H., and Hannun, Y.A. (2007). Activation of acid sphingomyelinase by protein kinase C delta-mediated phosphorylation. J. Biol. Chem. *282*, 11549–11561.
Zeidan, Y.H., Wu, B.X., Jenkins, R.W., Obeid, L.M., and Hannun, Y.A. (2008). A novel role for protein kinase Cδ-mediated phosphorylation of acid sphingomyelinase in UV light-induced mitochondrial injury. FASEB J. *22*, 183–193.
Zhang, Y., Bei, Y., Delikat, S., Bayoumy, S., Xin-Hua, L., Basu, S., McGinley, M., Chan-Hui, P.Y., Lichenstein, H., and Kolesnick, R. (1997). Kinase suppressor of Ras is ceramide-activated protein kinase. Cell *89*, 63–72.
Zhang, Y., Li, X., Carpinteiro, A., and Gulbins, E. (2008). Acid Sphingomyelinase Amplifies Redox Signaling in Pseudomonas aeruginosa -Induced Macrophage Apoptosis. J. Immunol. *181*, 4247–4254.
Zhi-Jun, Y., Sriranganathan, N., Vaught, T., Arastu, S.K., and Ansar Ahmed, S. (1997). A dye-based lymphocyte proliferation assay that permits multiple immunological analyses: mRNA, cytogenetic, apoptosis, and immunophenotyping studies. J. Immunol. Methods *210*, 25–39.

Zhu, J., and Paul, W.E. (2008). CD4 T cells: Fates, functions, and faults. Blood *112*, 1557–1569.
Zhu, J., Yamane, H., and Paul, W.E. (2010). Differentiation of Effector CD4 T Cell Populations. Annu. Rev. Immunol. *28*, 445–489.

Appendix

Posters and presentations

Begum S, Gulbins E, Grassmé H, Haimovitz Friedman A, Lang KS. Role of acid sphingomyelinase in T lymphocyte activation during Tuberculosis. **Poster**, Tag der Forschung der Medizinischen Fakultät, Essen, Germany, November 17, 2017

Begum S, Gulbins E, Grassmé H, Haimovitz-Friedman A, Lang KS. Role of acid sphingomyelinase in T lymphocyte activation during Tuberculosis. **Poster**, International workshop: “Sphingolipids- from basic science to novel therapeutic concepts”, Würzburg, Germany, June 28-30, 2018

Begum S, Gulbins E, Grassmé H. Role of acid sphingomyelinase in T lymphocyte activation. **Presentation**, “Meeting GRK 2098 with the integrated GRK/ SFB 1039”, Frankfurt, Germany, June 27-28, 2018

Acknowledgments

First, I would like to thank Prof. Dr. Erich Gulbins for giving me the opportunity to work on this project under his excellent scientific guidance.

I am also very grateful for the academic support of Prof. Dr. Karl Sebastian Lang, Dr. Heike Grassmé and Dr. Katrin Becker-Flegler for their patience, encouragement and counsel throughout my PhD time and for sharing their enthusiasm for science with me.

I would like to thank our collaboration partners: Adriana Haimovitz-Friedman and Richard Kolesnick in Memorial Sloan Kettering Cancer Center, New York, USA; for their intensive guidance during the second year of my PhD. Moreover, Special thanks to Dr. Fabian Schumacher at the Department of Toxicology/Institute of Nutritional Science in Potsdam, for his support with Mass spectrometry experiments.

I would also like to thank the members of the thesis committee for taking the time to evaluate my PhD thesis.

A huge thank you is also owed to my past and present colleagues and friends at the Department of Molecular Biology and Department of Immunology, for helping me out and creating a positive and fun work environment: Anne Koch, Karen Hung, Yuqing Wu, Dr. Cao Li, Jie Ma, Eyad Naser, Bärbel Pollmeier, Andrea Riehle, Carolin Sehl, Matthias Soddeman, Hannelore Disselhoff, Dr. Stephanie Kadow, Dr. Alexander Carpinteiro, Simone Keitsch, Claudine Kühn, Melanie Kramer, Siegfried Moyrer, Helga Pätsch, Bettina Peter, Barbara Wilker, Nadine Beckmann, Gabriele Hessler and Judith Bezgovsek.

Finally, I would like to thank my family and friends, particularly my father and my husband, for their unconditional love and friendship and their strong belief in me.

Declarations

Erklärung:

Hiermit erkläre ich, gem. § 7 Abs. (2) d) + f) der Promotionsordnung der Fakultät für Biologie zur Erlangung des Dr. rer. nat., dass ich die vorliegende Dissertation selbständig verfasst und mich keiner anderen als der angegebenen Hilfsmittel bedient, bei der Abfassung der Dissertation nur die angegeben Hilfsmittel benutzt und alle wörtlich oder inhaltlich übernommenen Stellen als solche gekennzeichnet habe.

Essen, den _____ _____

Unterschrift der Doktorandin

Erklärung:

Hiermit erkläre ich, gem. § 7 Abs. (2) e) + g) der Promotionsordnung der Fakultät für Biologie zur Erlangung des Dr. rer. nat., dass ich keine anderen Promotionen bzw. Promotionsversuche in der Vergangenheit durchgeführt habe und dass diese Arbeit von keiner anderen Fakultät/Fachbereich abgelehnt worden ist.

Essen, den _____ _____

Unterschrift der Doktorandin

Erklärung:

Hiermit erkläre ich, gem. § 6 Abs. (2) g) der Promotionsordnung der Fakultät für Biologie zur Erlangung der Dr. rer. nat., dass ich das Arbeitsgebiet, dem das Thema ‘’**Role of acid sphingomyelinase in T lymphocyte activation**’’ zuzuordnen ist, in Forschung und Lehre vertrete und den Antrag von **Salina Begum** befürworte und die Betreuung auch im Falle eines Weggangs, wenn nicht wichtige Gründe dem entgegenstehen, weiterführen werde.

_____

Name des Mitglieds der Universität Duisburg-Essen in Druckbuchstaben

Essen, den _____ _____

Unterschrift eines Mitglieds der Universität Duisburg-Essen

Curriculum Vitae

"The biography is not included in the online version for reasons of data protection".